DURABILITY OF NON-PROPRIETARY ULTRA-HIGH-PERFORMANCE

CONCRETE FOR PRETENSIONED BRIDGE GIRDERS

A Thesis

by

BRITTNI ANNE COOPER

Submitted to the Office of Graduate and Professional Studies of
Texas A&M University
in partial fulfillment of the requirements for the degree of

MASTER OF SCIENCE

Chair of Committee,   Mary Beth D. Hueste
Co-Chair of Committee, Anol K. Mukhopadhyay
Committee Members,   Stefan Hurlebaus
                     John B. Mander
                     Anastasia Muliana
Head of Department,   Robin Autenrieth

August 2020

Major Subject: Civil Engineering

ABSTRACT

Proprietary ultra-high-performance concrete (UHPC) has predominantly been used in bridge applications in the United States in connections, overlays, and girders. To facilitate further implementation, the Texas Department of Transportation (TxDOT) is supporting research to develop its own cost-efficient non-proprietary UHPC that will provide the same benefits as the proprietary mixes with a specific application to pretensioned bridge girders. This research presents an evaluation of the durability, particularly permeability, of select non-proprietary mixes made with locally available materials in Texas and provides a service life estimation based on the available methods and properties of these mixes.

Resistivity is a non-destructive test that is faster and more user-friendly than conventional permeability tests, while the formation factor is based on a numerical approach to quantify the porosity and pore connectivity. Determining the service life of the considered non-proprietary UHPC mixes provides an additional evaluation for durability. While multiple programs are available for service life prediction, their applicability to UHPC components needs to be better understood. Using available software, a more detailed analysis on the limitations and applicability to UHPC are made. Identifying the limitations of the software in the application to UHPC elements is crucial to the interpretation of the results and the subsequent comparative analysis between mixes used in similar applications.

It is concluded that the non-proprietary mixes studied have excellent permeability characteristics and microstructure development. The resistivity testing provided useful insight into the role of supplementary cementitious materials (SCMs) in UHPC microstructure development. The computed formation factors are used to calculate a diffusion coefficient. This diffusion coefficient aids in service life prediction and allows for a comparative assessment with other concrete mixes. While the limitations in the available software make it impossible to provide explicit results for service life prediction, the service life predictions coupled with the permeability testing indicate that the non-proprietary UHPC mixes have a strong potential to provide a service life exceeding conventional concrete mixes used in similar applications. The results also merit a further discussion for additional bridge applications outside of pretensioned bridge girders.

ACKNOWLEDGMENTS

CONTRIBUTORS AND FUNDING SOURCES

NOMENCLATURE

AASHTO — American Association of State Highway Transportation Officials

AC — Alternating Current

AM — Amarillo, TX

ASTM — American Society for Testing and Materials

AU — Austin, TX

C_2S — Di-Calcium Silicate

C_3S — Tri-Calcium Silicate

$Ca(OH)_2$ — Calcium Hydroxide

CC — Corpus Christi, TX

CIR — Center for Infrastructure Renewal

C_o — Initial Chloride Concentration (%)

C_s — Surface Chloride Concentration (%)

C-S-H — Calcium Silica Hydrate

$C_{x,t}$ — Chloride Concentration at a Specific Depth and Time (%)

D — Diffusion Coefficient (in^2/s)

DC — Direct Current

D_o — Chloride Ion Self-Diffusion Coefficient (in^2/s)

DOT — Department of Transportation

F — Formation Factor

FHWA — Federal Highway Administration

GGBS	Ground Granulated Blast-Furnace Slag
HPC	High Performance Concrete
HRWR	High Range Water Reducer
K_2O	Potassium Oxide
K_2SO_4	Arcanite
KICT	Korea Institute of Civil Engineering and Building Technology
KOH	Potassium Hydroxide
LaDOT	Louisiana Department of Transportation
m	Diffusion Decay Index
MSZ	Marine Spray Zone
Na_2O	Sodium Oxide
NaCl	Sodium Chloride
NaOH	Sodium Hydroxide
NIST	National Institute of Science and Technology
NSC	Normal Strength Concrete
PC	Precast Concrete
PSC	Pore Solution Concentration
PSR	Pore Solution Resistivity
RCPT	Rapid Chloride Penetration Test
SCC	Self-Consolidating Concrete
SCM	Supplementary Cementitious Material
SiO_2	Silicon Dioxide

SSD	Saturated Surface Dry
t	Time for Chloride Exposure Limit to be Reached (s)
TAMU	Texas A&M University
TxDOT	Texas Department of Transportation
UHB	Urban Highway Bridge
UHPC	Ultra-High-Performance Concrete
US	United States
w/c	Water-to-Cement Ratio
w/cm	Water-to-Cementitious Ratio
x	Depth to Reinforcement (in.)
XRD	X-ray Powder Diffraction
XRF	X-ray Fluorescence
β	Conductivity
ρ	Bulk Resistivity (kΩ-cm)
ρ_o	Pore Solution Resistivity (kΩ-cm)
ϕ	Porosity

TABLE OF CONTENTS

LIST OF FIGURES

LIST OF TABLES

1. INTRODUCTION

1.1. Background

Ultra-high-performance concrete (UHPC) is a newer class of concrete with exceptional strength and durability properties, making it an excellent option for infrastructure projects. It is defined by Graybeal (2011) in the Federal Highway Administration (FHWA) report (FHWA-HRT-11-038) as "a cementitious composite material composed of an optimized gradation of granular constituents, a water-to-cementitious ratio (*w/cm*) less than 0.25, and a high percentage of discontinuous internal fiber reinforcement." Graybeal (2011) emphasizes that UHPC has compressive strengths and post-cracking tensile strength exceeding 21.7 ksi (150 MPa) and 0.72 ksi (5 MPa), respectively. In the late 1990s, Lafarge Research Centre partnered with Bouygues and Rhodia to develop the proprietary UHPC patent Ductal® (Batoz and Behloul 2011). Since then, other commercial UHPC mixes have become available worldwide. However, due to the high cost of proprietary mixes, researchers have worked to develop non-proprietary UHPC mix designs with local materials. These mixes aim to achieve comparable strength and durability properties at a fraction of the cost of the proprietary UHPC mixes for realistic implementation on a state-by-state basis.

The first prestressed concrete bridge application in Texas was a post-tensioned, cast-in-place slab span of the San Bernard River Bridge that was built in Austin County in 1952. In 1957, the first precast, pretensioned concrete beam was completed on the Texas and New Orleans Railroad Overpass in Kennedy, Texas (Farris and Bettis 2019). The first

major prestressed project followed shortly after on the Corpus Christi Harbor Bridge, in Nueces County in 1959, and had the first precast, post-tensioned beams of 40 and 60 ft (12.2 and 18.3 m) (Jensen 2015). Advancements in construction, cost, and safety features in prestressed bridges led to widespread implementation in the 1980s. Prestressed concrete revolutionized bridge construction by increasing member strength, allowing longer span lengths, and minimizing costs. By introducing UHPC into these prestressed bridge applications, the goal is to continue increasing member strength and span lengths while also providing a longer service life with exceptional durability properties.

The knowledge on UHPC durability, thus far, is primarily based on research performed on proprietary UHPC. UHPC consists of fine particles, ranging from very fine cement to sand, that produces an optimum particle packing density. The densely packed particles combined with low water content leads to a dense microstructure and low permeability, which is indicative of increased durability. Because of that, this material is desirable for critical infrastructure projects like bridges. The most popular application of UHPC in bridges thus far has been for structural connections because the increased bond strength allows a short anchorage length and reduction in clear cover (Sritharan 2015). A stronger connection paired with better durability would mean increased time until repair and a decreased failure potential at that location. In UHPC overlay applications, a low permeability would limit the deterioration from deicing salts or freeze-thaw damage. A detailed durability study covering non-proprietary UHPC mixes, thus, becomes a necessity. Because permeability directly impacts durability, determining cost-efficient and accurate practices to measure this property will aid in further implementation of UHPC.

Such practices will also facilitate the study of the permeability properties of non-proprietary UHPC mixtures.

A detailed durability study through laboratory testing is needed for non-proprietary UHPC mixes to determine if local materials can provide comparable durability to proprietary UHPC mixes. To address this issue, durability testing, as it relates to permeability, will be a prime focus for this research. Using more advanced techniques like resistivity, pore solution resistivity (PSR), and formation factor, the susceptibility of non-proprietary UHPC mixtures to chloride penetration can be evaluated. In addition, abrasion testing can evaluate the wear and skid resistance property of mixes to ensure superior non-proprietary UHPC mixes.

1.2. Significance

Based on research on proprietary UHPC durability to date, UHPC is considered a long-lasting and durable concrete. However, a systematic and detailed durability study covering all aspects of durability using conventional as well as advanced techniques has not yet been reported. This research provides a systematic evaluation of relevant durability properties, primarily through evaluation of permeability of non-proprietary UHPC mixes made with local Texas materials using both existing as well as advanced test methods. ASTM C1202 (2017), *Standard Test Method for Electrical Indication of Concrete's Ability to Resist Chloride Ion Penetration*, also known as the rapid chloride penetration test (RCPT) has been widely considered to characterize concrete permeability as a conventional test method. Permeability measurement using the resistivity method has recently been developed, and the Florida and Louisiana Departments of Transportation

(DOTs) have implemented this method for quality control of paving concrete (AASHTO PP84 2018; Nassif et al. 2015). Research is underway to implement this method for bridge deck concrete (Nassif et al. 2015; TxDOT Project 0-6958 8/2020). Resistivity can provide a measure of permeability in a relatively short time, offer a cost-effective solution, and provide a user-friendly technique compared to the conventional RCPT method. Recently, using the formation factor, a parameter derived through normalizing bulk resistivity by PSR has been gaining importance as an effective way to measure permeability, the diffusion coefficient, and predict service life (Spragg et al. 2019). Resistivity and formation factor have yet to be applied to non-proprietary UHPC mixes, and there has been minimal research for proprietary mixes.

The application of UHPC in bridge superstructures, particularly non-proprietary UHPC, has limited implementation in the United States (US). Using the formation factor, service life estimations for non-proprietary UHPC mixes can provide an initial understanding of the durability performance of UHPC bridge superstructures. Further service life estimations using well-known software can provide a more thorough understanding of UHPC for bridge applications. Using UHPC for girders and decks can extend the service life of structural components. Whereas, those components made of normal strength or high-strength concrete will become the limiting factor as they will require more frequent maintenance. With a UHPC deck replacement or overlay, as shown so far in Iowa, New York, and Delaware, existing bridges can be upgraded with a stronger, more ductile, and less permeable material, thereby increasing the time between required maintenance (FHWA 2019).

1.3. Statement of Objectives and Scope

The objective of the proposed research is to determine durability properties, with a primary focus on permeability, of non-proprietary UHPC mixes, and the resulting improved service life predictions for bridge applications. Specifically, this study focuses on non-proprietary UHPC mixtures developed using locally available materials in Texas. The mixes in this study are intended for precast, pretensioned bridge girder applications, and performing detailed permeability measurements, as a major durability performance indicator, will be essential to ensure long-lasting, durable UHPC mixtures and explore suitable implementation options for UHPC. Resistivity measurements can be used to determine the permeability of a UHPC mix, and the measured resistivity values can be used to calculate the formation factor. The formation factor is then applied in the service life estimation to quantify the benefits of using UHPC for precast, pretensioned bridge applications in Texas, and further confirmed through software predictions. The applicability of the software to UHPC is addressed. It is anticipated that UHPC will offer longer service life because of superior durability and ensure long-lasting, durable bridges.

1.4. Research Tasks

1.4.1. Background and Literature Review

The literature review includes a summary of current UHPC bridge applications, a state-of-the-art section on the relevant and available studies on the selected topics of research, and evaluation of other non-proprietary mixture designs. Strides have been made to use UHPC in overlays, connections, and girders, in an effort to extend the service life of

bridges in the US. These UHPC applications have, primarily, utilized proprietary mixes. The state-of-the-art review summarizes the durability testing performed for proprietary and non-proprietary UHPC mixtures, while also including comparative information to NSC, HPC, and SCC. Other useful sources cover the relevant pore solution characterization techniques, formation factor calculation, and service life estimations. Limitations of software modeling capabilities for UHPC service life predictions, due to the significant differences between UHPC and conventional concrete, are identified. Several state Departments of Transportation (DOTs) have developed their non-proprietary UHPC mixes, and a discussion on their mixture proportions and intended use in bridge applications is provided.

1.4.2. Select Non-Proprietary UHPC Mix Designs

The non-proprietary mix designs selected for this research include local Texas materials. While the development of each UHPC mixture is not in the scope of this thesis research, a summary of the UHPC mix proportions developed as part of a larger study are provided. The cement, fly ash, and silica fume characteristics are included as needed for the pore solution characterization. A summary of the materials includes a Type I/II cement, silica fume, Class F fly ash, river sand finer than 0.05 in. (No. 16 sieve), high range water reducer (HRWR), and steel fibers.

1.4.3. Laboratory Testing to Determine Durability

The following tests were performed in the laboratory or through subsequent calculations to determine the durability of the selected mixes. Where ASTM C1856 (2017) for UHPC

testing provides modifications to standard tests, these modifications are implemented accordingly. A summary is found in Table 1.1.

Table 1.1. Summary of Durability Testing for Non-Proprietary UHPC

Test Name	Standard	ASTM C1856 (2017) Modification
Rapid Chloride Ion Penetration (RCPT)	ASTM C1202 (2017)	Yes
Bulk Resistivity	ASTM C1876 (2019)	No
Surface Resistivity	AASHTO T358 (2017)	No
Pore Solution Resistivity and Formation Factor	ASTM C1876 (2019); AASHTO PP84 (2018)	No
Abrasion Resistance	ASTM C944 (2012)	Yes

Surface and bulk resistivity were measured for each mix to determine if the UHPC mix designs have significantly different permeability properties. These measurements were validated by the more conventional method for permeability indication, RCPT. Abrasion resistance testing was performed to determine the wear resistance on select surfaces of the mixes with steel fibers. By changing the surface preparation, a more thorough representation of UHPC wear behavior is made. The pore solution is unique to each mix because it is formed from a combination of the cementitious ions and water used in mixing. Two of the three methods for pore solution characterization, per AASHTO PP84 (2018) or ASTM C1876 (2019), are used, and the formation factor is calculated for each mix. The formation factor is a parameter calculated as the ratio of bulk resistivity,

found from ASTM C1876 (2019) testing, to pore solution resistivity, found from AASHTO PP84 (2018) or ASTM C1876 (2019). It provides a numerical quantification to the pore size and tortuosity in the system (Layssi et al. 2015). By performing these detailed tests, this research aims to determine if these non-proprietary UHPC mixes have comparable permeability properties to proprietary mixes while also providing a better understanding of using resistivity and the formation factor for UHPC.

1.4.4. Service Life Evaluation

With the formation factors, a service life estimate for each non-proprietary mix is initially made using the error function to Fick's second law. This equation only provides an initial estimation for service life because of the assumptions associated with it, and further service life predictions are explored using service life modeling software. ConcreteWorks (Riding et al. 2017) and Life-365 (Ehlen 2018) are the two software programs used in this research with the latter undergoing more extensive use. However, this software package has limited applicability to UHPC, and a thorough discussion on those limitations is required before use. By highlighting the current software limitations, this study aids in outlining the necessary considerations required before applying to UHPC. Once the applicability of UHPC in Life-365 is understood, the formation factors can be used for a simulation of a bridge deck and girder. A comparative assessment is made to other mixes used in similar structural applications like self-consolidating concrete (SCC), high-performance concrete (HPC), or conventional precast concrete (PC). Supplementary evaluations are made for service life in different regions of Texas to reflect the various temperature and exposure conditions. Non-proprietary UHPC for bridge applications has

limited implementation to date in the US, and this evaluation provides a quantifiable comparison to advocate for non-proprietary UHPC use in pretensioned bridge girders. Based on these results, additional recommendations are made for durability quality and prestressed bridge applications.

1.4.5. Summary and Conclusions

The first objective of this study was to determine the permeability of non-proprietary UHPC mixes through bulk resistivity, surface resistivity, and rapid chloride ion penetration testing. Abrasion resistance testing was performed as a supplemental study. A pore solution resistivity was determined for each mix studied, and through that, a formation factor value was calculated. Using the error function solution to Fick's second law, an initial service life estimation is made for the non-proprietary UHPC mixes and later assessed through Life-365 predictions. The Life-365 estimations are compared to that of other mixes used in similar applications. The conclusions from the Life-365 and the laboratory study are summarized to determine durability and service life the benefits of using non-proprietary UHPC for pretensioned bridge girders. Finally, recommendations are provided for future research.

1.5. Outline of Thesis

There are six primary sections outlined in this thesis.

- Section 1 provides the background, significance, objectives, and scope of the research.

- Section 2 includes a comprehensive literature review of recent UHPC bridge applications, the durability of UHPC in terms of permeability and abrasion resistance, current and standardized practices for durability testing, service life estimations, and a summary of the state DOT non-proprietary mix designs and their intended use for bridges.

- Section 3 presents the non-proprietary mix designs studied and the characteristics of the selected materials, testing procedures, and equipment setups used.

- Section 4 includes the results of the durability testing for resistivity, RCPT, abrasion resistance, the pore solution characterization methods, and calculated formation factor values.

- Section 5 presents the service life prediction results and evaluation from the error function solution to Fick's second law and Life-365.

- The final section, Section 6, consists of the summary, conclusions, and future research recommendations.

2. LITERATURE REVIEW

2.1. UHPC for Bridge Applications in the United States

Between 2006 and 2019, there have been over 250 UHPC bridge applications in the US (FHWA 2019). These applications include connections, components like girders and decks, overlays, and repairs; however, the most popular use of UHPC in US bridges is for structural connections (Sritharan 2015). The following sections summarize select UHPC applications in the US.

2.1.1. Prestressed UHPC Girders

The first UHPC superstructure bridge in the United States was the Mars Hill Bridge in Wapello County, Iowa, completed in 2006 using the proprietary mix Ductal® (Graybeal 2009). Sritharan (2015) notes that while the design was conservative, costs were kept low, and the three-girder bridge was ultimately successful. A modified Iowa DOT bulk tee C-beam shape with additional prestressing satisfied the design requirements with the number of 0.6 in. (15 mm) strands increasing from 22 to 49. The author noted that the relatively high tensile strength and prestressing resulted in the elimination of the transverse reinforcement, decreased girder depth by 6 percent, increased span length by 37 percent, and thereby allowed a single span rather than a two-span bridge.

Graybeal (2009) summarized the second UHPC superstructure bridge constructed in 2008 in Richmond County, Virginia, named the Cat Point Creek Bridge. One of the ten

spans used a Ductal® UHPC Virginia BT-45 girder without any modifications to the cross-section and eliminated all mild shear reinforcement.

The first UHPC pi-girder bridge constructed in the US was the Jakway Park Bridge, built in late 2008 in Buchanan County, Iowa, using Ductal® proprietary UHPC. Bierwagen et al. (2010) described the second-generation pi-girders in the center span as 51 ft 2 in. (15.6 m) long with a design compressive strength of 21.5 ksi (148 MPa). Modifications from the first generation girder were required and included adding 5 and 8 in. (127 and 203 mm) radii to the web and deck connection, increasing the interior deck thickness between the webs to 4-1/8 in. (105 mm), decreasing the web spacing by 4 in. (100 mm), including mild reinforcement in the deck, and using grouted reinforcement pockets at 18 in. (457 mm) spacing (Bierwagen et al. 2010). The Massachusetts Institute of Technology (MIT) and the FHWA collaborated to develop these girders (Ulm 2004).

Giesler et al. (2018) worked to implement non-proprietary UHPC prestressed girders for a bridge in New Mexico. These girders were adapted to full-scale girder designs that were tested in a lab facility. Results indicate that their implementation is not far away.

2.1.2. K-UHPC Bridge

In 2015, Buchanan County, Iowa, constructed another UHPC bridge named the Hawkeye Bridge or the Deacon Avenue Bridge. The Korea Institute of Civil Engineering and Building Technology (KICT) developed a proprietary mix called K-UHPC, and this was the first bridge in the US to use this brand of UHPC (Kim 2016). There are strict guidelines to meet the mix requirements. The author states the silica fume must have a surface area larger than 23,250 in^2/g (150,000 cm^2/g) and silicon dioxide (SiO_2) content above 96

percent. The two types of steel fibers have lengths of 0.63 in. (16 mm) and 0.79 in. (20 mm), and both have a diameter of 0.0079 in. (0.2 mm). Shrinkage is controlled by a glycol-based reducing agent and a calcium sulfa aluminate-based expansive agent (Kim 2016). The K-UHPC girders are prefabricated second-generation pi-girders. These girders are 52 ft (15.8 m) long, 5 ft 4 in. (1.6 m) wide, and 2 ft 4 in. (0.7 m) deep. Seven 0.6 in. (15 mm) diameter longitudinal strands ran in each of the bottom flanges of the 12 girders, and three 0.6 in. (15 mm) transverse strands ran in the middle of each of the crossbeams.

2.1.3. UHPC Overlays

Significant work has been done in Europe, notably Switzerland, since the mid-2000s for UHPC overlay application. In 2005, a bridge over the River la Morge, near Sion, Switzerland, was outfitted with the first UHPC overlay (Denarié 2005). Five years later, a more challenging project on a high traffic road that serviced more than 20,000 vehicles per day per lane, with a 5 percent slope used UHPC to reduce traffic delays to 14 days and reduce construction costs by 30 percent compared to conventional rehabilitation methods (Brühwiler and Denarié 2013). In 2014 and 2015, a 1.7 in. (45 mm) UHPC overlay was applied to the Chillon Viaduct on the border of Lake Geneva (Bernardi et al. 2016). The authors summarized that during the 11-week project, up to 105 cubic yards (80 cubic meters) were cast per day to cover the 1.3-mile (2.1 km) road. More than 20 overlay applications have been applied in Switzerland to rehabilitate old bridge decks (Brühwiler and Denarié 2013). Implementation of UHPC overlays in the US began more recently.

Haber et al. (2017) reported on field testing results of UHPC overlays. The authors found a decrease in the dead load and overlay thickness. They also report that typical

concrete overlays are between 2.5 in. (64 mm) and 6 in. (152 mm) thick with a dead load of 30 to 75 psf (1.4 to 3.6 kPa). UHPC components are typically thinner making them more lightweight, with a thickness of 1 to 2 in. (25 to 51 mm) and a dead load of 12 to 26 psf (0.6 to 1.2 kPa).

In 2016, the Mud Creek Bridge in Buchanan County, Iowa, was selected to receive a UHPC overlay. It was built in the 1960s and is 100 ft (30.5 m) long and 28 ft (8.5 m) wide. Wibowo and Sritharan (2018) describe the replacement of the deck with a specific mix commercially known as Ductal® NaG3 TX. The authors reported that after a year of evaluation, the 1.5 in. (38 mm) UHPC overlay added more ductility and did not display any issues with the surface or interface bond.

The Blackbird Station Road Bridge in Townsend, Delaware, was the second bridge in the US to receive a UHPC overlay in 2017 (Dean et al. 2019). The authors note that Switzerland established a minimum UHPC overlay depth of 1 in. (25 mm), and due to unexpected camber differences, the Delaware DOT decided to decrease the thickness to between 3/4 in. (13 mm) and 1 in. (25 mm). This overlay was applied in two segments over two days. Since completion, the bridge has been inspected yearly, and the durability reports are positive. Chain-dragging and sounding hammers were used to check for delamination in addition to visual inspection (Dean et al. 2019). The report states that visual inspection detected no cracking or deterioration on the surface, and the difference in the two segments is indistinguishable. Additionally, there is no indication of delamination between the overlay and beams.

The Iowa DOT placed its second UHPC overlay on a bridge over the Floyd River in Sheldon, Iowa, in 2018 (WALO USA 2018). The 205 ft (62.5 m) long and 44 ft (13.4 m) wide bridge deck received a 1-3/4 in. (44 mm) thick overlay of Ductal®. It took ten days to pour a total of 9020 square feet (838 square meters) of concrete.

According to FHWA (2019), two additional UHPC overlay projects are complete. Three bridges on Route 17B in Callicoon, New York, and the State Route 1 at Bower Beach Road in Frederrica, Delaware, received UHPC overlays in 2019.

2.2. State-of-the-Art

The following section includes a comprehensive literature review for the tests discussed in the previous sections and introduces the available service life modeling. The parameters incorporated in the models are discussed.

2.2.1. UHPC Durability Characteristics

The durability of UHPC is better understood when compared to other classes of concrete. Ahlborn et al. (2008) summarized the durability characteristics of normal strength concrete (NSC), high-performance concrete (HPC), and proprietary UHPC based on prior literature. In RCPT, there are five classifications for chloride ion penetration that are ranked from lowest to highest: negligible, very low, low, moderate, and high. NSC typically has a low, moderate, or high chloride penetration rating and measures above 2000 Coulombs. HPC performs slightly better at 500 to 2000 Coulombs, which falls in the very low or low classification. UHPC exhibits a negligible chloride penetration rating with less than 100 Coulombs. Diffusion coefficients for each are also different. NSC

typically has an average diffusion coefficient of 1.55×10^{-9} in^2/s (1.0×10^{-12} m^2/s), HPC with

7.75×10^{-10} in^2/s (5.0×10^{-13} m^2/s), and UHPC with 3.1×10^{-11} in^2/s (2.0×10^{-14} m^2/s). Other

durability test comparisons are available. However, these tests were not part of the

research scope for the current study. The authors included freeze-thaw, air permeability,

water absorption, and scaling resistance comparisons. UHPC statistically performs the

best in all categories, followed by HPC and then NSC.

Thomas et al. (2012) studied chloride ingress for UHPC and HPC in Treat Island,

Maine. The chloride penetration depth on HPC and UHPC specimens were measured. The

HPC specimens had a measured chloride depth up to 0.91 in. (23 mm), while UHPC

specimens recorded less than half that with up to 0.39 in. (10 mm). The authors explained

that due to the discontinuous pore structure, which gives UHPC superior performance,

pores at the surface are unlikely to form a connection more than a few millimeters deep.

Thus, keeping chloride damage from reaching important reinforcement features.

Additionally, UHPC has been used for the rehabilitation of reinforced concrete

structures to increase durability. The positive durability properties of proprietary UHPC

are exploited under extreme environmental conditions, like de-icing salts and marine

environments, and mechanical loadings, like concentrated forces and fatigue impact

(Brühwiler and Denarié 2013). The authors also note, that for the crash barrier parts,

UHPC provides lower permeability and less ingress of water.

2.2.2. Rapid Chloride Penetration Tests (RCPT)

The rapid chloride penetration tests measure the charge passed through a sample and

classify the charge to one of five classifications. UHPC typically falls in the least

permeable category, which is negligible. Although ASTM C1202 (2017) states the test is not valid for longitudinal steel reinforcement, researchers have used steel fibers in their testing despite the potential for a conductive path to be created between the two ends. The following sections provide a summary of their results.

2.2.2.1. Proprietary UHPC Mixes

Graybeal (2006) tested Ductal® specimens with steel fibers at 28 and 56 days for RCPT charge passed values. There were four different curing conditions: steam treatment, tempered steam, delayed steam, and untreated or ambient air. For the steam treatment regime, four hours after demolding, specimens were subjected to 194°F (90°C) steam at 95 percent relative humidity for 48 hours. Tempered steam specimens followed the same method as the steam treatment, except 140°F (60°C) steam was used instead. Delayed steam also followed the steam treatment regime, except treatment begins 15 days after casting instead of four hours. The untreated or ambient air specimens were left to cure in the lab environment from casting until testing. The author evaluated the chloride ion penetrability ranges based on the classification provided in ASTM C1202 (2017). The author discovered that all steam curing regimes, except the steam treatment, which was only tested at 28 days, produced a negligible chloride ion penetrability at both 28 and 56-days. The untreated ambient air regime produced a very low chloride ion penetrability result at 28 days, and a negligible chloride ion penetrability result at 56 days.

Ahlborn et al. (2008) also studied the Ductal® mixture under three different curing and testing age regimes. Even with steel fibers, the system measured in the negligible range, meaning less than 100 Coulombs charge passed. The thermally treated specimens

had lower charges than the air-cured specimens. The authors further indicated that UHPC mixes with higher amounts of silica fume produced lower charge passed than mixes with lower silica fume contents.

Haber et al. (2018) studied six proprietary mixes from Europe, the US, and Canada containing 2 percent by volume steel fibers. Mix U-A is a US laboratory-developed mix, U-B and U-C are from a European supplier, U-D is a US based subsidiary mix from a multinational corporation, and U-E originates from Canada. While ASTM C1202 (2017) and the ASTM C1856 (2017) modification do not allow for metallic fibers, the authors determined that the fiber presence only significantly affected results for mix U-B. Because UHPC is typically in the negligible range in terms of chloride ion penetrability, very high charge measurements, 5100 Coulombs for 28 days, and 2501 Coulombs for 56 days, from U-B specimens were disregarded. The authors determined that the steel fiber presence increased the standard deviation between the two specimens in each test group. All mixes experienced a decrease in charge passed results from 28 to 56 days. Table 2.1 provides a summary of the results from the proprietary UHPC research.

Table 2.1. RCPT for Proprietary UHPC

Mix	Age (days)	Ahlborn et al. (2008)		Graybeal (2006)				Haber et al. (2018)
		AA	TT	AA	TS	DS	S	LSWB
U-A	28	-	-	-	-	-	-	302
	56	-	-	-	-	-	-	53
U-B	28	-	-	-	-	-	-	5100
	56	-	-	-	-	-	-	2501
U-C	28	-	-	-	-	-	-	425
	56	-	-	-	-	-	-	298
U-D	7	-	10	-	-	-	-	-
	28	75	15	360	39	18	18	789
	56	-	-	76	26	-	-	495
U-E	28	-	-	-	-	-	-	470
	56	-	-	-	-	-	-	303

Notes:
1. Unit is Coulombs
2. U-A: US laboratory developed mix
3. U-B: U-C: European supplied mix
4. U-D: US subsidiary of a multinational corporation
5. U-E: Canadian supplied mix
6. AA: Ambient air
7. TT: Thermally treated
8. TS: Tempered steam
9. DS: Delayed steam
10. S: Steam
11. LSWB: Lime saturated water bath

2.2.2.2. Non-Proprietary Mixes

Alkaysi et al. (2016) studied non-proprietary mixes from Wille and Naaman. These mixes varied cement type and quantity of silica powder to create nine mix designs. The cement types included white cement, Type V cement, and a blend of Type I and ground granulated blast furnace slag (GGBS), and the silica powder quantities are 0, 15, and 25 percent. Silica fume and steel fiber content remained constant at 25 and 1.5 percent, respectively. The authors intended to determine the effect of the varying parameters on permeability using RCPT measurements. Only two mix designs resulted in a negligible rating at 28 days. The Type V cement with 0 percent silica powder performed the best, at 57

Coulombs, followed by the white cement with 25 percent silica powder, at 89 Coulombs. The blend of Type I cement and GGBS had the same value of 137.5 Coulombs for 0 percent and 25 percent silica powder. Other mixture values measured between 229 and 939.5 Coulombs. The authors determined that the effect of the parameters was ultimately unclear, and attributed this to all mixes still being close to the optimum particle packing density. Although there was minimal change between data, it was found that increasing the silica powder content increased permeability, which conflicts with those results found by Ahlborn et al. (2008). However, the authors were able to conclude the mix designs containing the GGBS replacement offer better overall resistance to chloride-ion penetration regardless of silica powder content.

Berry et al. (2017) also found promising results for their mix design. The two samples measured charge passed values of 75 and 56 Coulombs at 56 days. These values fall in the negligible chloride ion penetration range based on the ASTM C1202 (2017) classification. Steel fibers were present during their test. However, the authors considered the test valid.

2.2.2.3. Self-Consolidating Concrete (SCC)

TxDOT Report 0-5134-2 by Trejo et al. (2008) studied 12 SCC mixes with two release strengths, two different aggregates, and three volumes of coarse aggregates. These mixes were compared to four conventional PC mixes from Texas. The RCPT results from these mixes can serve as a comparison to UHPC for prestressed bridge applications. There were three specimens tested for each age for each mix. SCC mixes containing river gravel with 16-hour target compressive strengths of 5 ksi (34.5 MPa) rated low to very low in the

chloride ion penetration range at 28 days. In contrast, the mixes having 16-hour target compressive strengths of 7 ksi (48.3 MPa) performed slightly worse with more results in the low classification at 28 days. All mix designs rated as having very low chloride ion penetration at 56 days.

Comparatively, the limestone SCC mixes with 5 ksi (34.5 MPa) 16-hour compressive strength showed results both in the low and very low chloride ion penetration range, and mixes having 7 ksi (48.3 MPa) 16-hour compressive strength still rated in the low chloride ion penetration range at 28 days. At 56 days, all mixtures rated in the very low range similar to those found with the river gravel mixes.

At 28 and 56 days, the conventional PC mixes for 5 ksi (34.5 MPa) with river gravel and 7 ksi (48.3 MPa) with limestone measured in the low range. For the 5 ksi (34.5 MPa) limestone mix, all samples measured in moderate at 28 days and decreased to low at 56 days. The 7 ksi (48.3 MPa) river gravel mixture measured very low at 28 and 56 days. Figure 2.1 provides a summary of the average RCPT results from the literature along with their respective chloride ion penetration classification. The SCC and conventional PC mix values are at 56 days. The gray shading indicates the relevant classifications of chloride ion penetration (negligible, very low, and low) based on the RCPT results.

Figure 2.1. Charge Passed for Non-Proprietary UHPC, SCC, and Conventional PC Mixes

2.2.3. Resistivity

Resistivity is a fast and cost-efficient way of estimating the permeability of hardened concrete. This section elaborates on the background, UHPC research, and applications.

2.2.3.1. Background

Spragg et al. (2013) studied the factors affecting electrical resistivity measurements in conventional cementitious systems. The authors found that sample geometry, temperature,

and curing affect the pore structure, degree of saturation, and degree of hydration. As temperature increases, ion movement increases in the pore solution, which causes a decrease in the resistivity. Additionally, the authors determined that specimens sealed for curing and testing displayed higher resistivity values than the specimens sealed during curing only. When the resistance is measured instead of the resistivity, a sample geometry correction factor k is used. The k value depends on the type of resistivity test, electrode spacing, and specimen geometry. The temperature during testing influences the ion movement. Therefore, the authors proposed an equation based on the Arrhenius law that converts the resistivity at the testing temperature to the resistivity at 23°C (73.4°F). Sealed samples were found to have higher resistivity as the degree of hydration increases.

Layssi et al. (2015) expand on those factors discussed by Spragg et al. (2013). Temperature fluctuations in the sample and environment can increase or decrease ion movement, which directly impacts the resistivity reading for conventional concrete. When temperatures increase, ion movement increases, and resistivity values decrease. A low resistivity value indicates a higher permeability, which may not be the case when recorded at appropriate testing temperatures in ASTM C1876 (2019) or AASHTO T358 (2017). Layssi et al. (2015) explain that changing the temperature by 1.8°F (1°C) can change the resistivity measurement by 3 percent. When measuring resistivity, the sample needs to be in saturated surface dry (SSD) conditions, and the authors state the sample's degree of saturation will determine the amount of liquid in the pore network. The measurement equipment should use a signal frequency between 0.5 and 1.0 kHz. The authors explain

that this range typically gives an accurate representation of the sample's resistance, and any frequency below 0.5 Hz will give overestimated results.

AASHTO T358 (2017) and AASHTO PP84 (2018) have a table correlating RCPT and resistivity. The applicability of these limits for UHPC needs to be verified, which is beyond the scope of this study. Spragg et al. (2013) summarize why there is a big push to use resistivity measurements instead of RCPT. When compared to the testing and specimen preparation time for ASTM C1202 (2017), resistivity is a quick, nondestructive test that provides results in minutes. In a study performed by the Louisiana Department of Transportation (LaDOT) by Rupnow and Icenogle (2011), the ASTM C1202 (2017) procedure requires an initial equipment cost of $18,000 and 8 hours of technician hours per test. On the contrary, surface resistivity testing equipment has an initial cost of $2,800 with 0.33 technician hours per test. The LaDOT aimed to replace RCPT with surface resistivity, and within the first year, estimated saving $101,000 in personnel costs (Rupnow and Icenogle 2011). The authors have also suggested that using surface resistivity for quality control could result in savings of $1.5 million per year for contractors on a state level.

2.2.3.2. UHPC Resistivity Results

Haber et al. (2018) studied resistivity for five proprietary mixes from Europe, the US, and Canada. The presence of steel fibers is not allowed by AASHTO T358 (2017), the newer surface resistivity standard, because it can cause a higher standard deviation amongst the measured values, and the presence of steel fibers can give an inaccurate reading. Despite this concern, these mixes used 2 percent by volume steel fibers in the 4x8 in. (100x200

mm) cylinders, and the authors concluded including metallic fibers in the sample is only possible if they do not create a conductive path. The authors were able to establish that the surface resistivity values measured correctly correlated to the RCPT results.

Haber et al. (2018) measured resistivity values until 56 days for 4x8 in. (100x200 mm) cylinders. At seven days, all specimens for U-A, U-C, U-D, and U-E were in the moderate range. At 14 days, these specimens moved to the very low range, except those for U-A. Values for U-A, exceed 254 kΩ-cm and are classified as negligible. By 56 days, mixes U-C, U-D, and U-E are still in the very low category, and Mix U-A continued further into the negligible range.

2.2.3.3. Applications

Layssi et al. (2015) also discussed the applications of resistivity. As stated previously, it can be compared to the popular RCPT because there is an inverse relationship between the charge passed and resistivity. There is a similar inverse relationship between resistivity and corrosion. A linear relationship exists between resistivity measurements taken from a saturated surface dry (SSD) sample and the Nernst-Einstein equation. This equation describes the diffusion coefficient. The authors comment that resistivity can also detect cracks. When cracks initiate and propagate, the pore connectivity alters, and such changes will cause the resistivity measurement to change.

2.2.3.4. Pore Solution Resistivity (PSR)

Earlier, it is mentioned that PSR needs to be determined in order to calculate the formation factor. PSR either needs to be measured experimentally or estimated by applying predictive models. The National Institute of Standards and Technology (NIST) model,

while efficient to use because it only requires the mix proportions and material chemical composition, has limited accuracy. One assumption is that the sodium (Na^+) and potassium (K^+) alkali free factor is 75 percent, which can lead to errors in mixes containing fly ash (NIST 2017). Tanesi et al. (2019) reported a 60 percent error in pore solution resistivity values using this model. When cement contacts water, the cement releases positive and negative ions, typically potassium, sodium, calcium, hydroxide, and sulfate, and the resulting ion and water combination is unique to the mix. Correctly characterizing the pore solution of UHPC can be difficult due to the high packing density. Thus, additional characterization methods have been proposed by several researchers (Spragg et al. 2013). Tanesi et al. (2019) adopted a curing and conditioning method called the bucket test. In this method, samples are submerged and cured in a synthetic solution with a known resistivity value instead of in the moisture room or lime-saturated water bath, as is recommended in AASHTO T358 (2017) and ASTM C1760 (2012). After conditioning and allowing the content to reach equilibrium, the resistivity of the specimen solution and the synthetic solution is assumed to be equal. The authors argue that this method resolves the alkali leaching and simplifies pore solution resistivity measurements. However, the authors noted that the accuracy of this method is dependent on how different the actual specimen pore solution resistivity value is from the synthetic solution.

2.2.4. Formation Factor

As described by Spragg et al. (2013), the formation factor is the inverse of porosity and connectivity, aims to characterize the resistance to chloride ion penetration, and can quantify the microstructure. It is the ratio of bulk resistivity to pore solution resistivity or

26

the ratio of the self-diffusion coefficient to the diffusion coefficient (Spragg et al. 2013).

Higher formation factor values will indicate low porosity and connectivity and slow ion

movement. Formation factor equations are presented as Equation (2.1) (Snyder 2001):

$$F = \frac{1}{\phi\beta} = \frac{\rho}{\rho_o} = \frac{D_o}{D}$$

(2.1)

Where:

ϕ	=	Porosity
β	=	Connectivity
ρ	=	Bulk resistivity (kΩ-cm)
ρ_o	=	Pore solution resistivity (kΩ-cm)
D_o	=	Chloride ion self-diffusion coefficient (in^2/s)
D	=	Diffusion coefficient (in^2/s)

The formation factor can directly relate to the durability of a system because it

quantifies the pore connectivity, and was used to define the durability of proprietary

UHPC mixes by Spragg et al. (2019). Multiple proprietary UHPC mixes, without steel

fibers, were studied. The cast cylinders are placed in a storage solution of known

resistivity, as described by Tanesi et al. (2019). Resistivity measurements on the cylinders

are taken periodically. The proprietary UHPC mixes were compared to two other mixes

used in similar applications. The first mix has a *w/cm* of 0.35, 3 percent entrained air, 30

percent paste volume, and Type I/II cement. This mix is a precast type concrete with a 28-

day compressive strength of 7.5 ksi (52 MPa). The second is a non-shrink cementitious

grout with water to solids ratio of 0.16 and compressive strength of 8.6 ksi (59 MPa). For

the UHPC mixes, a formation factor ranging between 39,000 and 130,000 was calculated

at 28 days. The authors noted that such a broad range could be indicative of particle packing effectiveness, *w/cm*, or cementitious chemistry. With values this high, it is difficult to conclude that one mix performs significantly better than the other. The average formation factor values were 7820 and 79,400 at 7 days and 28 days, respectively. Both comparison mixes have a formation factor of less than 1000 at 91 days. Overall, conclusions indicate that at 28 days, the proprietary UHPC mixtures have a significantly higher formation factor than common cement-based materials.

2.2.5. Chloride Service Life Prediction Models

Service life models for concrete account for varying factors in the environment, structural component, location, and design to estimate the chloride initiation and propagation periods. Other calculations using the formation factor can provide an initial estimate of service life. The capabilities and limitations of two commercial software packages in terms of estimating the service life of UHPC structural components are discussed in the following sections.

2.2.5.1. ConcreteWorks

ConcreteWorks is a software program developed by the Center for Transportation at the University of Texas at Austin and sponsored by TxDOT (Riding et al. 2017). The software provides a feature that estimates the chloride service life based on structural component type, location, mix design, and various input parameters. The model is based on Fick's second law and assumes that diffusion is the only form of chloride ingress (Riding et al. 2017). Riding et al. (2017) also explains that the software assumes the concrete is uncracked during corrosion initiation, and once the designated chloride concentration is

reached, corrosion occurs at a linear rate. For prestressed concrete, service life is equal to the time it takes to reach the chloride threshold, which means prestressed concrete will only register a service life for the chloride initiation period, while reinforced concrete will register the initiation plus the propagation period. ConcreteWorks limits the model to a 100-year prediction for mass concrete and 75 years for bridge deck concrete. Service life estimations are not available for precast concrete or pavements. Because the service life of proprietary UHPC is expected to exceed 75 and even 100 years, using the service life feature in this software may have limited applicability. Other components that make up the models include the diffusion coefficient, *w/cm*, surface concentration, threshold, and the initial profile.

As concrete ages and hydrates, porosity decreases, the pore structure becomes more discontinuous, and subsequently, diffusion will decrease. The diffusion coefficients are a function of the 28-day old concrete, decay constant, activation energy, universal gas constant, reference temperature, and concrete temperature.

Riding et al. (2017) also describes the effect of water content and supplementary cementitious materials (SCMs) on diffusivity values and how the model can account for these inputs. The authors explain that diffusion increases as the water-to-cement ratio (*w/c*) increases and will decrease as finer SCMs increase the packing density and minimize pore interconnectedness. The model accounts for the SCM replacement of silica fume and fly ash.

Surface concentrations for chloride can be challenging to model for structures with more variable environmental conditions. Those in marine environments are easier to

model than those in decks or parking garages, and the surface concentrations will also vary seasonally (Riding et al. 2017). For example, parts of northern Texas might require deicing during the winter months, which will increase the surface concentration, while during the summer, deicing is unnecessary in the state, and the concentration will decrease. The authors state that ConcreteWorks supports bridges and parking garage structures and define different marine environment types that designate proximity to the ocean. The maximum surface concentration values used in this program are the same as those used in Life-365 (Riding et al. 2017).

The chloride threshold is the chloride value at which corrosion begins. As stated earlier, for prestressed structures, the service life ends at this time due to the consequences of strand corrosion. For reinforced concrete, the service life prediction continues. This threshold must account for those characteristics above and the steel type. A chloride threshold of 0.07 percent was used for mass concrete with black steel and epoxy coated steel, and this value was increased to 0.7 percent for 316 stainless steel (Riding et al. 2017). Calcium-nitrate-based and amines and esters corrosion inhibitors are available in this software, and the associated threshold values are the same as those in Life-365 (Riding et al. 2017).

2.2.5.2. Life-365

Life-365 has a service life prediction model that can predict corrosion initiation, propagation, repair schedule, and life cycle cost (Ehlen 2018). Because Life-365 is typically used for reinforced concrete, and this research is focused on prestressed concrete, only the first sequence is of interest in this study because the service life of prestressed

30

concrete is typically only considered as the initiation phase (Riding et al. 2017). Life-365 describes the initiation period as the time it takes for chlorides from the environment to penetrate the concrete and accumulate at the surface of the steel reinforcement in large enough quantities for corrosion to begin (Ehlen 2018). The authors state that this makes initiation a function of mix design, reinforcement depth, exposure type, temperature, and the chloride threshold concentration. This prediction model also uses Fick's second law as the primary equation and has additional features that account for a reference time, location, structural component, exposure level, clear cover, and mix design in a similar manner as ConcreteWorks (Ehlen 2018). The final service life estimation combines all available factors. One defining limitation for the applicability of this software to UHPC is the inability to model a mix design with *w/cm* lower than 0.25. By the definition of UHPC given by Graybeal (2011), this limitation should exclude all UHPC mixes from modeling. However, Life-365 has an analysis period of up to 500 years and has the potential to offer more insight into service life than ConcreteWorks for UHPC.

2.2.5.3. Error Function Solution to Fick's Second Law

As discussed, results from resistivity, RCPT, and formation factor can all be related, and researchers are now attempting to use the formation factor to calculate service life. Weiss et al. (2018) noted that there is excellent potential to relate these measured and calculated values to long-term durability. As shown in Equation (2.1), the formation factor and self-diffusion coefficient can replace the original diffusion coefficient in the error function solution to Fick's second law using the Nernst-Einstein relationship (Snyder 2001). The prediction equation is presented as Equation (2.2).

$$C_{x,t} = C_o + (C_s - C_o)\left(1 - erf\left(\frac{x}{2\sqrt{\frac{D_o}{F}t}}\right)\right)$$ (2.2)

Where:

$C_{x,t}$ = Chloride concentration at depth x (%)

C_o = Initial chloride concentration (%)

C_s = Surface chloride concentration (%)

x = Depth to reinforcement (in)

D_o = Chloride ion self-diffusion coefficient (in^2/s)

F = Formation factor

t = Time for exposure limit to be reached (s)

Spragg et al. (2019) used the above equation to relate the calculated formation factor to a corrosion initiation estimation for proprietary UHPC and two other mixes used in similar applications. Chloride concentrations, cover depth, and the self-diffusion coefficient are assumed based on literature and the Life-365 chloride model. The authors used the respective values in their calculations: $C_{x,t}$ is 0.05 percent, C_o is taken as 0.02 percent, C_s is 0.5 percent for moderate chloride exposure, x is 2 in. (50 mm), D_o of 2.95x 10^{-6} in^2/s (1.9x10^{-9} m^2/s), and F of 34,500. The formation factor value is conservative and based on the lower bound confidence interval. The authors estimated corrosion initiation for four proprietary UHPC mixes at 210 years. The other two mixes were estimated to have 2.2 and 5.7 years before corrosion initiation. The authors note that while more refinement and work should be done on diffusion predictions, the aim to use formation

factor as a future quality assurance or quality control parameter for construction is promising.

However, Bentz et al. (2014) summarized the applicability of Equation (2.2) to real-world conditions and lists those factors not accounted for that influence service life. The software models, like ConcreteWorks and Life-365, do account for some of these factors. Bentz et al. (2014) summarized that Equation (2.2) assumes the chloride ion diffusion coefficient is independent of outside variables, the chloride surface concentration is constant for the system, and only diffusion ion transportation occurs. In reality, the surface concentration will vary on the structure, the diffusion coefficient will depend on time and depth to reinforcement, and capillary action will enhance ion movement as well as diffusion (Bentz et al. 2014). While the diffusion coefficient is equal to the ratio of the self-diffusion coefficient to the formation factor, the problem remains. Thus, predictions from this equation should be used for comparisons or a guide instead of fact.

Bentz et al. (2014) further highlight how these assumptions could lead to grossly overrated service life. The reinforcement bars highly influence the chloride concentration, and the above formula does not account for their presence. The authors created a model that kept all parameters the same except added a reinforcing bar. It produced a service life that was 12 to 27 percent less than the original value. When a model with a damaged interfacial transition zone between the rebar and concrete was studied, a similar 11 to 23 percent drop in service life was predicted. Chloride thresholds affect the service life outcome even more. The authors report that steel type and coating are significant factors

as the initiation concentration is 4.6 times higher when comparing epoxy coated steel to uncoated. The service life, when including an epoxy coated bar, is five to six times higher than predicted. Fick's second law, ConcreteWorks, and Life-365 operate under the assumption that cracking has not occurred.

2.2.5.4. Modeling UHPC for Service Life

While ConcreteWorks and Life-365 are available for service life determination of concrete components, these programs are limited in terms of ultimately capturing the unique mix design and characteristics of UHPC. These software packages do not have the programming properties to process such low w/cm, lack of coarse aggregate, cement type, or high 28-day compressive strength. Given the mixes studied in this research have one-day compressive strengths between 10 to 14 ksi, system maturation occurs much faster than HPC or NSC. Thus, using the formation factor in the error function solution to Fick's second law can serve as an initial estimation for service life. With the software limitations in mind, further quantification can be made using Life-365 for comparison to concrete that is conventionally used for bridge decks and girders.

2.2.6. Abrasion Resistance

The effect of surface preparation, mix design, and curing regime on abrasion resistance of UHPC is an important consideration for selecting mixtures that will be used for bridge superstructures.

2.2.6.1. Proprietary UHPC Mixes

Graybeal (2006) studied Ductal® and used three cylindrical 6 in. (152 mm) diameter by 3 in. (76 mm) tall specimens from steel molds for each of the four curing regimes in the

study, and the same three specimens per regime were used for each of the studied surfaces. After running the test on the desired surface under a 44 lbf (197 N) load, the damage was removed, and the new surface preparation was put in place. The tested surfaces include steel cast, sandblasted, and surface ground. The surface ground conditions were met using an end grinder. The specimens subject to all types of steam curing performed better than those under ambient air curing, which means steam-treated specimens experienced less mass loss. The authors determined that steel cast surfaces have higher initial abrasion resistance. However, once the cutters damaged the specific type of surface preparation, the specimens behave similarly.

Hartwell (2011) studied the abrasion resistance of Ductal® JS1000 for cast-in-place deck joints. Three different temperatures, four ages, and three surface preparations were studied. The ages include 2, 4, 7, and 28 days. In addition to age, these specimens were cast and cured at three different temperatures: 40, 70, and 100°F (4.4, 21.2, and 37.8°C). The cast 4x8 in. (100x200 mm) cylinders were cut in half at the selected testing age, and the resulting two cylinders produced four surface preparations. The rough surface results from the cast top, the formed surface is in contact with the mold, and the two diamond cut surfaces are from splitting the cylinder. The author found that the diamond cut surface lost the least amount of mass under a 22 lbf (98 N) load. Formed surface results, which came from the surface in contact with the mold bottom, performed worse than the rough surface at an early age and lower compressive strength. However, they performed better at later ages and higher compressive strength. The author attributed the formed surface results to fiber orientation. Fibers are approximately parallel to the surface, and

once the surface is breached, the fibers are more likely to be ripped up. The rough surface, at the top of the specimen, is more likely to have small air bubbles that affect surface performance. A summary of the results is found in Figure 2.2.

Weldon et al. (2010) summarized the comparison between HPC and proprietary UHPC in terms of abrasion resistance. The relative volume loss for an HPC mix with a compressive strength of 8.7 ksi (60 MPa) is 2.75 while the Ductal® mix with 2 percent fibers and cured at 90°C (194°F) has a relative volume loss of 1.2. The HPC experienced more than double the loss when compared to UHPC.

Notes: 1. S: Steam curing   3. TS: Tempered steam curing
        2. AA: Ambient air curing   4. DS: Delayed steam curing

Figure 2.2. Average Mass Loss Per Two-Minute Abrasion Cycle for Ductal®

2.2.6.2. Non-Proprietary UHPC Mixes

Berry et al. (2017) developed a non-proprietary mix and tested abrasion resistance using 22 lbf (98 N) and 44 lbf (197 N) loadings. The 3-1/4 in. (83 mm) rotating cutter per ASTM C944 (2012) was used. The two specimens experienced an average of 0.024 lb (11.1 g) of mass loss under the 22 lbf (98 N) load. With the additional load, 44 lbf (197 N), the specimens averaged 0.061 lb (27.5 g) of mass loss.

2.3. UHPC Mix Designs

2.3.1. Proprietary Mix Designs

Proprietary mixes typically are more expensive than non-proprietary options due to higher steel fiber volumes and less local material use. The proprietary mixes in Table 2.2 can be used as a comparison for those non-proprietary mixes in Table 2.3. In the late 1990s, the Lafarge Research Centre partnered with Bouygues and Rhodia to develop a patent for Ductal® (Batoz and Behloul 2011). Multiple completed bridge projects in the US and Switzerland have used this product (Bernardi et al. 2016; FHWA 2019; WALO USA 2018; Wibowo and Sritharan 2018). K-UHPC was developed by KICT and used in Buchanan County, Iowa, on the Hawkeye Bridge (Kim 2016).

Table 2.2. Proprietary Mix Designs (lb/yd^3)

Name	Ductal®	K-UHPC*
Author	Russell and Graybeal (2013)	Park et al. (2015)
Cement	1200	1329
Silica fume	390	332
Ground quartz	355	-
Quartz sand	1720	1462
HRWR	52	24
Accelerator	51	-
Shrinkage reducing agent	-	13
Expansive agent	-	100
Water	184	311
Steel Fiber (%)	2.5	1.5–2.0

Notes: *An unspecified filling powder makes up an additional 399 lb/yd^3 (237 kg/m^3) and has an average particle size of 10 µm and SiO$_2$ content over 96 percent.

2.3.2. Non-Proprietary Mix Designs

Ongoing research has led to the development of non-proprietary UHPC in multiple states. Development began with the New Mexico DOT for application in prestressed bridges and has since spanned over multiple states with published mix designs (Weldon et al. 2010). Those DOTs with a published non-proprietary mix design have been provided in Table 2.3. Researchers have developed successful UHPC mixes using SCMs like silica fume, silica powder, fly ash, and GGBS.

Table 2.3. Non-Proprietary Mix Designs (lb/yd^3) for State DOTs

State Organization	1	2	3	4	5	6	7		8
Cement	1264	1500	1300	1517	650	1117	1570	1571	1214
Silica fume	158	260	273	280	327	71	304	304	162
Fly ash	158	-	364	-	-	619	-	-	-
GGBS	-	-	-	-	650	-	-	-	588
Silica powder	-	-	-	512	-	-	-	-	-
Sand	1900	1574	1820	1582	1975	1704	1604	1605	1612
HRWR	71	101	59	35	39	20	39	44	56
Water	221	325	312	334	286	288	363	363	310
Steel fibers (%)	1.5	1.8	1.5	2.0	1.5	1.5	2.1	2.1	2.0

Notes:
1. New Mexico DOT (Weldon et al. 2010)   6. Missouri DOT (Khayat and Valipour 2018)
2. Washington State DOT (Qiao et al. 2016)   7. Caltrans (Subedi et al. 2019)
3. Montana DOT (Berry et al. 2017)   8. Nebraska DOT (Mendonca et al. 2020)
4. Colorado DOT (Kim 2018)   9. GGBS: Ground-granulated blast-furnace slag
5. Michigan DOT (El-Tawil et al. 2018)   10. HRWR: High range water reducer

The researchers have developed their non-proprietary UHPC mix designs for different bridge applications. Qiao et al. (2016) worked on developing and testing their selected mix for bridge joint connections applications for Washington State. The work performed by Berry et al. (2017) was essential in developing a mix for the Montana Department of Transportation Bridge Bureau for field-cast joint applications between flanges of adjacent girders and deck panels and girders. In Colorado, the primary objective was developing cost-effective UHPC for joints between precast girders and other bridge members (Kim 2018). Extensive optimization was required in order to get a non-proprietary UHPC mix in Michigan implemented in a bridge rehabilitation project (El-Tawil et al. 2018). Khayat and Valipour (2018) focused on non-proprietary UHPC for bonded bridge deck overlays and determined the minimum thickness for the most cost-

efficient result. Caltrans (California Department of Transportation) wanted a mix to use in connections in seismic regions, and their study effectively provided two promising mix designs that could be used in grouted corrugated duct applications where longitudinal reinforcing bars extending from precast members are anchored in ducts of connecting elements such as footings (Subedi et al. 2019). A non-proprietary mix using local Nebraska materials was, most recently, created for connecting precast superstructure components, and a field-scale connection between two bridge deck panels was cast with the developed mix (Mendonca et al. 2020). The authors note that the panel connection with the non-proprietary mix had comparable structural capacity to that of proprietary UHPC.

3. TESTING PROCEDURES

Several standard test methods can indicate a concrete's susceptibility to chloride ion penetration. These include ASTM C1202 (2017), *Standard Test Method for Electrical Indication of Concrete's Ability to Resist Chloride Ion Penetration*, AASHTO T358 (2017), *Standard Test Method for Surface Resistivity Indication of Concrete's Ability to Resist Chloride Ion Penetration*, and ASTM C1876 (2019), *Standard Test Method for Bulk Electrical Resistivity or Bulk Conductivity of Concrete*. These standards are not applicable to concrete mixtures containing metallic fibers or reinforcing steel. This research also utilizes ASTM C944 (2012), *Standard Test Method for Abrasion Resistance of Concrete or Mortar Surfaces by the Rotating-Cutter Method*, which evaluates the surface preparations and ability to withstand wear resistance. ASTM C1856 (2017), *Standard Practice for Fabrication and Testing Specimens of Ultra-High Performance Concrete*, provides the procedures for UHPC fabrication and necessary modifications to existing test methods. ASTM C1856 (2017) currently has modifications for ASTM C1202 (2017) and ASTM C944 (2012).

3.1. Chloride Ion Penetration (ASTM C1202)

This test is used to determine the resistance of a concrete mixture to chloride-ion penetration by passing an electrical charge through a 2 in. (50 mm) thick cylindrical specimen. The top section of the specimen is exposed to sodium chloride and the bottom section to sodium hydroxide. Using a 60 V direct current (DC), the charge passed after six hours is measured, and the resulting charge directly relates to a chloride penetration

classification. Higher charges indicate more ion movement and chloride penetration. Table 3.1 summarizes the relationship between charge passed and chloride ion penetration class in ASTM C1202 (2017).

Table 3.1. Chloride Ion Penetration Based on Charge Passed (adapted from ASTM C1202 2017)

Chloride Ion Penetration Classification	Charge Passed (Coulombs)
High	>4000
Moderate	2000 – 4000
Low	1000 – 2000
Very Low	100 – 1000
Negligible	<100

Laboratory specimens are prepared and cured in conditions per ASTM C192 (2016). For mixes containing only Portland cement, 28-day moist curing is specified. For mixes, such as UHPC that have SCMs in addition to Portland cement, 56-day moist curing is specified. Because the UHPC mixes used in this study contain SCMs, the extended curing time of 56 days was used. The ASTM C1856 (2017) modification for UHPC indicates that ASTM C1202 (2017) is not applicable for specimens containing metallic fibers due to potential interference with results, and that test specimens be 4 in. (100 mm) in diameter.

A 1.97 ± 0.12 in. (50 ± 3 mm) thick section is cut from the top of a cylinder with a wet diamond or silicon carbide saw. Cuts should be parallel to the top surface, and any

uneven surfaces should be ground away. The specimens are allowed to dry for at least one hour before applying a rapid setting epoxy sealant along the outside surface of the sample. It is necessary to ensure that the sample is evenly coated before leaving to dry. The dry samples are placed on their side so that both ends are exposed, the desiccator is sealed, and the pump is started. For the first three hours, the pressure in the desiccator must be kept less than 50 mm Hg. The de-aerated water is siphoned until the specimens are entirely submerged, and the vacuum is run for an additional hour before turning off the pump and allowing air to enter the desiccator. The specimens are soaked for an additional 18 ± 2 hours.

Before testing, a rubber gasket is placed on the top and bottom of the specimen and mounted into the voltage cells. The cells are clamped together to seal them. Alternatively, a cell sealant is used to mount the specimens but must then be left to dry. The top part of the specimen is exposed to the negative terminal containing 3.0 percent sodium chloride (NaCl) solution, and the bottom to the positive terminal containing 0.3 N sodium hydroxide (NaOH) solution. These cells should remain filled during the testing duration. A 60 ± 0.1 V power supply is applied, and initial measurements are recorded using the Germann Instruments, Inc. Proove'it supply unit and associated software. The ambient temperatures, equipment, and the solution must be between 68 and 77°F (20 and 25 °C) at the start of the test, and ambient temperatures should remain in this range until testing concludes. Current readings are recorded at least every 30 minutes for a total duration of 6 hours. Figure 3.1 shows the complete test setup for RCPT with the cells and equipment and a close-up view of the top of the cell with a thermometer in the NaCl port.

|(a) Rapid Chloride Penetration Equipment | (b) Close-Up View of Cell |
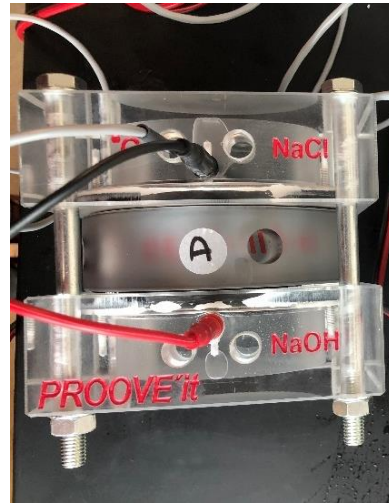
Figure 3.1. ASTM C1202 Test Setup and Cells

3.2. Bulk Resistivity (ASTM C1760; ASTM C1876)

The bulk resistivity test is used to quickly indicate the resistance of concrete to penetration from fluids and other dissolved ions, which is indicative of the pore size and connectivity. Resistivity signifies how a system opposes electrical charge while conductivity, measured in ASTM C1760 (2012), *Standard Test Method for Bulk Electrical Conductivity of Hardened Concrete*, quantifies the strength of an electrical charge that can pass through a system. Conductivity is the reciprocal of resistivity. The test specimens in ASTM C1876 (2019) are soaked in a simulated pore solution of known resistivity for at least six days before testing. In contrast, the ASTM C1760 (2012) curing conditions are the same as ASTM C1202 (2017). An alternating current (AC) passes between the two parallel

surfaces at the top and bottom of the specimen. The resulting potential difference or resistivity is either measured or can be calculated depending on the testing apparatus.

This test, like RCPT, is not applicable to specimens containing metallic fibers or longitudinal steel reinforcement. Resistivity is a non-destructive test. So, to allow for multiple tests to be performed on the same specimen, ASTM C1760 (2012) and ASTM C1876 (2019) were used for bulk resistivity curing and testing. This combination means that the same specimen has multiple readings and results from three durability tests. Curing regimes are per ASTM C1760 (2012), which is moisture room curing, and specimens were tested using the test setup described in ASTM C1876 (2019).

Bulk resistivity specimens are permitted to be either 4 in. or 8 in. (100 mm or 200 mm) long, but the ratio of length to diameter must be at least one. After demolding, the diameter is measured at two perpendicular angles on the top and bottom surface, and the length is recorded every 90 degrees along the sides.

Testing should be completed within five minutes, and then, the specimens are returned to the curing environment. Since specimens were used for multiple tests, a total of three to five 4x8 in. (100x200 mm) cylinders were made per batch. Measurements with the Giatec RCON resistivity meter were taken at 7, 14, 28, 56, and 90 days. To perform the test, the average specimen dimensions are entered, the test frequency is set to 1 kHz, and measurements are recorded in resistivity. Two sponges are soaked in a conductive fluid supplied by the manufacturer and placed between the two plate electrodes and test specimen. A 6.6 lb (3 kg) weight is applied to the top to provide compression. The general bulk resistivity test setup is shown in Figure 3.2.

Figure 3.2. Bulk Resistivity Testing Equipment and Specimens

3.3. Surface Resistivity (AASHTO T358)

Surface resistivity testing is similar to bulk resistivity as it also provides a quick indication of chloride ion resistance. Four electrodes, instead of two, are arranged in a line and pressed onto the surface of the specimen. The inner electrodes measure electrical potential difference while the outer apply the AC. The current, difference, and sample geometry are used to calculate resistivity. This value is related to the resistance of the specimen to chloride ion penetration.

The surface resistivity test is also not valid for specimens containing metallic fibers, and the sample size is similar to that required in ASTM C1876 (2019), which is why the same specimens were used for all permeability tests. A 4x8 in. (100x200 mm) diameter sample is prepared per ASTM C192 (2016). After demolding, the dimensions are measured in the same manner described in ASTM C1876 (2019). Measurement

locations are marked on the top and sides of the specimen. One mark is assigned as 0 degrees and moving in a counterclockwise direction the remaining marks are assigned as 90, 180, and 270 degrees. Specimens should be moist cured for their testing duration at 73.4 ± 3.6°F (23 ± 2°C) and 100 percent relative humidity.

As in ASTM C1876 (2019), the specimens are quickly returned to the curing environment to prevent drying, and testing temperatures should be between 68 and 77°F (20 and 25°C). Using a Proceq Resipod Resistivity Meter with 1.5 in. (38 mm) electrode spacing, the specimen is placed on its side with the 0 degrees mark on top, and the four-point electrode is centered along the specimen parallel to the longest dimension. The meter is pressed down and the measurement is recorded once it stabilizes. This process is repeated for 90, 180, and 270 degrees until four total measurements are obtained. The specimen is rotated back to the 0 degrees mark, and a second reading is obtained at each location. The surface resistivity of the sample is the average of the eight readings. In Table 3.2, the surface resistivity for both cylinder sizes are correlated to a chloride ion penetration resistance based on the table from AASHTO T358 (2017). The general surface resistivity test setup, along with the required specimen labeling, is shown in Figure 3.3.

Table 3.2. Chloride Ion Penetration and Surface Resistivity (adapted from AASHTO T358 2017)

Chloride Ion Penetration Classification	Charge Passed (Coulombs)	4x8 in. Cylinder (kΩ-cm)	6x12 in. Cylinder (kΩ-cm)
High	>4000	<12	<9.5
Moderate	2000 – 4000	12 – 21	9.5 – 16.5
Low	1000 – 2000	21 – 37	16.5 – 29
Very Low	100 – 1000	37 – 254	29 – 199
Negligible	<100	>254	>199

(a) Surface Resistivity Equipment

(b) Specimen Labeling

Figure 3.3. Surface Resistivity Testing Equipment and Specimens

3.4. Formation Factor and Pore Solution Resistivity (AASHTO PP84)

The formation factor is a numerical characterization of the porosity and connectivity and has advantages over electrical test methods like ASTM C1202 (2017) and ASTM C1760

(2012). These electrical-based tests, while also influenced by porosity and pore connectivity, are also influenced by the pore fluid conductivity. The fluid conductivity does not indicate resistance to penetration. Therefore, using the formation factor can avoid this influence. The PSR is required to calculate the formation factor. A more thorough explanation of the determination of these two factors is in *Standard Practice for Developing Performance Engineered Pavement Mixtures* AASHTO PP84 (2018).

AASHTO PP84 (2018) lists three methods to characterize the pore solution: (1) assuming a constant resistivity value of 0.1 Ω-m, (2) estimating with the NIST model (NIST 2017), and (3) experimentally measuring. The most accurate method for pore solution determination is experimentation. The first experimental method is pore solution expression, which requires a 2x4 in. (51x100 mm) cementitious paste cylinder. The hardened sample is compressed in a high-pressure system, and the expressed pore solution is collected in a small vial. The resistivity can be measured using a pore solution resistivity cell. Another experimental method uses embedded sensors. These are placed right after casting, and as the concrete sample hydrates, each sensor measures the change in resistivity.

The NIST model is the second most accurate way to estimate the conductivity of the pore solution according to AASHTO PP84 (2018). Using chemical components from the cementitious materials, mix design, and degree of hydration, the NIST model can produce the electrical conductivity of the pore solution (NIST 2017). The inverse of conductivity gives resistivity of the pore solution. The least accurate way to capture the PSR is by assuming the constant resistivity value.

Due to the dense microstructure of UHPC, pore solution expression was not performed, and because developing a new method for pore solution resistivity calculations is not under the scope of research, the NIST model is used for pore solution resistivity estimation. The constant resistivity assumption of 0.1 Ω-m per AASHTO PP84 (2018) can provide a range for the potential formation factor values.

Once the PSR is determined, the formation factor can be calculated, and is the ratio of bulk resistivity to PSR, as given in Equation (2.1). AASHTO PP84 (2018), like AASHTO T358 (2017), has a table correlating the chloride ion penetration category, charge passed, resistivity, and formation factor. The PSR used to calculate the formation factor in this table is assumed at 0.1 Ω-m (AASHTO PP84 2018). Table 3.3, adapted from AASHTO PP84 (2018), expands on the information given in Table 3.2 by adding the formation factor correlation.

Table 3.3. Permeability Correlations (adapted from AASHTO PP84 2018)

Chloride Ion Penetration Classification	Charge Passed (Coulombs)	Surface Resistivity for a 4x8 in. Cylinder (kΩ-cm)	Formation Factor Using a PSR of 0.1 Ω-m
High	>4000	<12	<520
Moderate	2000 – 4000	12 – 21	520 – 1040
Low	1000 – 2000	21 – 37	1040 – 2080
Very Low	100 – 1000	37 – 254	2080 – 20,700
Negligible	<100	>254	>20,700

3.5. Abrasion Resistance by the Rotating-Cutter Method (ASTM C944)

The abrasion resistance test is used to indicate the abrasion or wear resistance of concrete or mortar mixtures typically used for highway or bridge applications. This standard typically specifies a 6 in. (152 mm) diameter specimen. However, the ASTM C1856 (2017) modification requires the smallest specimen size to accommodate the device and using a 44 ± 0.4 lbf (197 ± 2 N) load instead of the typical 22 ± 0.2 lbf (98 ± 1 N).

The specimens used for this experiment are cut from a 4x8 in. (100x200 mm) cylinder that cured for 28 days at $68 \pm 3.6°F$ ($20 \pm 2°C$) in 95 percent relative humidity. At 28 days, the specimens were equally cut in thirds by a wet saw to create three different surface preparations: cast, surface ground, and molded. The cast surface is from the top third section of the cylinder, the ground surface from the middle third, and the molded surface is from the bottom third. After cutting the cast surface specimen, top third, away from the cylinder, the cut surface of the remaining cylinder is ground for 120 seconds in an end grinder to achieve a smooth finish. This remaining cylinder was then cut in half to create the ground and molded surface. The molded surface is from the bottom cylinder that was in contact with the plastic mold during casting. The height, diameter, and mass of each specimen are recorded before testing. The approximate dimensions of each were 4 in. (102 mm) in diameter and 2.5 in. (64 mm) in height. There were three specimens tested per surface preparation.

The dressing wheels used were slightly larger than those mentioned in ASTM C944 (2012). Instead of an overall diameter of 1.5 in. (38 mm) the wheels had a diameter of 2-3/8 in. (60 mm). The pin on the machine was too large to accommodate the inner

51

diameter of the commercially available 1.5 in. (38 mm) dressing wheels. The dressing wheels currently on the machine have an overall diameter of 1.5 in. (38.1 mm) and an inner diameter of 17/32 in. (13.5 mm). This inner diameter is slightly larger than the 0.5 in. (12.7 mm) diameter specified in ASTM C944 (2012). However, these smaller wheels were used on one sample per surface preparation to serve as a baseline for comparison purposes. Figure 3.4 shows the two dressing wheels with the 1.5 in. (12.7 mm) wheel on the left and the 2-3/8 in. (60 mm) wheel on the right. The wheels were changed every 90 minutes per standard recommendation, and a total of 10 minutes of abrading were applied to each specimen.

Figure 3.4. Dressing Wheels Used for the Abrasion Resistance Testing

To begin testing, the dressing wheels and washers are mounted on the horizontal pin of the rotating cutter. There are 22 wheels and 24 1.0 to 1.25 in. (25 to 32 mm) diameter washers on the pin. Each side is secured with bolts, but the wheels should be free to rotate. The mass of each specimen is recorded before testing. The specimen is placed on the

abrasion bench with the surface plane to the rotating cutter. Using a double load of 44 ± 0.4 lbf (197 ± 2 N), the machine is started, and the cutter is lowered onto the surface. Contact is continued for two minutes at 200 rpm. At the end of each two-minute sequence, the powdered debris is brushed off and the mass is recorded. The two-minute abrading sequences were repeated five times. Figure 3.5 shows the abrasion head with the 2-3/8 in. (60 mm) dressing wheels and test specimen.

Figure 3.5. 2-3/8 in. (60 mm) Dressing Wheels with Specimen for ASTM C944 Testing

3.6. Compressive Strength of Cylindrical Concrete Specimens (ASTM C39)

ASTM C39 (2018), *Standard Test Method for Compressive Strength of Cylindrical Concrete Specimens*, has a modification in ASTM C1856 (2017). The modification requires a 3x6 in. (75x150 mm) UHPC cylinder for compressive strength tests. An

additional modification in ASTM C1856 (2017) requires cylinders to be end ground so the ends are plane to within 0.002 in. (0.05 mm). Neoprene pads with capping compounds are not permitted. The loading rate for UHPC is also increased to 145 ± 7 psi/s (1.0 ± 0.05 MPa/s). Compression strength tests were performed at 1-day and 28 days using either the MTS Silentflo 515 in the Materials Laboratory or the MTS 311.41S 500 in the High Bay Laboratory for verification between batches and to ensure adequate strength was achieved.

3.7. Flow Test for Hydraulic Cement Mortar (ASTM C1437)

ASTM C1437 (2015), *Standard Test Method for Flow of Hydraulic Cement Mortar*, is used to determine the flow of mortars containing cementitious materials and also has an ASTM C1856 (2017) modification that requires the mold to be filled in a single layer without tamping or vibration.

The mold is placed on top of the flow table and filled with a single layer of fresh UHPC. The mold is lifted from the table and the mixture is allowed to spread undisturbed for 2 ± 5 seconds. Figure 3.6 shows a picture of the mold before the UHPC is poured and the spread result. The maximum and minimum diameter of the spread are recorded, and the average is taken as the flow value. This test was used as a measure of repeatability between different batches of the same mix design.

(a) Flow Table and Mold   (b) Spread Example
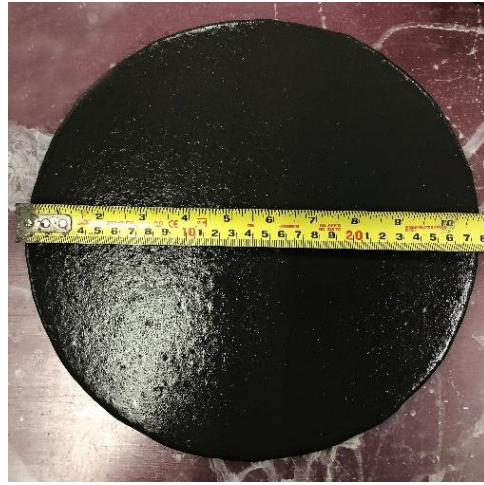
Figure 3.6. Flow Table Mold and Spread

4. DURABILITY TESTING OF NON-PROPRIETARY UHPC MIXTURES

This research includes a detailed evaluation of the durability of non-proprietary UHPC mixtures made with local Texas materials. Using novel test methods like resistivity, pore solution resistivity, and formation factor to characterize permeability, durability can be assessed more efficiently and economically as compared to other methods like RCPT. The formation factor can be calculated through the pore solution resistivity. Abrasion resistance testing, as a supplemental measure, can provide a more thorough understanding of UHPC wear resistance behavior.

The non-proprietary UHPC mixtures were fully evaluated to determine their respective durability properties. Several vital tests for permeability include RCPT and resistivity, and the further look at pore solution, formation factor, and the service life. All testing was performed at the Center for Infrastructure Renewal (CIR) on the Texas A&M University (TAMU) System RELLIS Campus. Curing regimes were based on ASTM standards and availability of the required equipment and facilities at the CIR. Thus, all specimens in this research were cured at $68 \pm 3.6°F$ ($20.0 \pm 2.0°C$) with 95 percent relative humidity. Because multiple batches were made for each mix, two tests were used as a check for repeatability because these two tests guarantee indirect adequacy of UHPC quality (Graybeal 2013).

4.1. Texas Non-Proprietary Mixes

The mixes developed for this study include local Texas materials. They include a Type I/II cement with a C_3S content of 65 percent and C_2S content of 8 percent with a median

particle size of 3.6 micron. The high C_3S content helped produce mixes with high early strength without the aid of heat treatment or accelerator. The silica fume has a median particle size of 2.9 microns, and the Class F fly ash has a median particle size of 12.7 micron. The river sand was washed, dried, and sieved before mixing. Particles finer than 0.05 in. (1.19 mm) (No. 16 sieve) were used. A 1.5 percent by volume dose of 0.5 in. (13 mm) long and 0.008 in. (0.2 mm) diameter steel fibers were used that have an aspect ratio of 65, and tensile strength of 400 ksi (2750 N/mm^2). A HRWR, more specifically a polycarboxylate based superplasticizer, was also used.

Due to the testing requirements for specimens with and without steel fibers, slight mixture adjustments must be made to account for the loss of volume from the steel fibers. The goal is to keep the mechanical properties constant so that the mix is reflective of actual mix conditions, which would include steel fibers. Like Wille et al. (2011), when steel fibers were removed, the same volume was replaced by sand. Table 4.1 provides the mix designs with fibers.

Table 4.1. Non-Proprietary UHPC Mix Designs (lb/yd^3)

Description	Mix 1	Mix 2	Mix 3
Cement (Type I/II)	1445	1238	1579
Silica fume	217	186	63
Fly ash	72	310	121
Sand	1671	1662	1715
Water	329	312	320
HRWR	27	24	26
Steel fiber (%)	1.5	1.5	1.5
w/*cm*	0.190	0.180	0.182

The most notable differences in the mix designs in this study are the SCM proportions. Mix 1 has a silica fume content of 15 percent and fly ash content of 5 percent, Mix 2 has 15 percent silica fume and 25 percent fly ash, and Mix 3 has 4 percent silica fume and 8 percent fly ash by cement weight. The proportions in Mix 3 are the most unconventional for a typical UHPC mix due to the extremely low silica fume content to achieve high early strength without heat-treatment or an accelerator agent for prestressing. Khayat and Valipour (2018) and Mendonca et al. (2020) have similar content at 4 percent and 8.25 percent, respectively, but the proprietary mixes generally have silica fume contents more than 20 percent. The effect of SCMs, especially silica fume, should be revealed in the permeability testing.

4.2. Material Characterization

In order to characterize the pore solution, x-ray fluorescence (XRF) is used to find the chemical properties of the cement and fly ash. XRF data for the fly ash was obtained. However, inferences based on the x-ray powder diffraction (XRD) data for the cement were made to find the chemical compound masses required for pore solution characterization. In the XRD data for the cement, the arcanite (K_2SO_4) is measured as 0.49 percent. In separate research on the HPC project under TxDOT Project 0-6958 (8/2020), a machine learning model to predict available alkali using bulk oxide composition is currently in progress, which uses an alkali free factor of 77 percent (Mukhopadhyay and Saraswatula 8/2020). Using this value from Mukhopadhyay and Saraswatula (8/2020), the contributing K_2O content can be calculated as 0.64 percent. A conservative estimate of 0.2 percent was taken as the Na_2O for the cement.

Table 4.2. XRF and XRD-based Data for Type I/II Cement and Class F Fly Ash

Compound	% Mass	
	Fly Ash	**Cement**
SiO_2	53.90	-
Na_2O	0.34	0.20
K_2O	0.93	0.64

The data from Table 4.2 is used to characterize the pore solution by direct input into the NIST model, where pore solution conductivity in Siemens per meter (S/m) is given (NIST 2017). The inverse is the resistivity.

4.3. Mixture Compressive Strengths and Flow Table Tests

Immediately after completed mixing a workability test that measures the flow value, ASTM C1437 (2015), with the UHPC modification in ASTM C1856 (2017), was used to determine if the mix was in the typical limits. Two compression tests at 1-day and 28 days were also used to verify the strength of the mixes at the two critical ages using ASTM C39 (2018) with the UHPC modification in ASTM C1856 (2017). This modification requires an end ground 3x6 in. (75x150 mm) cylinder. A general summary is available that includes the mixes, number of batches per mix, steel fiber presence, mixing volume, mixing room and mixture temperature, and results from the flow table test. This is presented in Table 4.3. The ideal spread value range for the three mixtures is between 9 and 11 in. (229 and 279 mm). The expected typical spread values for Mix 1 are 8.4 to 9.7 in. (213 to 246 mm), for Mix 2 are 9.5 to 10.8 in. (241 to 274 mm), and for Mix 3 are 10.4 to 11.9 in. (264 to

302 mm). The recorded spread value for Mix 1b, with no fibers, did slightly exceed the typical range for Mix 1, while the other batches for each mix gave measured flows in the expected range.

Table 4.3. General Mixture Summary for the Durability Tests

Mix ID	Batch ID	Fibers (Y/N)	Batch Volume (ft²)	Room Temperature (°F)	Mixture Temperature (°F)	Spread (in.)
Mix 1	a	Y	0.47	-	-	8.8
	b	N	0.40	-	-	10.0
	c	N	0.55	65.3	70.9	9.7
	d	Y	0.51	67.7	75.7	9.6
Mix 2	a	N	0.40	-	-	9.8
	b	N	0.55	65.3	72.9	10.8
	c	Y	0.51	67.7	75.9	9.5
Mix 3	a	N	0.55	66.5	75.2	10.6
	b	N	0.50	67.6	79.2	11.9
	c	Y	0.51	67.7	78.2	10.6

Additional data for compression tests are available. Three cylinders were tested at two ages, 1-day and 28 days, to verify that the target strength was met. Compressive strength is influenced by the presence of steel fibers and spread value, which affects air void content (Alkaysi and El-Tawil 2016; El-Tawil et al. 2018). Therefore, the variance in the compressive strength within 10 to 20 percent is acceptable. Target strengths were more critical at the 1-day mark because field-cast UHPC connections should achieve 0.65 percent of the 28-day compressive strength before sustained loads are applied to minimize

the creep (Graybeal 2019). If UHPC has a compressive strength of 21.7 ksi (150 MPa) according to Graybeal (2011), then a compressive strength of 14 ksi (96.5 MPa) should be achieved before loading. These mixes are intended for pretensioned girders where release within 16 to 24 hours is ideal. Therefore, it is important to validate that these mixes are achieving adequate strength in the desired time frame.

Initial compressive tests were run with a neoprene pad and a steel capping compound, which is not in accordance with the ASTM C1856 (2017) modification for ASTM C39 (2018). An end grinder was available for use on later mixes to meet the end preparation requirements in ASTM C1856 (2017). Four batches were made for Mix 1. Based on previous testing, the average 1-day compressive strength for this mix is between 10.5 to 11.6 ksi (72.4 to 80.0 MPa) and at 28 days is 16.1 to 17.6 ksi (111 to 121 MPa). The results are shown in Table 4.4. The compressive strength for Mix 1c at 1-day was just under the expected strength range at 10.3 ksi (71.0 MPa), and at 28 days, Mix 1a, with steel fibers, exceeded the 17.6 ksi (121 MPa) expected strength. However, both variances were well within the allowable tolerance. The remaining results were within the expected range.

Table 4.4. Compression Test Results for Mix 1

Batch	Fibers (Y/N)	Age at Compression Test (days)	Strength (ksi)	Avg (ksi)	Std Dev	Surface Preparation	Testing Equipment Used
a	Y	1	11.04 11.09 11.06	11.1	0.0	Cap	TTI
		28	19.06 18.52 16.62	18.1	1.0	Ground	TTI
b	N	1	11.12 11.64 11.64	11.5	0.2	Cap	TTI
		28	17.73 17.02 18.16	17.6	0.5	Ground	TTI
c	N	1	10.61 9.54 10.80	10.3	0.6	Ground	HBL
		28	16.37 19.35 16.22	17.3	1.4	Ground	TTI
d	Y	1	11.14 11.82 11.55	11.5	0.3	Ground	TTI
		28	15.51 15.91 17.16	16.2	0.7	Ground	HBL

Notes: 1. TTI: MTS Silentflo 515   2. HBL: MTS 311.41S 500

Similarly, for Mix 2, compression tests were performed at the same ages, with a summary in Table 4.5. Due to the lower cement content, the 1-day average is slightly lower than Mix 1. However, the 28-day strength can exceed that of Mix 1. Three batches were made for this mix, and the typical compression strength for mixes with fibers range

from 9.1 to 10.2 ksi (62.7 to 70.3 MPa) at 1-day and 16.1 to 18.2 ksi (111 to 125 MPa) at 28 days.

Table 4.5. Compression Test Results for Mix 2

Batch	Fibers (Y/N)	Age at Compression Test (days)	Strength (ksi)	Avg (ksi)	Std Dev	Surface Preparation	Testing Equipment Used
a	N	1	10.00	10.3	0.3	Cap	TTI
			10.16				
			10.74				
		28	15.49	16.1	0.5	Ground	TTI
			16.12				
			16.80				
b	N	1	9.97	9.0	0.9	Ground	HBL
			7.87				
			9.28				
		28	19.36	18.1	1.9	Ground	TTI
			19.60				
			15.48				
c	Y	1	10.15	10.2	0.5	Ground	TTI
			10.85				
			9.51				
		28	17.68	16.2	1.3	Ground	HBL
			16.24				
			14.53				

Notes: 1. TTI: MTS Silentflo 515   2. HBL: MTS 311.41S 500

Mix 3 has the highest cement content out of the three mixes and obtained the highest compression strengths at both testing ages. Similar to Mix 2, three batches were also prepared for Mix 3. The typical compressive strength values are reported as 13.1 to

14.0 ksi (90.3 to 96.5 MPa) at 1-day and 17.9 to 21.0 ksi (123 to 145 MPa) at 28 days. The results are shown in Table 4.6. While the 1-day compression test results were lower than the typical range, they are within 10 to 20 percent, and the repeatability between the three batches was confirmed.

Table 4.6. Compression Test Results for Mix 3

Batch	Fibers (Y/N)	Age at Compression Test (days)	Strength (ksi)	Avg (ksi)	Std Dev	Surface Preparation	Testing Equipment Used
a	N	1	11.58 12.57 11.19	11.8	0.6	Ground	TTI
		28	20.25 19.91 18.11	19.4	0.9	Ground	TTI
b	N	1	11.47 12.25 11.58	11.8	0.3	Ground	TTI
		28[*]	- - -	-	-	-	-
c	Y	1	11.53 11.77 11.70	11.7	0.1	Ground	TTI
		28	18.16 16.49 19.34	18.0	1.2	Ground	HBL

Notes: * Testing was not completed at 28 days due to temporary laboratory closure.
1. TTI: MTS Silentflo 515   2. HBL: MTS 311.41S 500

4.4. Rapid Chloride Ion Penetration Test

Multiple batches were made for all three mixes, and RCPT tests were performed on Mix 1c and Mix 2b following the procedures of ASTM C1202 (2017). A test matrix is for RCPT is provided in Table 4.7.

Table 4.7. Rapid Chloride Ion Penetration Test Matrix

Mix ID	Batch ID	Fibers (Y/N)	Number of Samples	Sample Size (in.)	Age at Testing (days)
Mix 1	c	N	4	4x2	56
Mix 2	b	N	4	4x2	56

Two cells were available for testing, so only two tests could be run at once. During the test, periodical checks were performed to ensure both ends of the cell remained filled with the solutions, and there were no leaks.

Results were obtained at 56 days for both mixes, and all specimens tested measured in the negligible chloride ion penetration range based on ASTM C1202 (2017) and shown in Table 3.1. This range requires a charge passed value, in Coulombs, of less than 100. Figure 4.1 shows the values measured for the four specimens in each mix, with Mix 1 having a slightly lower average of 65.7 Coulombs than Mix 2 with 74.2 Coulombs. The negligible and very low chloride ion penetration classifications are also shown. However, Mix 2 results have a higher standard deviation, which could be due to the higher SCM contribution in the mix. SCMs are known to affect chloride ion penetration. Initial results

indicate a positive durability result for the developed non-proprietary mixes because a negligible chloride ion penetration classification, which is below 100 Coulombs not only indicates low permeability but low ion movement and a discontinuous pore structure.
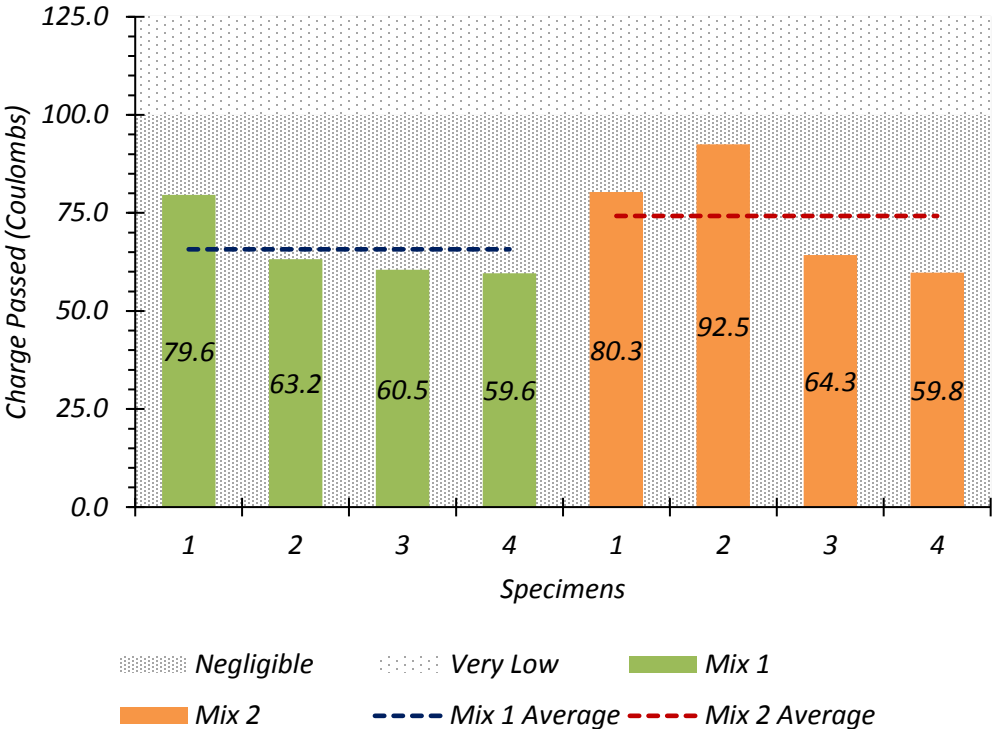
Figure 4.1. Rapid Chloride Ion Penetration in Coulombs for Mixes without Steel Fibers

4.5. Resistivity Measurements

4.5.1. Test Matrix

The test matrix, presented as Table 4.8, is valid for both bulk and surface resistivity testing

for the three mixes. Bulk and surface resistivity measurements are recorded on three to

five specimens at the same age, depending on the batch.

Table 4.8. Resistivity Test Matrix

Mix ID	Batch ID	Fibers (Y/N)	Number of Samples	Sample Size (in.)	Age at Testing (days)
Mix 1	a	Y	3	4x8 cylinder	7, 14, 28, 56, 90
	b	N	3	4x8 cylinder	7, 14, 28, 56, 90
	c	N	5	4x8 cylinder	7, 14, 28, 56
Mix 2	a	N	3	4x8 cylinder	7, 14, 28, 56, 90
	b	N	5	4x8 cylinder	7, 14, 28, 56
Mix 3	a	N	5	4x8 cylinder	7, 14, 28, 56
	b	N	4	4x8 cylinder	7, 14, 28

For Mix 1b, measurements at each age are an average of three specimens, while it

is an average of five specimens for Mix 1c. The same specimen allocation was used for

the Mix 2 resistivity mixes. Mix 3a had five specimens, and Mix 3b had four specimens.

To determine if steel fibers would influence the readings, Mix 1a included steel fibers, and

resistivity measurements were taken at the select ages.

4.5.2. Bulk Resistivity

The impact on the bulk resistivity measurements due to the steel fibers in Mix 1a is significant. In Table 4.9, it is shown that these measurements are approximately 25 percent of those measurements without steel fibers, and these trends are further displayed in Figure 4.2. In Figure 4.3, the bulk resistivity measurements from both batches have been averaged and then normalized by Mix 2 to show the comparisons between mixes.

Table 4.9. Average Bulk Resistivity Measurements (kΩ-cm)

Mix ID	Batch ID	Age (days)				
		7	14	28	56	90
Mix 1	a	6.3	13.0	28.9	55.5	71.0
	b	24.0	48.7	110	221	281
	c	23.1	45.3	104	197	-
Mix 2	a	24.9	51.3	117	233	311
	b	22.8	44.8	101	193	-
Mix 3	a	17.5	30.2	58.0	105	-
	b	17.9	31.2	59.6	-	-
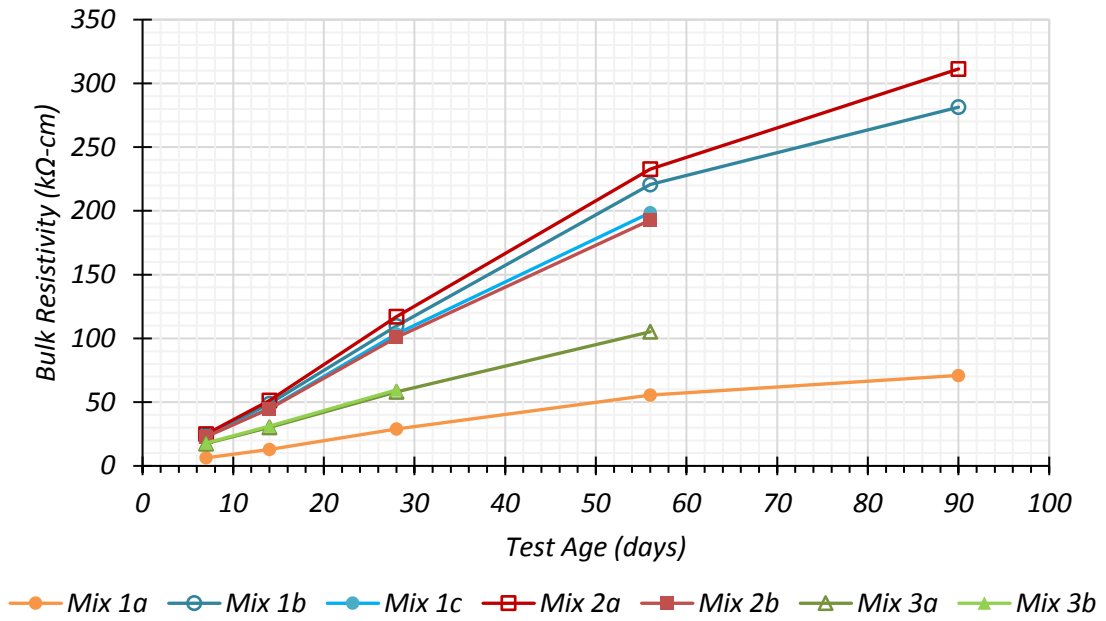
Figure 4.2. Bulk Resistivity Results
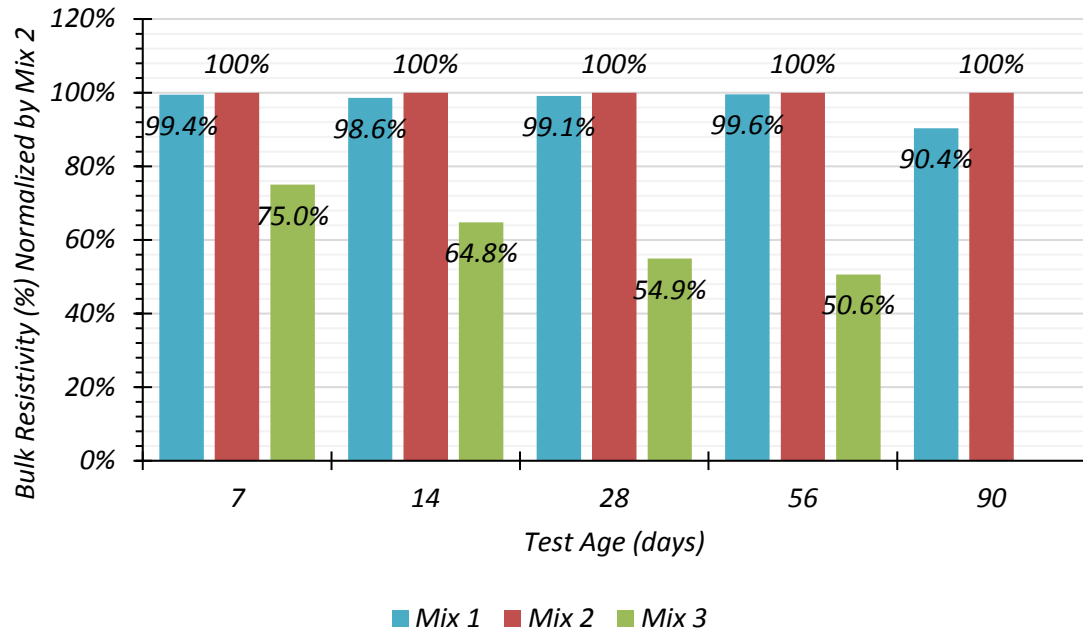
Figure 4.3. Bulk Resistivity Results Normalized by Mix 2

As shown in Figure 4.3, for Mix 1 and 2, without steel fibers, the results are similar until 90 days. At this age Mix 1 is 10 percent lower than Mix 2. Mix 2 has a higher SCM proportion, 17.9 percent fly ash and 10.7 percent silica fume, compared to Mix 1 with 4.2 percent fly ash and 12.5 percent silica fume. Fly ash begins reacting after 56 days, and although thought to be an inert material because of the minimal water in the UHPC system, in combination with the silica fume, it could be providing additional benefit to the microstructure development.

Mix 3, which contains significantly fewer SCMs than Mix 1 and 2, achieves approximately 75 percent of the resistivity reading of Mix 2 at seven days, before falling to 65 percent of those values at 14 days, 55 percent at 28 days, and 51 percent at 56 days. The large difference in silica fume contribution could be causing the differences in results between Mix 1 and 2 and Mix 3. When silica fume reacts with $Ca(OH)_2$, it produces calcium silica hydrate (C-S-H), fills micropores, accelerates cement hydration, and helps to densify the microstructure (Mindess et al. 2003). The absence of silica fume could result in a less dense microstructure, which is why the results from Mix 3 get consistently lower as the concrete ages. Mix 3 has a SCM proportion of 6.8 percent fly ash and 3.6 percent silica fume, which is unconventional when compared to the SCM packed mixes for proprietary mixes (see Table 2.2) and non-proprietary mixes (see Table 2.3). The positive effects of the SCMs in terms of resistivity, which include higher packing density, is not able to manifest in Mix 3 and are displayed in the resistivity results.

4.5.3. Surface Resistivity

The surface resistivity results are directly comparable to the RCPT results, according to Table 3.2 by AASHTO T358 (2017). This testing plan is provided in Table 4.8, while Table 4.10 provides the average surface resistivity measurements for all seven batches.

Table 4.10. Average Surface Resistivity Measurements (kΩ-cm)

Mix ID	Batch ID	Age (days)				
		7	14	28	56	90
Mix 1	a	12.6	16.6	29.1	57.8	69.9
	b	24.5	46.7	118	226	277
	c	23.3	43.6	99.8	202	-
Mix 2	a	30.0	50.3	117	237	321
	b	24.1	42.8	98.5	200	-
Mix 3	a	16.8	27.9	54.7	101	-
	b	16.5	30.0	58.9	-	-

The surface resistivity results follow the same trends discovered in the bulk resistivity measurements. Particularly, the Mix 1a specimens containing steel fibers, are still showing significantly lower results than the Mix 1 batches without fibers. From 7 days to 56 days, the surface resistivity measurements for Mix 1 and 2 are, again, similar to the bulk resistivity results. As stated, this could be due to the same silica fume contribution by cement weight for both mixes. At 90 days, Mix 2a is 16 percent higher than Mix 1b, which can be attributed to the fly ash contribution in Mix 2. At 7 days, Mix

3 is 33 percent lower than Mix 1 and 2, 36 percent at 14 days, 47 percent at 28 days, and 53 percent at 56 days.

In Figure 4.4, surface resistivity is plotted as the concrete matures, and is overlaid on the RCPT classification levels. At seven days, Mix 1 with the fiber reinforcement and Mix 3 correlate to the moderate range, and Mix 1 and 2 are in the low range. By 28 days, all mixes without fibers are in the very low range.
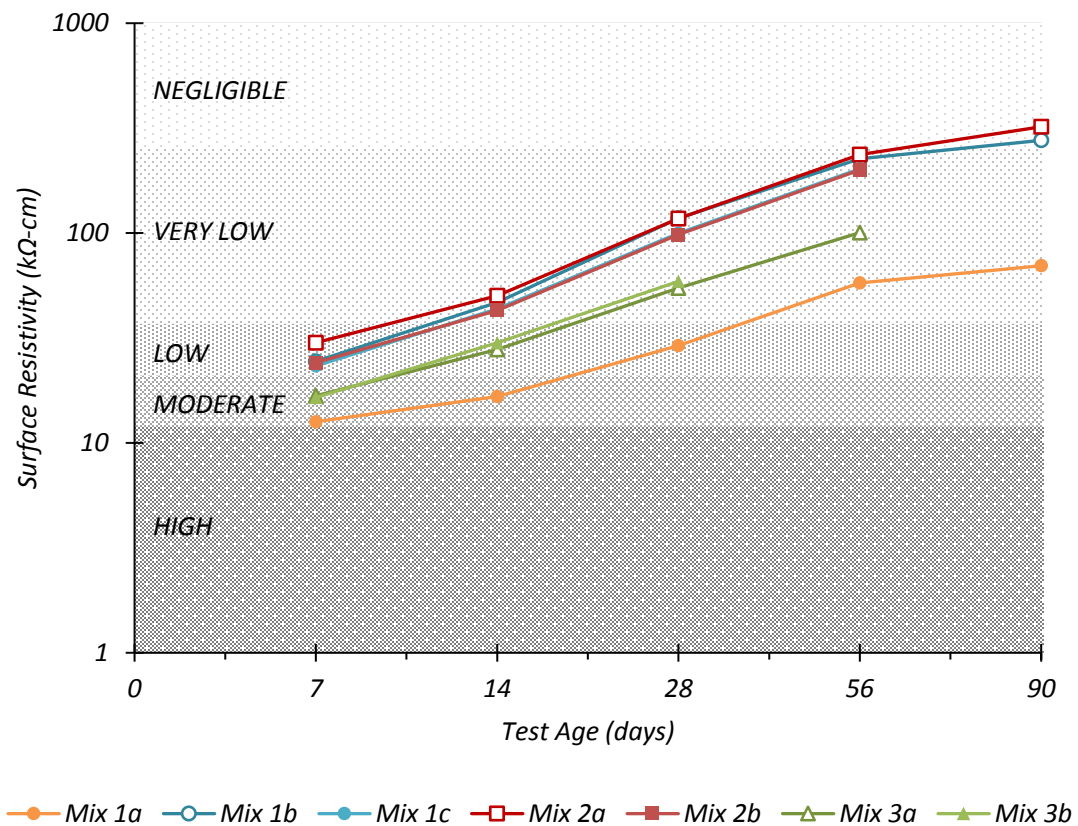
Figure 4.4. Surface Resistivity Results

4.6. Pore Solution Resistivity

The pore solution was found using the NIST model, which uses the mix proportions and material chemical composition to estimate the conductivity of the system (NIST 2017). This model assumes a 75 percent alkali free factor for sodium and potassium, which means that 75 percent of those oxides go towards defining the pore solution. The mass of water, cement, silica fume, and fly ash are entered along with their respective percent masses of Na_2O, K_2O, and SiO_2. These were determined earlier using XRF from Table 4.2. NIST (2017) provides assumptions for the silica fume composition of 0.2 percent Na_2O and K_2O, and a manual assumption of 96 percent SiO_2 is used. An estimated degree of hydration must also be assumed in order for the model to provide a conductivity output. A higher degree of hydration will result in higher conductivity.

To better understand the applicability of the NIST model for UHPC, additional mix designs from Texas were also entered into the model and are displayed in Table 4.11. NIST (2017) allows for a degree of hydration input up to 100 percent, but it is unrealistic that the mixes will achieve that level. Additionally, the NIST model does overestimate the fly ash contribution to the pore solution according to Tanesi et al. (2019), and a lower degree of hydration can help provide a more conservative estimate. According to Acker and Behloul (2004), HPC has an approximate degree of hydration of 80 percent at a w/c of 0.35. Since this HPC mix design has 5 percent silica fume and 20 percent fly ash, a 70 percent degree of hydration was chosen for the HPC bridge deck to provide a more conservative estimate. Ordinary concrete has a degree of hydration at approximately 90 percent at a w/c of 0.45, and since mixture does not have additional SCMs 80 percent

hydration was used (Acker and Behloul 2004). The SCC mixture has a very low water content, and UHPC with a *w/c* of 0.30 has a hydration of 69 percent (Acker and Behloul 2004). Since this mixture also contains high amounts of fly ash, 20 percent, a 60 percent was used for the degree of hydration. According to Acker and Behloul (2004), UHPC with a *w/c* of 0.20 would have a degree of hydration around 47 percent. Mix 1 and 2 have a *w/c* higher than this, and 47 percent is, therefore, more conservative. The presence of silica fume and fly ash will affect the result because more alkalis are contributed to the solution. However, it can be noted that *w/c* will have a significant impact on PSR. As *w/c* increases, PSR increases.

Table 4.11. NIST Model (NIST 2017) Conductivity Results for Different Mix Designs

Author	UHPC			Trejo et al. (2008)		TxDOT Project 0-6958 (8/2020)
Mix Type	Mix 1	Mix 2	Mix 3	SCC	PC	HPC
w/c	0.23	0.25	0.20	0.29	0.36	0.42
Water (lb)	329	312	320	208	225	245
Cement (lb)	1445	1238	1579	720	625	584
Silica fume (lb)	217	186	63	0	0	29
Fly ash (lb)	72	310	121	180	0	117
Hydration (%)	47	47	47	60	80	70
σ_{ps} (S/m)	21.29	26.59	31.27	23.47	16.34	15.39

Notes: 1. S: Siemens   2. PC: Conventional precast concrete mix

The inverse of conductivity is resistivity. Taking the inverse of 21.29, 26.59, and 31.27 S/m means the PSR values are 0.047, 0.038, and 0.032 Ω-m. A further look at these

values can be found when the proportion of silica fume and fly ash in a mix is plotted

against the PSR. For a constant *w/cm*, the proportion of silica fume, fly ash, and degree of

hydration, the fly ash and silica fume proportion can be varied individually. The curve

obtained from the NIST model will be specific to each *w/cm*, SCM contribution, and

hydration, but it can help provide a visual of at what point along the curve the PSR is being

taken. Table 4.12 provides the proportions of cement, silica fume, and fly ash for the

UHPC mixes.

Table 4.12. UHPC Mix Design Proportions and Percent by Mass

Material	Mix 1		Mix 2		Mix 3	
	Proportion of C	% by Mass	Proportion of C	% by Mass	Proportion of C	% by Mass
C	1.00	83.3	1.00	71.4	1.00	89.6
SF	0.15	12.5	0.15	10.7	0.04	3.6
FA	0.05	4.2	0.25	17.9	0.08	6.8

Notes: 1. C: Cement   3. FA: Fly ash
        2. SF: Silica fume

For Mix 1, the constant values are *w/cm* of 0.190, 4.2 percent fly ash, and 47

percent hydration. The silica fume proportion is varied from 0 to 20 percent, and as silica

fume increases, the cement contribution decreases to keep the same *w/cm* value of 0.190.

The *w/c* will increase because as the silica fume proportion is increasing, the cement must

decrease. A similar approach was taken to model the individual characteristics of Mix 2

and 3 for silica fume. For Mix 2, the *w/cm* is fixed at 0.180, the fly ash proportion 17.9

percent, and the hydration still at 47 percent. Mix 3 will have a *w/cm* of 0.182 and a fly ash proportion at 6.8 percent. Figure 4.5 shows the silica fume curves for each mix along with the point along the curve where the PSR is being taken.
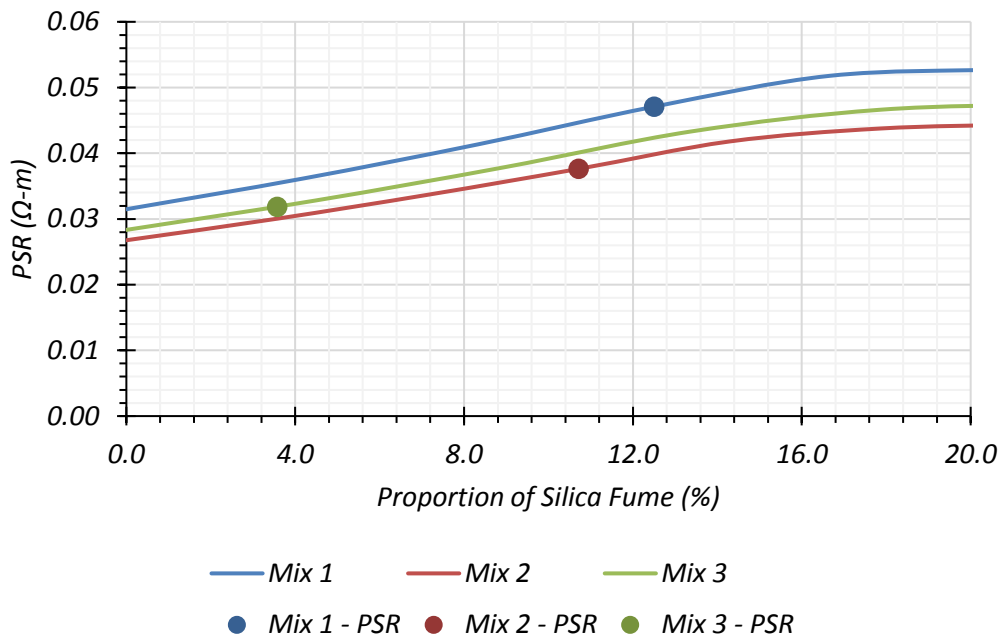
Figure 4.5. Silica Fume Proportion as a Function of PSR for UHPC Mixes

As the silica fume proportion in cementitious material increases, the PSR will increase linearly until a mix contains approximately 20 percent silica fume for mixes with a *w/cm* between 0.180 and 0.190 and fly ash proportions between 4.2 and 17.9 percent. Past that proportion, the PSR still increases linearly but at a lower rate. Mixes with the lowest fly ash contribution will have the highest PSR. Mix 1, with a fly ash proportion of

4.2 percent provides the curve with the largest PSR values, while Mix 2, with the highest fly ash proportion, provides the lowest. The PSR curve for Mix 3 is between these two. The PSR for the three mixes is taken along the curves at 12.5 percent, 10.7 percent, and 3.6 percent silica fume proportion.

When put in terms of fly ash proportion for silica fume varying from 3.6 to 12.5 percent, the same *w/cm* range, and hydration, a similar PSR curve can be created. For Mix 1 with the same *w/cm* of 0.190, a silica fume proportion of 12.5 percent, and hydration of 47 percent, the fly ash proportion can be varied between 0 and 30 percent. The cement content, like the silica fume example, will decrease to accommodate the changing fly ash proportion to keep the same *w/cm*. Thus, *w/c* will increase as the fly ash proportion increases. The same concept is applied to Mix 2 with a *w/cm* of 0.180 and silica fume proportion of 10.7 percent and Mix 3 with a *w/cm* of 0.182 and silica fume content of 3.6 percent. The location of the PSR along each curve for each mix is marked, and the resulting curves are displayed in Figure 4.6.

There is a linear decrease in PSR as the proportion of fly ash increases. This has the opposite trend of silica fume proportion, which has an increasing PSR as silica fume increases. Mix 1 and 2 have the largest silica fume proportions, at 12.5 and 10.7 percent, and highest PSR curves. The difference between the two curves will be the *w/cm* used in the model. Mix 3, with the lowest silica fume proportion at 3.6 percent, has the lowest PSR curve. The PSR value for each mix is, again, plotted along the fly ash curve.
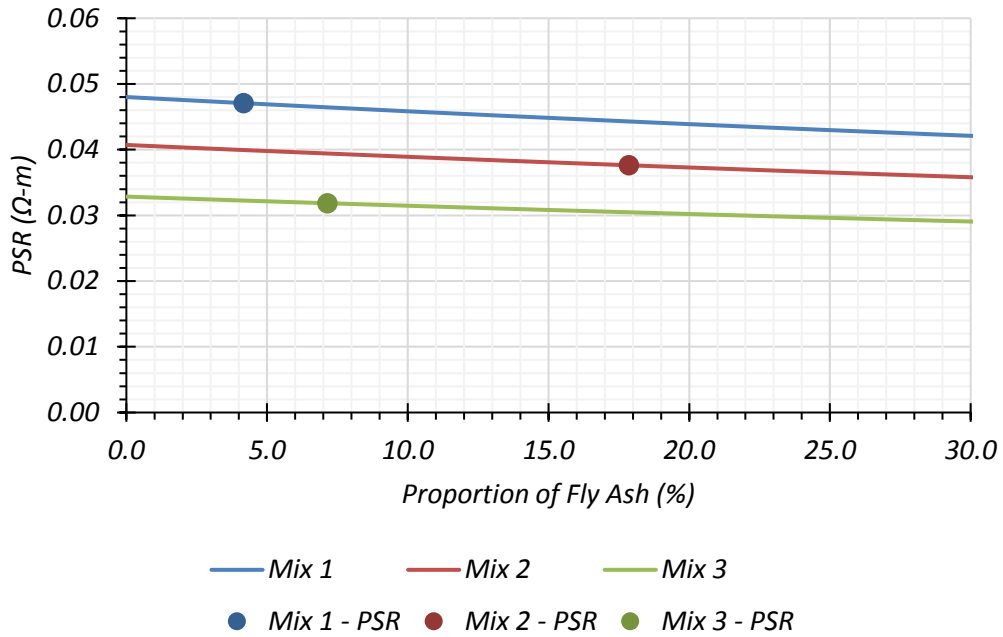
Figure 4.6. Fly Ash Proportion as a Function of PSR for UHPC Mixes

4.7. Formation Factor

Recall Equation (2.1), where the formation factor is calculated as the ratio of bulk resistivity to PSR.

$$F = \frac{1}{\phi\beta} = \frac{\rho}{\rho_o} = \frac{D_o}{D}$$

The PSR was calculated using the inverse of the conductivity values from the NIST model, in Table 4.11, and using the conservative estimate of 0.1 Ω-m from AASHTO PP84 (2018). The inverse of conductivity (S/m) is resistivity (Ω-m). The inverse of 21.29, 26.59, and 31.27 S/m for the UHPC mixes means the PSR values are 0.047, 0.038, and 0.032 Ω-m. It should be noted that the bulk resistivity values are recorded in kΩ-cm, and

the PSR values will have to be converted to the appropriate units. Any error from the NIST model prediction is magnified in the formation factor calculation, which is why the most conservative approach, using 0.1 Ω-m, is also calculated. Due to the high bulk resistivity values, a high formation factor value is predicted despite any error in the PSR determination. At 28 days, the bulk resistivity is averaged for two batches per mix, which means the eight measurements between Mix 1b and 1c are averaged, eight for Mix 2a and 2b are averaged, and nine for Mix 3a and 3b are averaged. The formation factor is then calculated. Table 4.13 has the summary information for resistivity and the calculated formation factor.

Table 4.13. Formation Factor for Non-Proprietary UHPC at 28 Days

Mix ID	Bulk Resistivity Average at 28 days (kΩ-cm)	Pore Solution Resistivity from the NIST Model (kΩ-cm)	Formation Factor from NIST Model	Formation Factor Using 0.01 kΩ-cm
Mix 1	106	0.0047	22,488	10,588
Mix 2	107	0.0038	28,407	10,688
Mix 3	58.7	0.0032	18,435	5871

To classify a mixture in the very low range for permeability according to ASTM C1202 (2017) and Table 3.3, the formation factor between is 2080 and 20,700. Exceeding 20,700 classifies a mixture in the negligible range for permeability. Using the NIST model PSR estimates, the calculated formation factor for Mix 1 and 2 exceed 20,700, which

means these mixes correlate to the negligible chloride penetration rating. Mix 3, at 18,435, falls in the very low range. When a higher, more conservative PSR is used, all values still exceed 2080, which is required to classify in the very low range. The higher formation factor indicates, regardless of PSR assumptions, a low chloride ion penetration, discontinuous pore structure, and a dense microstructure; all of which correlate to better durability performance.

4.8. Abrasion Resistance

The larger diameter dressing wheel and load will result in a higher percentage of total mass loss and mass loss per cycle compared to the results in the literature. The dressing wheels originally on the machine are 1.5 in. (38 mm) and serve as a comparison to the larger wheels. For the 1.5 in. (38 mm) diameter wheels with a load of 44 lbf (197 N), one specimen per surface were tested while three specimens per surface were tested for the 2-3/8 in. (60 mm) wheels.

Figure 4.7 displays the abrasion resistance results as the total percentage of mass loss for each surface type, mix, and dressing wheel after 10 minutes of abrading. For the 1.5 in. (38 mm) and 2-3/8 in. (60 mm) dressing wheels, the ground surface performed the best for all mixes. However, the cast and molded surfaces behaved differently for each wheel. The smaller wheel produced a higher mass loss for a molded surface than the cast surface for two of the mixes, while the bigger wheel produced mass losses significantly larger for cast surfaces than molded surfaces. Also, for the larger wheel, the concrete with the highest compressive strength performed better for all surface preparations, which correlates to the findings by Pyo et al. (2018) that conclude the abrasion resistance is

directly related to the compressive strength of the concrete. The results with the larger wheel could be applicable to bridge deck concrete, and with the total percentage of mass losses less than 1.25 percent for all mixes, the results are promising. When compared to NSC, UHPC typically exhibits three to seven times lower abrasion mass loss (Pyo et al. 2018). Additional work is required to see if changing specimen curing, cement type, or age will have a significant impact on the results with the larger wheel. Due to the limited data on abrasion resistance testing for non-proprietary UHPC, this data can prove to be an essential reference.
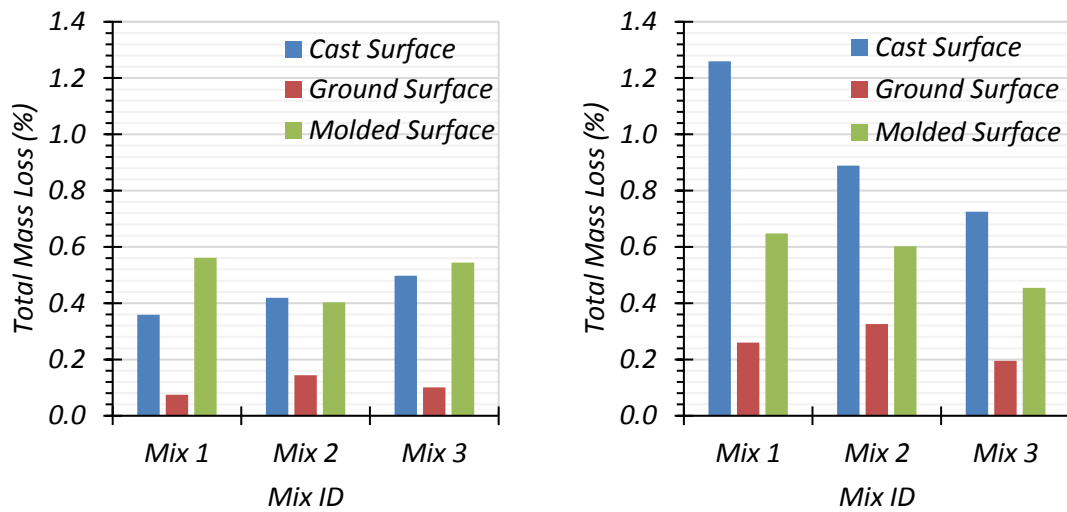
(a) 1.5 in. Dressing Wheels   (b) 2-3/8 in. Dressing Wheels

Figure 4.7. Percentage of Total Mass Loss after 10 Minutes for Abrasion Resistance

In Figure 4.8, the specimens for Mix 1, 2, and 3 after 10 minutes under the 1.5 in. (38 mm) dressing wheel are shown. The original surface preparation for each surface type is shown at the top of the diamond formation, with Mix 1 specimens on the left, Mix 2 specimens on the right, and Mix 3 specimens at the bottom of the shape. In the center of some specimens, there is still part of the original surface, and on the ground surface, the tracks from the dressing wheels are noticeable.

(a) Cast – Mix 1, 2, 3   (b) Ground – Mix 1, 2, 3   (c) Molded – Mix 1, 2, 3
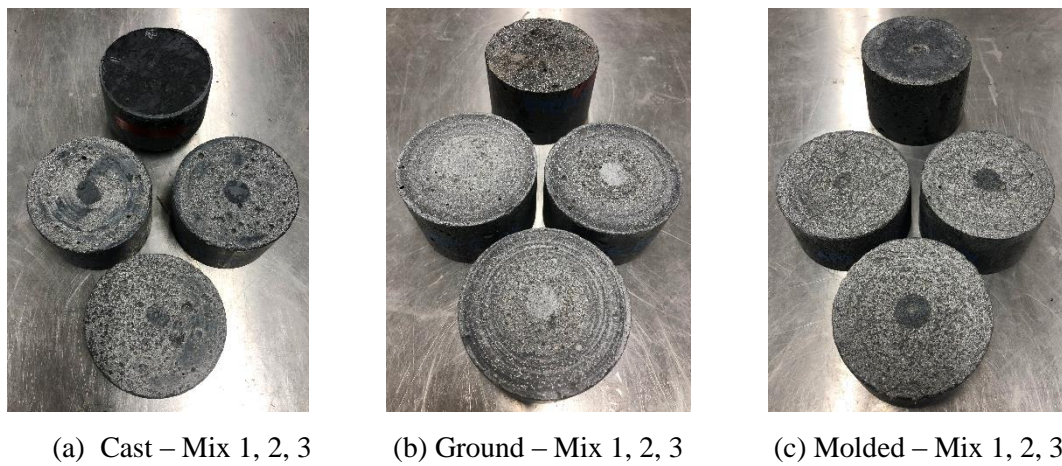
Figure 4.8. Abrasion Resistance Specimens after 10 Minutes of Abrading with 1.5 in. (38 mm) Dressing Wheels

Figure 4.9 shows the results for all specimens tested with the 2-3/8 in. (60 mm) dressing wheel. When compared to the specimens tested with the 1.5 in. (38 mm) dressing wheels, the specimens tested with the 2-3/8 in. (60 mm) dressing wheels show far more damage to the top surface. For the cast surfaces, the abraded surface revealed a large

number of air voids when compared to the ground and molded surface. The molded surface exhibited the least amount of air voids upon visual inspection. Because the test specimens came from a single cut 4x8 in. (100x200 mm) cylinder, the air void locations indicate more successful compaction at the bottom of the cylinder than at the top.

(a) Mix 1 – Cast Surface   (b) Mix 2 – Cast Surface   (c) Mix 3 – Cast Surface

(d) Mix 1 – Ground Surface   (e) Mix 2 – Ground Surface   (f) Mix 3 – Ground Surface

(g) Mix 1 – Molded Surface   (h) Mix 2 – Molded Surface   (i) Mix 3 – Molded Surface

Figure 4.9. Abrasion Resistance Specimens After 10 Minutes of Abrading with 2-3/8 in. (60 mm) Dressing Wheels

5. SERVICE LIFE PREDICTIONS

Life-365 is a commercially available software for service life modeling of conventional concrete (Ehlen 2018). This model uses Fick's second law as the primary equation and has additional features that account for variability in location, exposure type, structural component, and temperature (Ehlen 2018). For proprietary UHPC, service life estimations were made using the error function solution to Fick's second law, Equation (2.2), and including the formation factor (Spragg et al. 2019). However, as discussed in the literature, this equation assumes a chloride diffusion coefficient independent of outside variables and constant concentration and does not account for the type of reinforcement bars (Bentz et al. 2014). While Life-365 was designed for conventional concrete systems, its applicability to UHPC needs to be further explored, and then, a more thorough representation of service life prediction can be made.

Initial service life predictions for non-proprietary UHPC can be made similar to those performed by Spragg et al. (2019) for proprietary UHPC. The service life predictions are based on the formation factor calculated from bulk resistivity testing and PSR. In this study, the PSR from the NIST model (NIST 2017) along with the assumed value are used in the error function solution to Fick's second law, Equation (2.2), to provide an initial service life estimate. Because of the assumptions associated with this equation, the results only serve as a gauge and are be more thoroughly assessed through more comprehensive software estimations in Life-365. Life-365 can add simulations based on temperature, structural component, and location to the service life feature, which allows for more

comparative assessment between UHPC mixes and others used in similar applications. Once the applicability to UHPC is better understood, the formation factor can be implemented in this software to estimate service life. The service life predictions calculated in this section are only based on the corrosion initiation phase and do not include the subsequent propagation and cracking phase because the service life of a prestressed strand, according to Riding et al. (2017), is assumed to end at the chloride threshold which is equal to the initiation phase. The initiation phase, as described in the literature, is the time required for the chlorides from the environment to penetrate the concrete and collect on the surface of the steel in large enough quantities for corrosion to begin, and is, essentially, just the onset of corrosion (Ehlen 2018). The propagation phase, in Life-365, is defined as the time required for corrosion to reach an unacceptable level and the sum of the initiation and propagation phases are equal to the time of first repair (Ehlen 2018). The propagation phase has a default value of six years for black and stainless steel while the epoxy-coated steel has a default value of 20 years (Ehlen 2018). Additionally, service life predications are based on a component level and do not account for the entire structure or the differences in durability from one component to another.

5.1. Life-365 Parametric Study

Due to the limitations of the error function solution to Fick's second law, which were discussed in the literature review, service life predictions using Life-365 were performed to give a better indication of service life. Initial limitations of Life-365 were identified upon initiation of the parametric study. The lowest *w/cm* supported by Life-365 is 0.25, and was, therefore, used because it is closest to the *w/cm* of the non-proprietary UHPC

mixes in this study. Recall that the three non-proprietary UHPC *w/cm* values are between

0.180 and 0.190. Additionally, in Life-365, the mixture proportions must be entered as

percentages instead of mass. While this aspect is beneficial in the parametric study because

as one SCM content increases, the cement contribution is automatically decreased to still

maintain a cementitious content of 100 percent, it could be problematic for accurately

capturing the mechanisms of UHPC. UHPC has significantly higher cementitious content

than traditional concrete systems and based on the laboratory durability study and

literature review has shown to possess different mechanism characteristics. The full effect

of mixture proportions, *w/cm*, and SCMs for UHPC application is explored further.

Life-365 has seven options for surface chloride concentration, in Table 5.1, based

on the proximity to the ocean and structural component. Because this study is primarily

focused on the applicability of non-proprietary UHPC for pretensioned bridge girders, the

urban highway bridge (UHB) concentration values are used. To provide a comparison, a

more extreme exposure type, marine spray zone (MSZ), is also used.

**Table 5.1. Life-365 Chloride Surface Concentration Categories and Values
(adapted from Ehlen 2018)**

Proximity	Maximum C_s (%)
Marine Splash Zone	0.80
Marine Spray Zone	1.00
Within 0.5 miles (800 m) of the Ocean	0.60
Within 0.9 miles (1.5 km) of the Ocean	0.60
Parking Garage	0.80
Rural Highway Bridge	0.56
Urban Highway Bridge	0.68

Notes: 1. C_s: Chloride surface concentration

To determine the applicability of Life-365, a parametric study was conducted on a slab and beam example using the mixture proportions from the select non-proprietary mix designs. This study aimed to determine the effect of silica fume, fly ash, *w/cm*, location, and exposure type on the service life predictions.

5.1.1. Deck Example

A deck was analyzed to determine the effect of each parameter on the service life. While this research is primarily focused on UHPC pretensioned girders, the idea of a UHPC deck should not be eliminated. In fact, by performing this study, it can be determined whether a UHPC deck or overlay should be considered as an option to provide increased service life. A typical TxDOT bridge deck of 8.5 in. (216 mm) thickness with a 2.5 in. (64 mm) clear cover was used (TxDOT 2020). The constant parameters in this study include the thickness and clear cover mentioned and an analysis period of 500 years. Through preliminary evaluation, it was found that Life-365 is most sensitive to silica fume proportion, clear cover, fly ash proportion, and then *w/cm*.

5.1.1.1. Effect of Fly Ash

To determine the effect fly ash has on service life calculations in Life-365, two exposure conditions and three locations were chosen. The two exposure conditions include the UHB and MSZ, and the three locations in Texas include Corpus Christi (CC), Amarillo (AM), and Austin (AU). The UHB has a maximum chloride surface concentration of 0.68 percent, while the MSZ is a more extreme exposure with a maximum concentration of 1.0 percent. The location selection provides a temperature cycle that affects the diffusion properties of the concrete (Ehlen 2018). Using the default values, Corpus Christi will go

through a yearly temperature cycle where the absolute temperature difference is approximately 29°F (16.1°C). The absolute difference in Amarillo is 44°F (24.4°C) and in Austin is 36°F (20.0°C). The exposure selection relates to the surface chloride concentration and rate of chloride ingress. The combination of exposures and locations are found in Table 5.2.

Table 5.2. Location and Exposure Types for Parametric Study

Location	Exposure Type	Nomenclature	Maximum C_s (%)
Corpus Christi, TX	Marine Spray Zone	CC-MSZ	1.00
Corpus Christi, TX	Urban Highway Bridge	CC-UHB	0.68
Amarillo, TX	Urban Highway Bridge	AM-UHB	0.68
Austin, TX	Urban Highway Bridge	AU-UHB	0.68

Recall that Table 4.12 summarizes the mix proportions for each mix. Mix 1 has 83.3 percent cement, 12.5 percent silica fume, and 4.2 percent fly ash. Mix 2 has the highest SCM contribution with 71.4 percent cement, 10.7 percent silica fume, and 17.9 percent fly ash. Mix 3 has the lowest SCM contribution with 89.6 percent cement, 3.6 percent silica fume, and 6.8 percent fly ash. Because silica fume contribution has a significant effect on the service life, Mix 1 and 3 are used in the silica fume parametric study, and Mix 2 is used to understand the effect of fly ash.

To evaluate the influence of fly ash content, Mix 2 is considered with the *w/cm* adjusted to the lowest value available in Life-365, which is 0.25. The silica fume

proportion by mass is 10.7 percent, and black steel is considered. The location and exposure type are varied. Figure 5.1 shows the curves for each location when the percentage of fly ash is varied between 0 and 25 percent. The results show that as fly ash proportion increases at a fixed *w*/*cm*, silica fume content, location, and exposure, service life at 25 percent fly ash contribution is two to three times higher than the same mix without fly ash. When the study is run in the most extreme exposure and location, CC-MSZ, the service life predictions are the lowest while those run in AM-UHB are the highest. CC-UHB and AU-UHB produce similar curves with the location AU producing slightly larger predictions. For the 17.9 percent fly ash content used in Mix 2, the predictions vary from 162 to 472 years, all of which are quite high. These values are, most likely, overestimated due, in part, to the high silica fume content of 10.7 percent. When the benefits of fly ash are combined with an already high silica fume content, Life-365 appears to provide unrealistically high service life predictions. This sensitivity is tested further in the silica fume parametric study for Mix 1 and Mix 3.
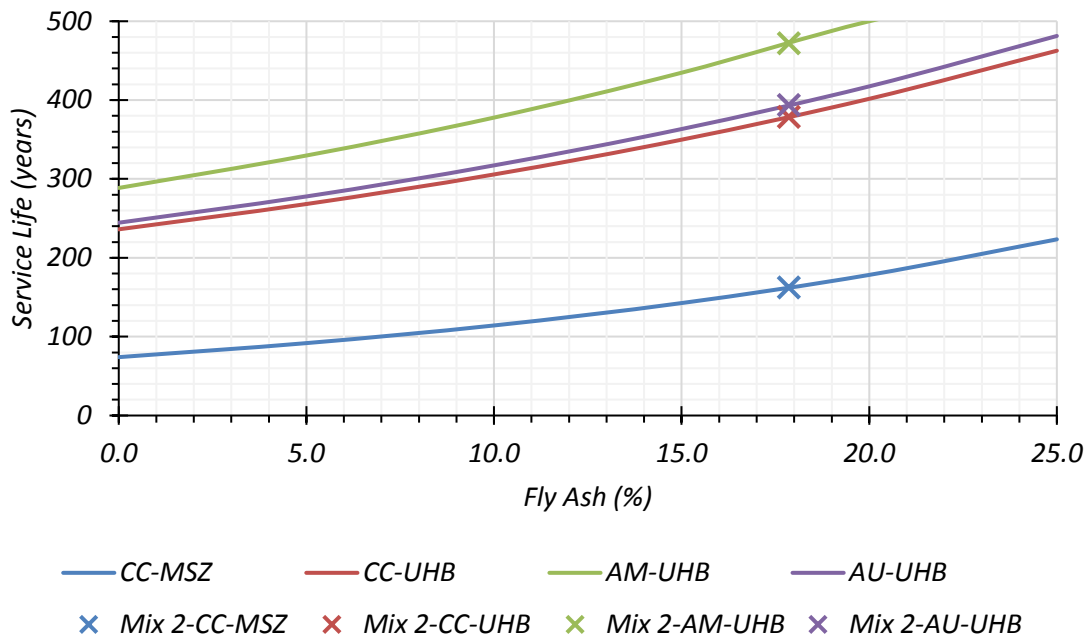
Figure 5.1. Impact of Fly Ash Content on Service Life Predictions for an 8.5 in. (216 mm) Deck using Adjusted Mix 2

5.1.1.2. Effect of Silica Fume

A similar approach was taken to determine the effect of silica fume on service life predictions. Life-365 is significantly affected by the presence of silica fume in the mixes. Mix 1 and 3 have comparable fly ash proportions at 4.2 and 6.8 percent. The average of the two, 5.5 percent, is used as a constant with the same minimum value of 0.25 *w/cm* selected and black steel assumption. Silica fume is varied from 0 to 15 percent by percent mass. Figure 5.2 shows the curves for each location considered, versus the percentage of silica fume. The values for Mix 3 are found along the curve. However, the values for Mix 1 would be slightly lower than the curve because the fixed fly ash content of 5.5 percent is higher than the actual, which is 4.2 percent. The increase in silica fume proportion, as

shown in Figure 5.2, results in a more exponential increase when compared to the effect of increasing fly ash, shown in Figure 5.1. A mix in the CC-MSZ exposure will see a service life prediction increase by 11 times if the maximum contribution of silica fume is added. In other locations and exposure conditions, this value is up to four times higher. This significant increase in service life with increasing silica fume content indicates that Life-365 could be oversensitive to changes in silica fume content that is not necessarily reflected in UHPC. Therefore, Life-365 predictions for Mixes 1 and 2 could be overestimated because of the abundant silica fume proportion while Mix 3 could be underestimated due to its low silica fume proportion. In a normal system, the filler effect of silica fume is exponentially more than fly ash, and it continues to hydrate while creating a dense microstructure, which was explained in the resistivity results.
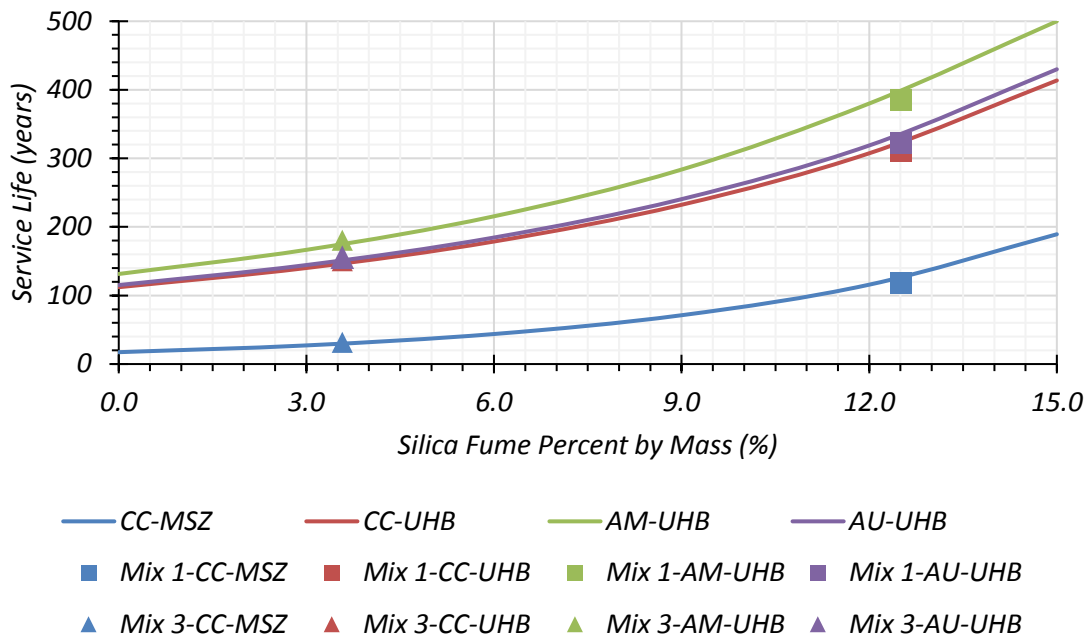
Figure 5.2. Impact of Silica Fume Content on Service Life Predictions for an 8.5 in. (216 mm) Deck using Adjusted Mix 1 and 3

The service life predictions for each mix at each location and exposure combination for the deck parametric study are summarized in Table 5.3. Mixes in the MSZ exposure have the lowest service life prediction due to the extreme environment, while those in the AM region have the highest service life prediction of the three locations.

Table 5.3. Service Life Predictions Based on Default Conditions in Life-365 for an 8.5 in. (216 mm) Deck with a 2.5 in. (64 mm) Cover

Mix ID	CC-MSZ	CC-UHB	AM-UHB	AU-UHB
Mix 1	119	311	385	323
Mix 2	162	379	472	394
Mix 3	32	151	180	156

Notes: The *w/cm* is set to the lowest value of 0.25.

93

5.1.1.3. Effect of w/cm

Because the considered UHPC mixes have a *w/cm* of 0.180 to 0.190, an additional study was performed to determine how changing the *w/cm* affected the results for service life estimates. A *w/cm* of 0.25 was used in all service life calculations because it is the lowest *w/cm* that can be assigned in Life-365. Mixes with a *w/cm* of 0.25 and 0.30 were considered using the mixture proportions for Mix 1, 2, and 3. Shown in Figure 5.3, the effect of *w/cm* was most apparent in the CC-MSZ condition, where each mix experienced higher reductions in service life as the *w/cm* increased. When *w/cm* is increased by 0.05, Mix 1 and 2 have a 24 percent decrease in service life predictions, and Mix 3 experienced a 23 percent decrease. When the exposure condition is changed to UHB, the differences are less noticeable. Service life only decreased by 12 to 16 percent for each mix as *w/cm* increased by 0.05. Compared to silica fume or fly ash contribution, the effect of the change in *w/cm* is much lower. As *w/cm* increases from 0.25 to 0.30, the service life decreases, but because the *w/cm* ranges for the three non-proprietary UHPC mixes is 0.180 to 0.190 there might be a small increase in service life, than what is derived in Table 5.3. Because Life-365 cannot accommodate a *w/cm* below 0.25, this cannot be verified, but the trends can provide insight into what might be expected for lower *w/cm* values.
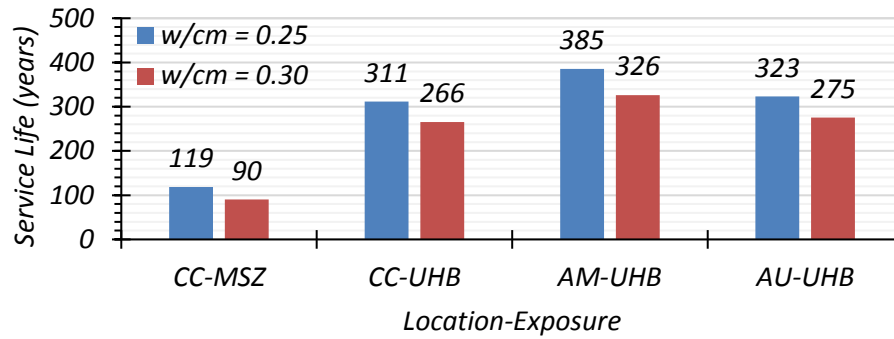
(a) Mix 1
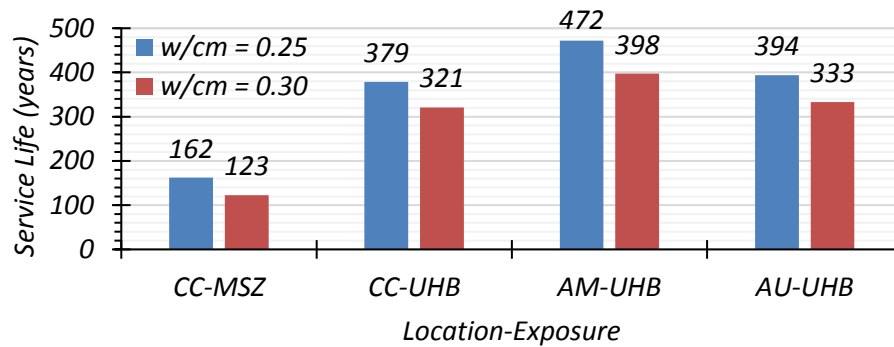
(b) Mix 2
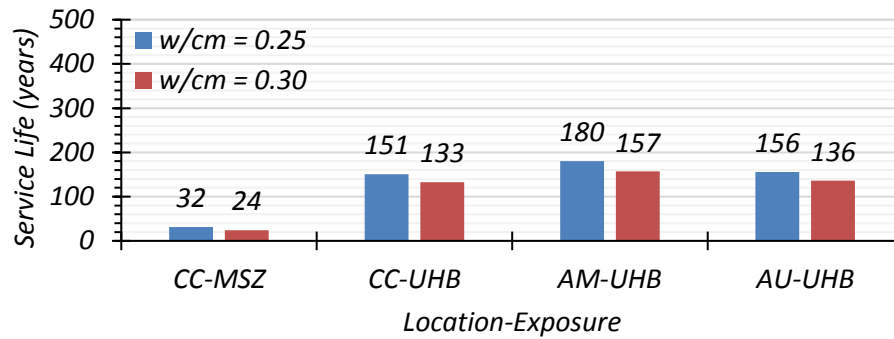
(c) Mix 3

Figure 5.3. Parametric Study on the Effect of *w/cm* on Service Life Predictions for an 8.5 in. (216 mm) Deck

5.1.2. Bridge Girder Example

The bridge girders under consideration have a smaller clear cover than the deck. A similar parametric study was performed on a beam with a similar area to the Tx34 I-girder. The Tx34 girders have an area of 627 in^2 (0.40 m^2) and a minimum clear cover of 1.5 in. (38 mm) (TxDOT 2020). To give the appropriate area, a 25x25 in. (635x635 mm) beam with a total area of 625 in^2 (0.40 m^2) and a clear cover of 1.5 in. (38 mm) was studied under the same conditions as the deck.

Similar trends were found for the effect of fly ash and silica fume in the beam with silica fume proportion affecting the service life calculation more than fly ash. The most notable difference between the deck and beam examples is the computed service life, which could be due to the decrease in clear cover. The service life of the beam is approximately 71 percent lower for the CC-MSZ exposure condition and 56 percent lower in the other locations with UHB exposure. Figure 5.4 provides the service life predictions based on the mixture proportions of the three non-proprietary UHPC mixes for different locations and exposure conditions.
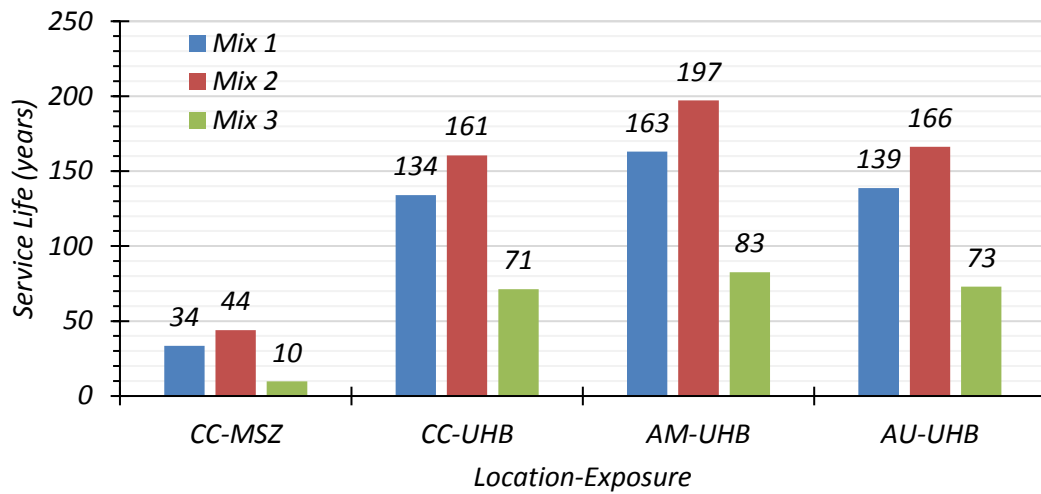
Figure 5.4. Service Life Predictions for a Tx34 Girder under Different Exposure Conditions

5.2. Limitations of Life-365 for UHPC

After the parametric study and subsequent evaluation, certain applicability issues became clearer with respect to modeling UHPC in Life-365. The *w/cm* limitation of 0.25 was investigated and a 12 to 16 percent reduction in service life was noted when *w/cm* increased by 0.05 in moderate exposure conditions. More significant effects were found when changing the silica fume and fly ash content, cover dimension, structural component, and exposure condition.

In combination with other factors like low water content, UHPC mixes rely on SCMs to create optimum particle packing. An additional limitation includes the available SCM parameters in this software. Life-365 only includes Class F fly ash, slag, and silica fume. The fly ash proportion cannot exceed 50 percent, slag cannot exceed 70 percent, and silica fume cannot exceed 15 percent. While the fly ash and slag proportions are

acceptable for UHPC, the silica fume maximum contribution is low. The proprietary mixes, displayed in Table 2.2, have silica fume contents exceeding 15 percent or another SCM, like silica powder, not available (Park et al. 2015; Russell and Graybeal 2013). In the non-proprietary mixes, displayed in Table 2.3, particularly the mixes from El-Tawil et al. (2018) and Subedi et al. (2019) have a silica fume contribution over 15 percent.

To provide further context on the role of silica fume, consider a conventional cast-in-place deck concrete with a w/cm of 0.40, cement content of 600 to 650 lb/yd^3 (356 to 386 kg/m^3), fly ash replacement level of 20 to 25 percent, and silica fume replacement of 5 percent. If the silica fume replacement increases from 5 to 15 percent, a significant increase in service life will be predicted by Life-365 because all the positive mechanisms of silica fume contribute to the hydration. These mechanisms include acting as a filler material, nucleation which results in accelerated cement hydration, and pozzolanic reaction. These attributes were also briefly discussed in the resistivity test results. Life-365 is designed to represent a conventional concrete system, which would undergo these positive mechanisms. When Life-365 is used for UHPC, it assumes that the silica fume mechanism and contribution are similar. However, UHPC has an added filler effect with the improved particle packing density, and there could be less contribution from accelerated cement hydration or pozzolanic reaction. The lack of water and very high cement content in UHPC may also restrict these contributions from fully taking effect, but Life-365 still assumes a very high contribution from these mechanisms. As a result, there is a chance for Life-365 to overestimate the effects of silica fume and produce a very high service life prediction. This could be the case for Mix 1 and 2 because of the high silica

fume proportion in the UHPC mix designs. For Mix 3, where silica fume content is low, Life-365 may be underestimating the service life because it assumes a lesser contribution from silica fume and the positive effects of high cement content and low w/cm are ignored.

Life-365 does not account for any type of superplasticizer. At such low w/cm and high powder content, the HRWR is required to form an adequate UHPC mix design. The dosage of HRWR may have more immediate effects on the workability or compression strengths of the concrete. However, long term durability could be affected if an insufficient dosage is used, which leads to less compaction and higher porosity (El-Tawil et al. 2018). Disregarding this parameter in the software could introduce unlikely expectations on performance.

Another drawback of Life-365 is the input for mixture proportions. Values are input as a percent instead of mass, which is where the differences in UHPC are found. Life-365 uses a default chloride threshold limit of 0.05 percent for service life calculations considering concretes containing 590 lb/yd^3 (350 kg/m^3) to 674 lb/yd^3 (400 kg/m^3) of cement, which indicates that program is meant for concretes with similar cement contributions (Ehlen 2018). The non-proprietary mixes developed in this study have cement contents that are double this range, from 1238 lb/yd^3 (734 kg/m^3) to 1579 lb/yd^3 (937 kg/m^3). This is additionally true in the other proprietary and non-proprietary UHPC mixes mentioned in the literature review (Berry et al. 2017; Khayat and Valipour 2018; Kim 2018; Mendonca et al. 2020; Park et al. 2015; Qiao et al. 2016; Russell and Graybeal 2013; Subedi et al. 2019; Weldon et al. 2010). So, while a concrete mix design might have the same proportions of cement, silica fume, and fly ash, the quantity of each could be

entirely different. Using an example mix design of 80 percent cement, 10 percent fly ash, and 10 percent silica fume, the differences in mix design can be shown in Table 5.4. Mix A would be closer to a UHPC mix design while Mix B is a mix with a cement content more suitable for Life-365. The difference in powder contents will have a significant impact on the mixture and durability characteristics.

Table 5.4. Mix Design Examples by Percent Weight

Mix ID	80% Cement (lb)	10% Silica Fume (lb)	10% Fly Ash (lb)	Total Cementitious Material (lb)
Mix A	1200	150	150	1500
Mix B	640	80	80	800

UHPC does not consist of coarse aggregate, and there is not a current input for aggregate selection or size in Life-365. If the coarse aggregate is, improperly, assumed to account for a percentage of the concrete mix, when there is none, it is not reflective of UHPC. The particle sizes in the coarse aggregate, and some sands, are too large to create the dense matrix. Certain relationships in the program, like the relationship between the diffusion coefficient and *w/cm,* are produced for concrete containing an aggregate of normal density (Ehlen 2018). This, among other assumptions used in Life-365, could be the reason why the diffusion coefficient calculated by Life-365 is significantly higher than the typical diffusion coefficient of proprietary UHPC, found as 3.10×10^{-11} in^2/s (2.00×10^{-14} m^2/s) (Ahlborn et al. 2008).

To further display the effect of the mixing proportions and diffusion coefficient, another example in Life-365 can be considered. Under the same assumptions for an 8.5 in. (216 mm) deck, 2.5 in. (64 mm) reinforcement depth, location in Corpus Christi, TX, and under a MSZ exposure, changing the diffusion coefficient can alter the results. Using the diffusion coefficients from Ahlborn et al. (2008) for NSC, HPC, and UHPC, diffusion decay index calculated from Life-365, and the chloride threshold of 0.05 percent the service life predictions can be calculated. These values are in Table 5.5. The predictions increase as the diffusion coefficient gets smaller, and the coefficient for UHPC causes the highest service life prediction.

Table 5.5. Life-365 Service Life Prediction Based on Diffusion Coefficients

Mix Type	Diffusion Coefficient (in^2/s) from Ahlborn et al. (2008)	Assumed Diffusion Decay Index	Service Life Prediction (years)
NSC	1.55×10^{-9}	0.28	29
HPC	7.75×10^{-10}	0.28	135
UHPC	3.10×10^{-11}	0.28	337

When Life-365 is left to use default settings to predict the service life, there are different results. The results are presented in Table 5.6. Using a mix with the same proportions as Mix A and B in Table 5.4 of 80 percent cement, 10 percent silica fume, and 10 percent fly ash while varying *w/cm* based on literature, the results are different. The result for NSC and HPC for the default and custom cases are more comparable, which

makes sense based on the typical cement amounts, 590 to 675 lb/yd^3 (350 to 400 kg/m^3), that were considered in developing Life-365 (Ehlen 2018). The service life prediction for UHPC, while still the highest in both examples, are different. The service life based on the literature-based diffusion coefficient (337 years) is over three times higher than the 102 years determined using the Life-365 default diffusion coefficient.

Table 5.6. Life-365 Service Life Predictions Based on Default Conditions

Mix Type	*w/c* Range from Ahlborn et al. (2008)	*w/cm* Used in Life-365	Diffusion Coefficient (in^2/s)	Diffusion Decay Index	Service Life (years)
NSC	0.40 – 0.70	0.48	3.68x10^{-9}	0.28	29
HPC	0.24 – 0.35	0.28	1.22x10^{-9}	0.28	86
UHPC	0.14 – 0.27	0.25	1.03x10^{-9}	0.28	102

It should also be noted that Life-365 does not account for any type of mechanical loading on the structure. Only the material level influences, which include the mixture design or diffusion properties, are included along with the environmental conditions, like temperature variations based on location and exposure to chlorides, to calculate the service life. Due to this limitation, the service life could be overestimated by Life-365 and caution should be taken when interpreting the results. In summary, Life-365 does have significant limitations for UHPC when using the default conditions, and even with alternate methods, like overriding the diffusion coefficient or diffusion decay index in the program, it is difficult to provide a definitive service life prediction for the mixes in this study and other

UHPC mixes in literature. Further work to improve Life-365 to accommodate UHPC is required and beyond the scope of this research. However, in combination with extensive permeability testing, the results from Life-365 can be used in a comparative assessment.

5.3. Fick's Second Law Service Life Calculations

Recall Equation (2.2), which is the error function solution to Fick's second law.

$$C_{x,t} = C_o + (C_s - C_o)\left(1 - erf\left(\frac{x}{2\sqrt{\frac{D_o}{F}t}}\right)\right)$$

This equation was used by Spragg et al. (2019) to estimate the service life of proprietary UHPC, and because the prediction stops at the chloride threshold, this prediction is equal to the initiation phase. It substitutes the diffusion coefficient for the ratio of the chloride self-diffusion coefficient, D_o, to the formation factor, F. The relationship between the diffusion coefficient, chloride self-diffusion coefficient, and formation factor was established by Snyder (2001). Appropriate values for all variables must be assumed in order to solve this equation for time and get a service life prediction. The chloride threshold limit, $C_{x,t}$, is an integral part of computing the service life. Higher thresholds will increase the service life, and when trying to estimate the service life of a system that has, so far displayed, superior durability characteristics, using lower limits in the calculation will make it more comparable to conventional concrete.

The limitations of this equation were discussed in the literature and expanded on by Bentz et al. (2014). As discussed earlier, Life-365 accounts for varying temperature cycles and exposure conditions. These temperature cycles affect the diffusion coefficient

and the exposures selected will affect the rate of chloride ingress. This equation is unable to account for the effect of temperature, time, chloride buildup, or the reinforcement type.

To provide a direct comparison to the service life predictions completed by Spragg et al. (2019) for proprietary UHPC, recall the selected values for each variable. The authors used $C_{x,t}$ of 0.05 percent, C_o of 0.02 percent, C_s of 0.5 percent for moderate chloride exposure, x of 2 in. (50 mm), D_o of 2.95x10^{-6} in^2/s (1.9x10^{-9} m^2/s), and F of 34,500. The resulting diffusion coefficient for the proprietary UHPC would be 8.54x10^{-11} in^2/s (5.51x10^{-14} m^2/s). The authors also used a PSR value of 0.05 Ω-m to calculate the formation factor. This value is comparable to the PSR values calculated by the NIST model for the non-proprietary UHPC mixes, which were found in Table 4.13. If the same PSR value of 0.05 Ω-m is also applied to the non-proprietary UHPC mixes, instead of those values calculated by the NIST model and assumption of 0.1 Ω-m, the formation factor values for Mix 1, 2, and 3 become 21,175, 21,375, and 11,742, respectively, which do fall between those formation factors calculated in Table 4.13. The resulting service life predictions are 127, 129, and 71 years for Mix 1, 2, and 3, respectively. Spragg et al. (2019) calculated a conservative prediction of 210 years for the proprietary UHPC mixtures studied, and the results from the non-proprietary UHPC Mix 1 and 2 are approximately 37 percent lower while the Mix 3 prediction is 65 percent lower.

To provide appropriate comparisons to Life-365, the variables must be adjusted. A chloride threshold, $C_{x,t}$, of 0.05 percent is a default value in Life-365 and is based on a mixture containing 15 percent cement by volume (Ehlen 2018). This correlates to 590 lb/yd^3 (350 kg/m^3) to 674 lb/yd^3 (400 kg/m^3) of cement. Among other factors, an increase

in cement content by volume could increase the threshold value. However, by increasing this parameter, the service life will also increase, and it becomes unrealistic for comparative purposes. The initial chloride concentration, C_o, is set to 0 percent (Ehlen 2018). The surface concentration, C_s, is another parameter that can be varied based on the exposure type. For comparative purposes with Life-365, the UHB exposure with a surface concentration of 0.68 percent was used for this sample calculation. The MSZ exposure, with a concentration of 1.0 percent, could also be used. An additional value for the chloride self-diffusion coefficient, D_o, comes from literature. The cover distance, x, chosen is based on the cover distance for a deck according to TxDOT (TxDOT 2020). If a calculation for a girder were used, then the cover depth would decrease to 1.5 in. (38 mm) and the service life would subsequently decrease as well. The following assumptions for the variables are summarized in Table 5.7.

Table 5.7. Variable Assumptions for Fick's Second Law Corresponding to a Bridge Deck in the Urban Highway Bridge Exposure

Variable	Variable Description	Assumption	Source
$C_{x,t}$	Chloride concentration at depth x and time t that initiates corrosion (%)	0.05	Ehlen (2018)
C_o	Initial chloride concentration (%)	0	Ehlen (2018)
C_s	Surface chloride concentration (%)	0.68	Ehlen (2018)
x	Depth to reinforcement (in.)	2.5	TxDOT (2020)
D_o	Chloride ion self-diffusion coefficient (in^2/s)	3.0×10^{-6}	Yuan-Hui and Gregory (1974); Spragg et al. (2019)
F	Formation factor	22,488 (Mix 1) 28,407 (Mix 2) 18,435 (Mix 3)	From Table 4.13
t	Time for exposure limit to be reached (s)	-	-

Recall the formation factors based on the NIST model PSR values that were originally provided in Table 4.13. Using the values from Table 5.7 and the NIST model formation factor values, solving for t in Equation (2.2) yields a prediction of 233, 294, and 191 years for Mix 1, Mix 2, and Mix 3, respectively.

If a more conservative formation factor value is used, which means assuming a PSR of 0.1 Ω-m, as recommended by AASHTO PP84 (2018) for conventional concrete, the formation factor decreases to 10,588, 10,688, and 5871. These values are also shown in Table 4.13. However, the applicability of 0.1 Ω-m PSR for UHPC may be questionable because the pore solution concentration (PSC) of the UHPC system should be higher than conventional concrete due to the high cement content and low w/cm. The higher the PSC,

the higher the conductivity, and thus, the lower the resistivity. In this regard, the PSR estimation based on the NIST model appears to be more representative of the UHPC system. However, the more conservative estimate of 0.1 Ω-m is used to determine the resulting service life values for comparison. When using this higher PSR, the service life decreases to 110, 111, and 61 years respectively, for Mix 1, Mix 2, and Mix 3. If the cover distance is decreased, to model the cover for the girder, then the calculated service life decreases further. The initial service life predictions for the NIST model PSR values are promising. However, the significant decrease in service life when a more conservative formation factor is used shows the influence of the PSR when using Equation (2.2). Therefore, a more reliable method for assessing PSR followed by estimating service life for the UHPC system is necessary.

5.4. Service Life of UHPC Based on Custom Diffusion Coefficient

Some limitations for Life-365 were noticed during the parametric study, particularly the heavy influence of silica fume proportion, the software calculations for the diffusion coefficient, and resulting service life in more extreme exposures. To more accurately reflect UHPC, service life calculations using mixture proportions and *w/cm* were not used. Instead, custom inputs using the diffusion coefficient calculated from the formation factor are input into the program, which gives the potential for this software to more accurately reflect UHPC.

Using the relationship between D_o, F, and D, which were established in Equation (2.1) by Snyder (2001), the diffusion coefficient, D, can be calculated as the ratio of the chloride self-diffusion coefficient, D_o, to the formation factor, F. The formation factor is

a ratio of the bulk resistivity to the PSR. Similar to the error function solution to Fick's second law calculation, the formation factor calculated from the conservative PSR, 0.1 Ω-m, is used. Using the self-diffusion coefficient, from Yuan-Hui and Gregory (1974), in Table 5.7 as 3.0×10^{-6} in^2/s (1.9×10^{-9} m^2/s) divided by the formation factor the diffusion coefficient can be calculated and compared to the default diffusion coefficients calculated by Life-365. Additionally, once the diffusion coefficient from Life-365 is obtained, a formation factor can be calculated to compare to the laboratory value. These values are presented in Table 5.8.

Table 5.8. Diffusion Coefficient Calculated from the Formation Factor and Life-365

Mix ID	D_F (in^2/s)	D_L (in^2/s)	Formation Factor from Resistivity Testing	Formation Factor from Life-365
Mix 1	2.78×10^{-10}	6.83×10^{-10}	10,588	4310
Mix 2	2.76×10^{-10}	9.18×10^{-10}	10,688	3208
Mix 3	5.02×10^{-10}	2.98×10^{-9}	5871	989

Notes: 1. D_F: Diffusion coefficient calculated from the formation factor
               2. D_L: Diffusion coefficient calculated by Life-365

Lowering the diffusion coefficient will increase the service life calculation and calculating the diffusion coefficient based on the formation factor has effectively reduced this value for all mixes. It can be additionally shown that the formation factor, based on the diffusion coefficient from Life-365, while still considered in the very low chloride ion penetration classification according to the correlation established by AASHTO PP84

(2018) and repeated in Table 3.3, is severely underestimated for Mix 3. By entering this custom value, Life-365 bypasses the mixture inputs for material proportions and *w/cm*.

Another parameter that can be changed for UHPC is the diffusion decay index. The diffusion coefficient will reduce as the concrete matures and hydrates, and this value describes this change as a function of time (Ehlen 2018). By default, this value has a range in Life-365 of 0.20 to 0.60 with higher values indicating higher hydration and producing a higher service life. Because UHPC has an approximate hydration of 47 percent, according to Acker and Behloul (2004), the lowest value of 0.20 is chosen for the diffusion decay index.

5.4.1. Deck Slab

Using the same deck that was used in the parametric study, the diffusion coefficients calculated from the formation factor in Table 5.8, and a diffusion decay index of 0.20 a service life prediction for each non-proprietary UHPC mix was made. The predictions from Table 5.9 could indicate that UHPC would provide exceptional service life for deck applications with respect to chloride penetration. However, additional comparisons are required for mixes used in similar applications.

Table 5.9. Service Life Predictions for an 8.5 in. (216 mm) Deck Using Custom Inputs (years)

Mix ID	CC-MSZ	CC-UHB	AM-UHB	AU-UHB
Mix 1	240	479	500+	486
Mix 2	242	482	500+	500+
Mix 3	134	334	414	347

When these service life predictions are compared to those predictions based on the default conditions in Life-365, shown in Figure 5.5, they are higher. The most significant increases in service life are in Mix 3, which has a lower SCM content than the first two mixes. Life-365 analysis has indicated to SCM proportion based on the parametric study, and the predictions for Mix 3 could be much lower due to that. Using the diffusion coefficient from the default conditions in Life-365, found in Table 5.8, the formation factor is also calculated. This formation factor is 60 to 70 percent lower than the formation factor calculated from the bulk resistivity measurements and PSR of 0.1 Ω-m. Similar to the service life predictions, Mix 3 also has the largest difference in formation factor values. The formation factor from the default conditions is 83 percent lower than the one calculated based on laboratory testing. The tabulated service life predictions, in years, based on the two formation factors for the deck are found in Table 5.10.

Table 5.10. Service Life Predictions (years) for an 8.5 in. (216 mm) Deck based on the Formation Factor

Mix ID	Mix 1		Mix 2		Mix 3	
Formation Factor	10,588	4310	10,688	3208	5871	989
CC-MSZ	240	119	242	162	134	32
CC-UHB	479	311	482	379	334	151
AM-UHB	500+	385	500+	472	414	180
AU-UHB	486	323	500+	394	347	156
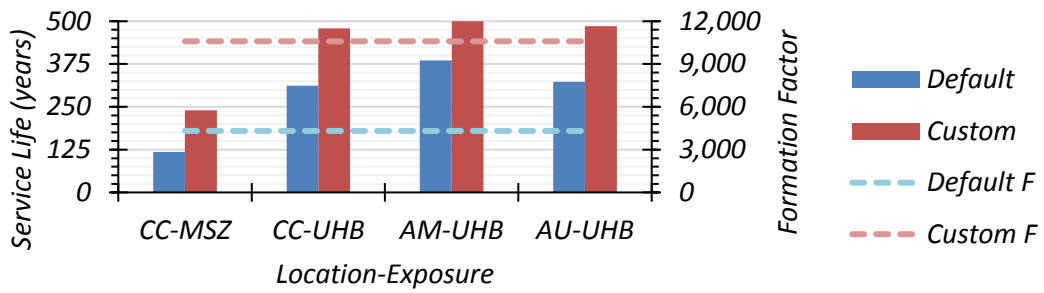
(a) Mix 1
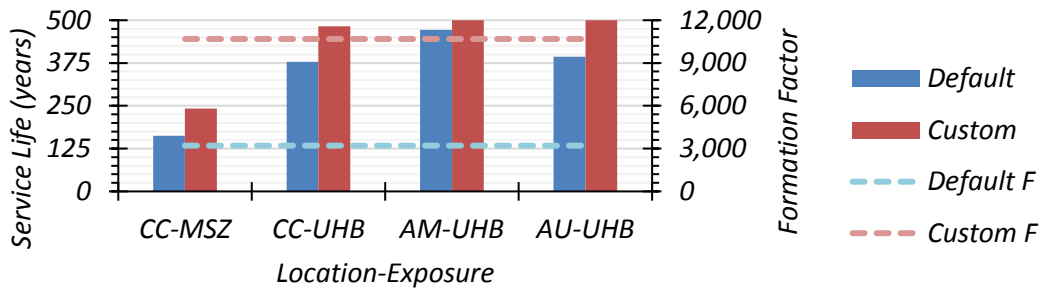
(b) Mix 2
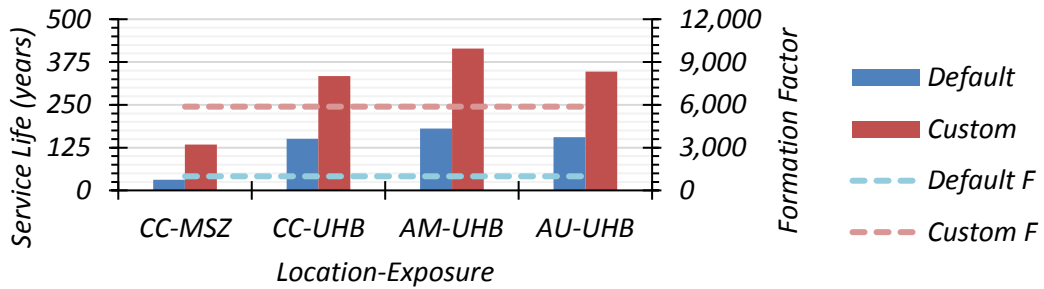
(c) Mix 3

Notes: 1. Default: Service life based on the default conditions in Life-365
         2. Custom: Service life based on the diffusion coefficient calculated from the formation
            factor and a diffusion decay index of 0.20
         3. Default F: Formation factor calculated from the Life-365 diffusion coefficient under
            default conditions
         4. Custom F: Formation factor calculated from bulk resistivity and a PSR of 0.1 Ω-m

**Figure 5.5. Comparing Service Life Predictions for an 8.5 in. (216 mm) Deck
based on the Formation Factor**

5.4.2. Tx34 and Tx54

The Tx34 bridge girder was partially analyzed in the parametric study and was found to have a shorter service life than the deck slab example when default conditions are used. In addition to the Tx34 girder, a larger beam based on a Tx54 bridge girder was studied. The Tx54 girder section has an area of 817 in^2 (0.53 m^2) and a minimum clear cover of 1.5 in. (38 mm) (TxDOT 2020). To give the appropriate area, a 30x30 in. (762x762 mm) beam with a total area of 900 in^2 (0.58 m^2) and a clear cover of 1.5 in. (38 mm) was studied under the same location and exposure conditions.

A similar correlation between the default and custom values is made for the two girder shapes. In Table 5.11, the default and custom formation factors along with the service life predictions are displayed for the 25x25 in. (635x635 mm) beam simulation for a Tx34 girder for each of the three mixes and the four combinations of location and exposure.

Table 5.11. Service Life Predictions (years) for a Tx34 Girder based on the Formation Factor

Mix ID	Mix 1		Mix 2		Mix 3	
Formation Factor	10,588	4310	10,688	3208	5871	989
CC-MSZ	67	34	68	44	38	10
CC-UHB	300	134	201	161	143	71
AM-UHB	248	163	250	197	175	83
AU-UHB	208	139	209	166	148	73
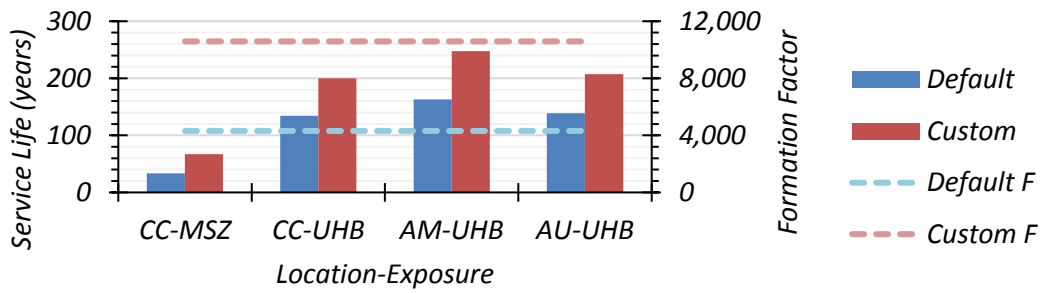
(a) Mix 1
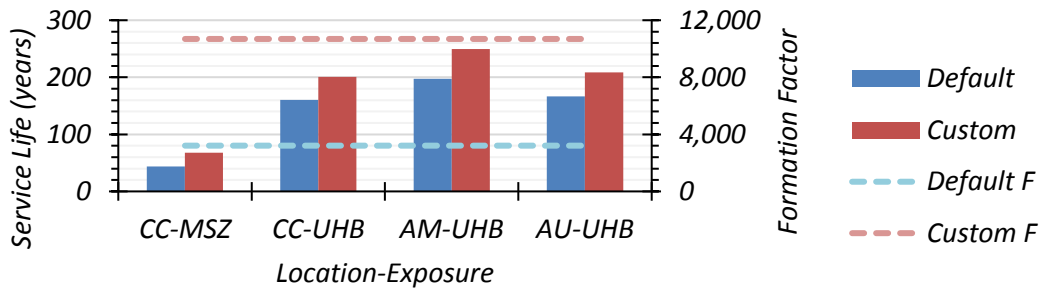
(b) Mix 2
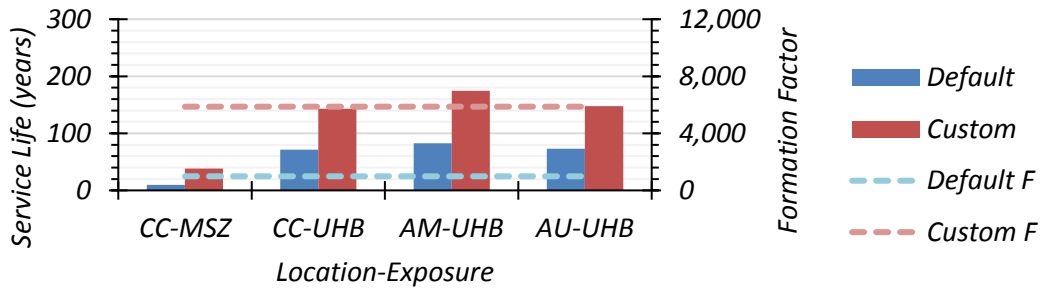
(c) Mix 3

Notes: 1. Default: Service life based on the default conditions in Life-365
2. Custom: Service life based on the diffusion coefficient calculated from the formation factor and a diffusion decay index of 0.20
3. Default F: Formation factor calculated from the Life-365 diffusion coefficient under default conditions
4. Custom F: Formation factor calculated from bulk resistivity and a PSR of 0.1 Ω-m

Figure 5.6. Comparing Service Life Predictions for a 25x25 in. (635x635 mm) Beam (Tx34) based on the Formation Factor

For the Tx34 simulation, shown in Figure 5.6, the benefit of the custom conditions is most clearly seen in the results for Mix 3. The default conditions estimate a service life that is 75 percent lower than the custom conditions in MSZ. Similarly, in the UHB exposure across all locations, the predictions for default conditions are still 51 percent lower than the custom conditions. Mix 1 has the next largest difference in service life prediction. Default conditions produce an estimate that is 50 percent lower for MSZ exposure and 33 percent lower in the UHB exposure. Mix 2 has the smallest difference in approximations at 35 percent for MSZ and 20 percent for UHB.

The service life predictions based on the custom and default formation factors are calculated for the 30x30 in. (762x762 mm) beam simulation, representing a Tx54 girder and produce similar results to the Tx34 girder simulation. The tabulated values are shown in Table 5.12.

Table 5.12. Service Life Predictions (years) for a Tx54 Girder based on the Formation Factor

Mix ID	Mix 1		Mix 2		Mix 3	
Formation Factor	10,588	4310	10,688	3208	5871	989
CC-MSZ	73	36	74	48	41	10
CC-UHB	210	140	211	168	150	74
AM-UHB	261	171	262	207	183	86
AU-UHB	218	145	220	175	155	76
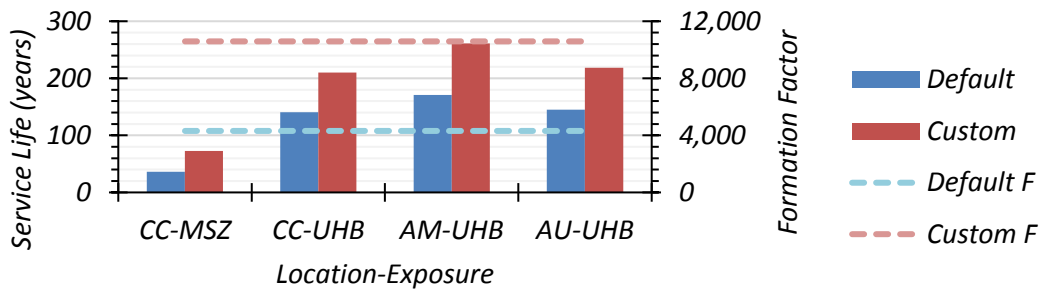
(a) Mix 1
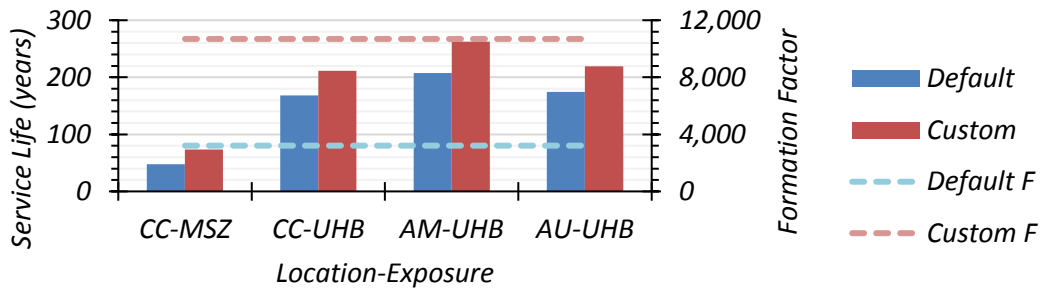
(b) Mix 2
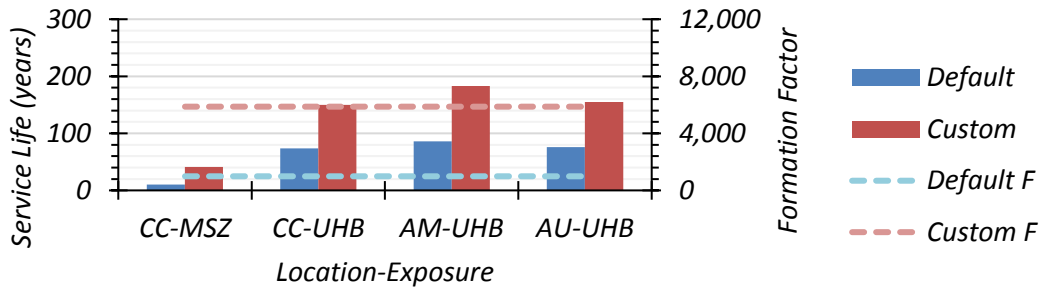
(c) Mix 3

Notes: 1. Default: Service life based on the default conditions in Life-365
2. Custom: Service life based on the diffusion coefficient calculated from the formation factor and a diffusion decay index of 0.20
3. Default F: Formation factor calculated from the Life-365 diffusion coefficient under default conditions
4. Custom F: Formation factor calculated from bulk resistivity and a PSR of 0.1 Ω-m

Figure 5.7. Comparing Service Life Predictions for a 30x30 in. (762x762 mm) Beam (Tx54) based on the Formation Factor

The results from the 30x30 in. (762x762 mm) beam simulation, representing a Tx54 girder, found in Figure 5.7, follows a similar trend to that of the Tx34 girder, shown in Figure 5.6. Mix 3 predictions are still vastly underestimated in the default conditions with the largest difference in prediction coming in the most extreme exposure. The default conditions, again, produce an estimate that is 75 percent lower in MSZ and 52 percent lower in UHB. Mix 1 has a decrease of 50 percent in default conditions under MSZ and 21 percent under UHB. The predictions for Mix 2 are closer with a 35 percent decrease in MSZ and a 21 percent decrease in UHB.

The service life of both girders can be directly compared for the custom conditions. The predictions for the Tx54 girder are 5 to 8 percent higher than the Tx34, and the simulations in the MSZ produce a much lower estimate. The direct comparison between the predictions is shown in Figure 5.8.

(a) CC-MSZ

(b) CC-UHB

(c) AM-UHB

(d) AU-UHB
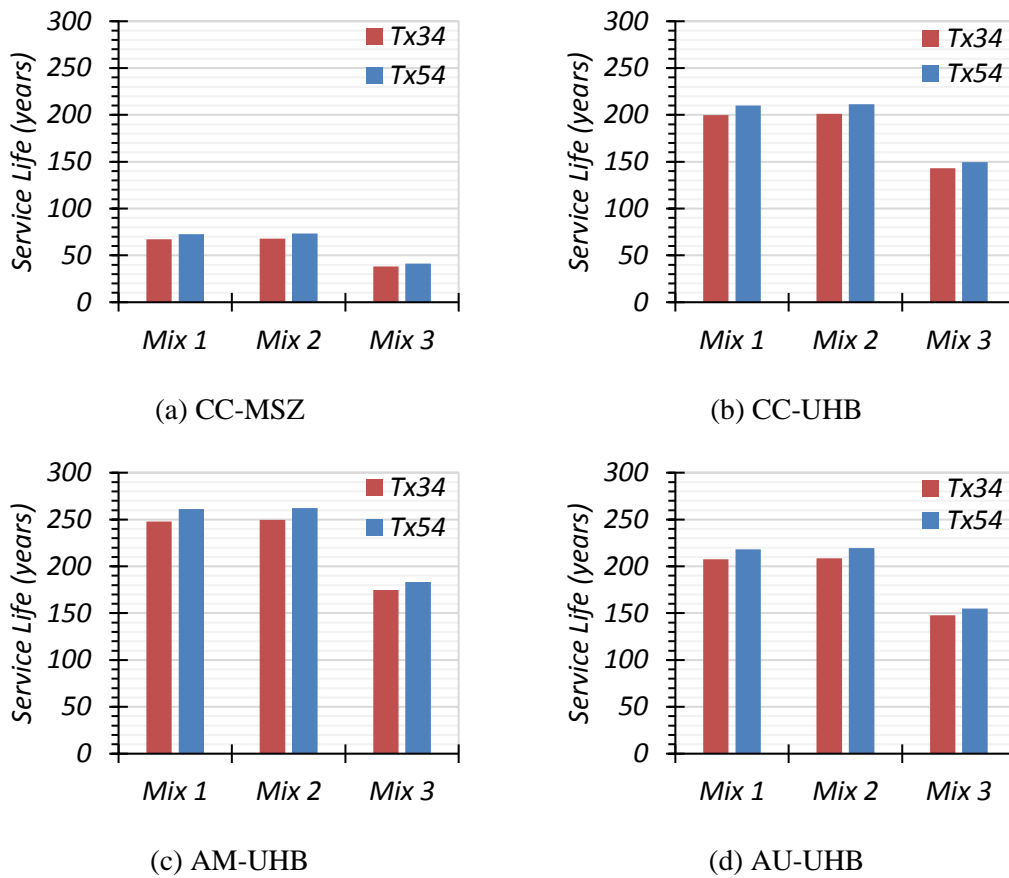
Figure 5.8. Service Life Predictions for a Tx34 and Tx54 using Custom Inputs

The predictions in AM under the UHB exposure have the longest predicted service life of the three locations and two exposure conditions. The simulations in the MSZ exposure are heavily affected with service life predictions less than 100 years for all three mixes. From the beam and slab simulations, the difference in service life predictions indicates that the girder would be the limiting structural component between the two if both were made of the same non-proprietary UHPC mix. For CC-MSZ, the girder predictions are approximately 71 percent lower than the slab. In more moderate exposures,

the girder predictions are between 52 and 57 percent less than the slab predictions. This difference could be decreased with a larger cover used for the girder simulation.

5.5. Comparison Between Fick's Second Law and Life-365 Predictions

The predictions from the error function solution to Fick's second law can be directly compared to the predictions from the custom inputs from Life-365 to determine the difference in results. Recall the variable assumptions in Table 5.7. In particular, the chloride threshold value of 0.05 percent and initial chloride concentration of 0 percent. Using these values along with the diffusion coefficients based on the formation factors for all three UHPC mixtures (Table 5.8), reinforcement depths for the bridge girder and bridge deck, and surface chloride concentrations for the MSZ and UHB, a prediction can be calculated for each mixture. The results are shown in Table 5.13.

Table 5.13. Service Life Predictions (years) Based on Fick's Second Law

Structural Component	Deck		Girder	
Exposure Type	UHB	MSZ	UHB	MSZ
Mix 1	111	93	40	33
Mix 2	112	94	40	34
Mix 3	62	51	22	19

These predictions are compared to the predictions from Life-365 across all locations and exposures. Recall the predictions from Table 5.9 for the service life predictions under custom conditions. The comparisons for the bridge deck simulation,

with a reinforcement depth of 2.5 in. (64 mm), are shown in Figure 5.9. Service life predictions under the MSZ exposure are more comparable than those under the UHB exposure. Under the MSZ exposure, the predictions based on Fick's second law are approximately 62 percent lower than the predictions based on the CC-UHB exposure from Life-365 across all mixes. Under the UHB exposure, the differences between the Fick's second law predictions and Life-365 are much larger. For Mix 1 and 2, the prediction based on Fick's second law is approximately 77 percent lower than the Life-365 service life prediction across the three locations. For Mix 3, the Fick's second law service life predictions are approximately 83 percent lower across the three locations.
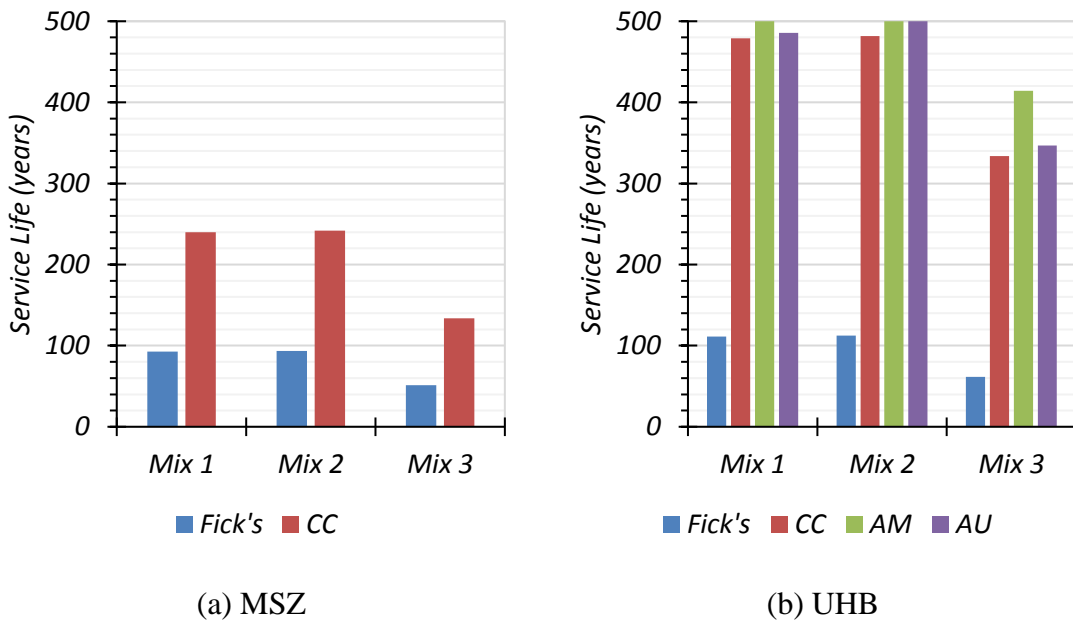
	(a) MSZ	(b) UHB

Notes: 1. Fick's: Service life prediction based on the error function solution to Fick's second law
2. CC: Life-365 service life prediction for Corpus Christi
3. AM: Life-365 service life prediction for Amarillo
4. AU: Life-365 service life prediction for Austin

Figure 5.9. Comparing Service Life (years) for an 8.5 in. (216 mm) Deck Using Fick's Second Law and Life-365

If a similar comparison is performed for the Tx34 bridge girder simulation, the difference in values is slightly smaller under the MSZ exposure but approximately the same under the UHB exposure. These values are presented in Figure 5.10. In the MSZ exposure, the value computed using the Fick's second law prediction is approximately 51 percent lower than the CC-MSZ Life-365 across all mixes. In the UHB exposure, Fick's second law is, on average, 81 percent lower than the Life-365 service life predictions for Mix 1 and 2. The difference in service life predictions for Mix 3 are a little larger at 86 percent across all locations.
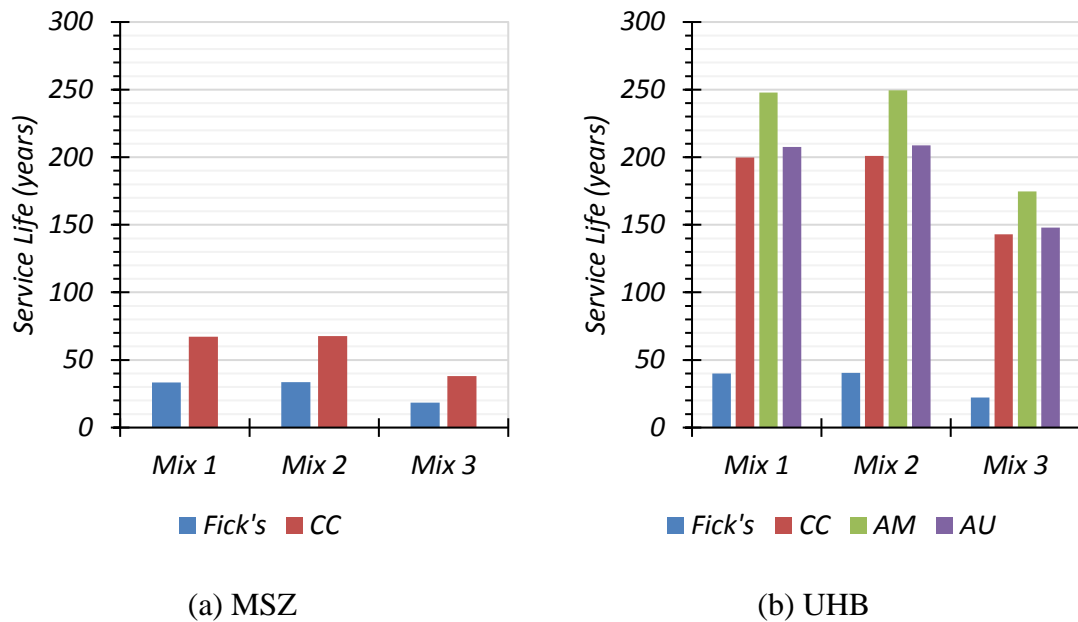
120

(a) MSZ   (b) UHB

Notes: 1. Fick's: Service life prediction based on the error function solution to Fick's second law
            2. CC: Life-365 service life prediction for Corpus Christi
            3. AM: Life-365 service life prediction for Amarillo
            4. AU: Life-365 service life prediction for Austin

Figure 5.10. Comparing Service Life (years) for a 25x25 in. (635x635 mm) Beam (Tx34) Using Fick's Second Law and Life-365

Service life calculations based on the error function solution to Fick's second law are consistently lower than those predictions from Life-365 with the MSZ exposure providing the closest comparisons between the two calculations options. The predictions using Fick's second law, as discussed in the literature, are known to have several limitations including, but not limited to, the assumptions associated with the diffusion coefficient, lack of reinforcement type, or constant surface chloride concentration. Life-365 service life predictions for UHPC have several different limitations including, but also not limited to, the silica fume mechanism, mixture proportion input, and the diffusion

121

coefficient relationships. These limitations go beyond the typical differences between the Fick's second law prediction and Life-365 predictions for conventional concrete, which could contribute to the large differences in the service life predictions for UHPC when comparing the results from the two methods.

5.6. Service Life of Mixes Used in Similar Applications Based on Custom Inputs

Using the diffusion coefficient from literature, a RCPT charge and formation factor can be correlated and provide a comparison to UHPC on multiple fronts. These comparisons are made using a combination of Equation (2.1), Table 3.3, and AASHTO PP84 (2018).

Russell and Graybeal (2013) provided a 28-day diffusion coefficient for proprietary UHPC of 2.02×10^{-10} in^2/s (1.3×10^{-13} m^2/s). Trejo et al. (2008) provided a 28-day diffusion coefficient of 2.50×10^{-9} in^2/s (1.61×10^{-12} m^2/s) for a SCC mix with a 16-hour target compressive strength of 7 ksi (48 MPa) in their study. Thomas et al. (2012) found a diffusion coefficient of 2.64×10^{-9} in^2/s (1.7×10^{-12} m^2/s) for a HPC mix with a *w*/*cm* of 0.35, 5 percent silica fume, and 20 percent fly ash that matches closely with the mix design from TxDOT Project 0-6958 (8/2020). Using Equation (2.1), the formation factor for the SCC and HPC mix can be calculated as the ratio of the chloride self-diffusion coefficient to the diffusion coefficient. This is done to provide a comparison to the UHPC mixes in this study and is presented in Table 5.14 using the relationships established in AASHTO PP84 (2018).

Table 5.14. Formation Factor and Chloride Ion Penetration Classification Based on the Diffusion Coefficients

Mix ID	Diffusion Coefficient (in²/s)	Formation Factor at 28 Days	Chloride Ion Penetration Classification
Proprietary UHPC	2.02×10^{-10}	14,615	Very Low
UHPC Mix 1	2.78×10^{-10}	10,588	Very low
UHPC Mix 2	2.76×10^{-10}	10,688	Very low
UHPC Mix 3	5.02×10^{-10}	5871	Very low
SCC	2.50×10^{-9}	1178	Low
HPC	2.64×10^{-9}	1118	Low

These diffusion coefficients, along with the diffusion decay index, can be used in Life-365 to calculate service life and provide a comparison to UHPC. All UHPC mixes have a diffusion decay index of 0.20. To calculate the decay index value for these additional mixes, Life-365 provides a conservative equation based on the SCM input (Ehlen 2018) and this is presented as Equation (5.1).

$$m = 0.2 + 0.4 \cdot \frac{FA}{50} \qquad (5.1)$$

Where:

m = Diffusion decay index

FA = Fly ash proportion in the mix design (%)

Using the mix proportions in Table 4.11, the diffusion decay index is calculated from Equation (5.1). For the HPC mix, the proportions from TxDOT Project 0-6958 (8/2020), have a fly ash contribution of 20 percent, and the diffusion decay index for this mix is 0.36. The SCC mix from Trejo et al. (2008) also has 20 percent fly ash and has the

same value of 0.36. The conventional PC mix has an approximate diffusion decay index of 0.26 according to Ehlen (2018) because it only contains Portland cement.

Using the same structural components and conditions, the four additional mixes can be evaluated for service life using Life-365. The maximum service life prediction is 500 years. For the deck slab, with the results shown in Figure 5.11, it is clear that the predictions for the UHPC mixes exceed that of HPC, SCC, and a conventional PC mix. The service life prediction for the proprietary UHPC is the highest and is compared to the non-proprietary UHPC results. Under CC-MSZ exposure, the proprietary UHPC mix has a service life approximately 27 percent higher for UHPC Mix 1 and 2 and 59 percent higher than UHPC Mix 3. For the UHB exposure, the difference between proprietary and non-proprietary UHPC Mix 1 and 2 is indistinguishable due to the 500-year service life analysis limitation in Life-365. UHPC Mix 3 has the lowest predicted service life of the UHPC mixes and can be used as a reference to the SCC, HPC, and conventional PC mixes. When compared to the UHPC Mix 3 in CC-MSZ, SCC has a predicted service life that is 51 percent lower, HPC 52 percent lower, and the conventional PC mix is 92 percent lower. The UHB exposure produces more comparable results across the three locations where SCC is an average of 33 percent less, HPC is 34 percent less, and conventional PC is 74 percent less.
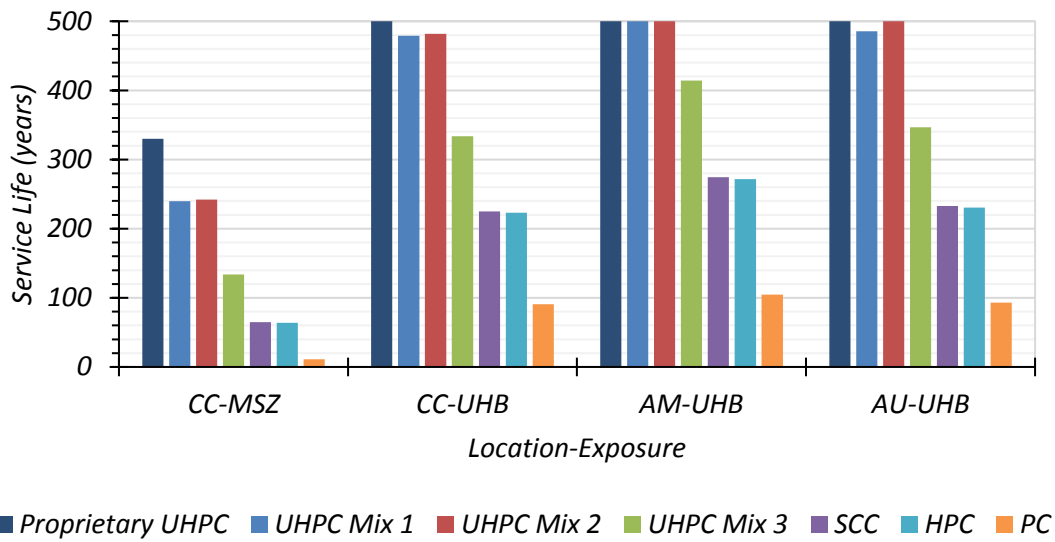
Figure 5.11. Service Life Predictions for UHPC, HPC, SCC, and a Conventional PC Mix for an 8.5 in. (216 mm) Deck

For the girder simulations, the trend is almost identical and is shown in Figure 5.12 and Figure 5.13. In the MSZ, the UHPC predictions are double the SCC and HPC results and significantly greater than the conventional PC results for both girder simulations. This result correlates to the rehabilitation study performed by Brühwiler and Denarié (2013), who stated that the positive durability properties of proprietary UHPC are exploited under extreme environmental conditions, like de-icing salts and marine environments, and mechanical loadings, like concentrated forces and fatigue impact. For the Tx54 simulations, compared to the proprietary UHPC, the non-proprietary UHPC Mix 1 and 2 have a service life prediction in the MSZ exposure approximately 26 percent lower while UHPC Mix 3 is 59 percent lower. In the UHB exposure, on average, UHPC Mix 1 and 2 have a service life prediction 18 percent lower than the proprietary UHPC and UHPC Mix

3 has a service life 42 percent lower. For the UHB exposures in the Tx54 simulation, compared to UHPC Mix 3, SCC has an average prediction that is 31 percent lower, HPC is 33 percent lower, and conventional PC is 68 percent lower. In the Tx34 simulation, the difference between proprietary and non-proprietary UHPC service life predictions are similar. Under the MSZ exposure, UHPC Mix 1 and 2 have a prediction approximately 25 percent lower, and UHPC Mix 3 has a prediction approximately 58 percent lower. In the UHB exposure, the difference between the proprietary UHPC predictions and non-proprietary UHPC Mix 1 and 2 predictions are 17 percent lower while UHPC Mix 3 is 41 percent lower. Under the same UHB exposure, the SCC and HPC predictions are approximately 31 percent and 32 percent lower than the UHPC Mix 3 predictions, respectively. UHPC vastly outperforms the conventional PC mix for both girder simulations across all locations and exposures studied.
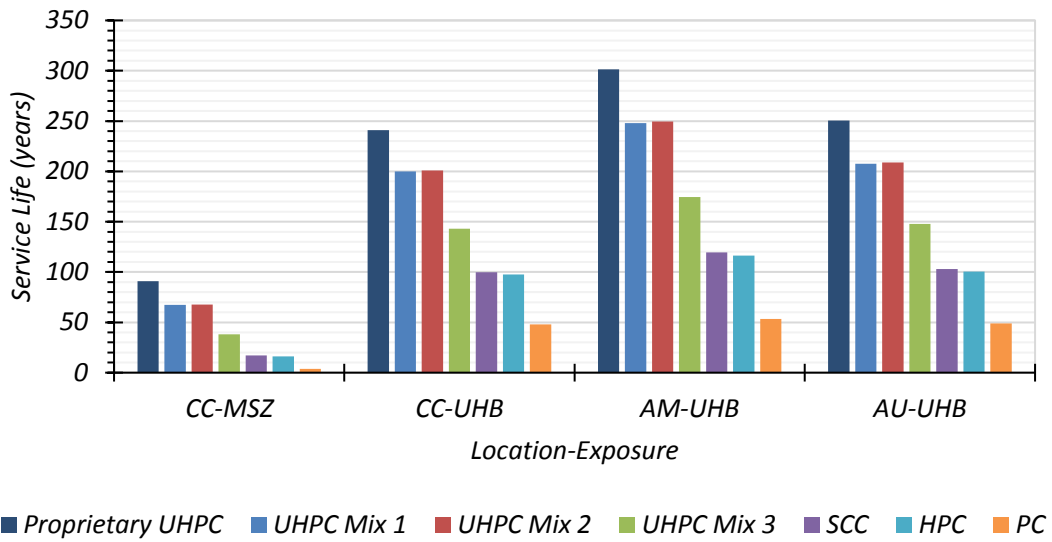
Figure 5.12. Service Life Predictions for UHPC, HPC, SCC, and a Conventional PC Mix for a 25x25 in. (635x635 mm) Beam (Tx34)
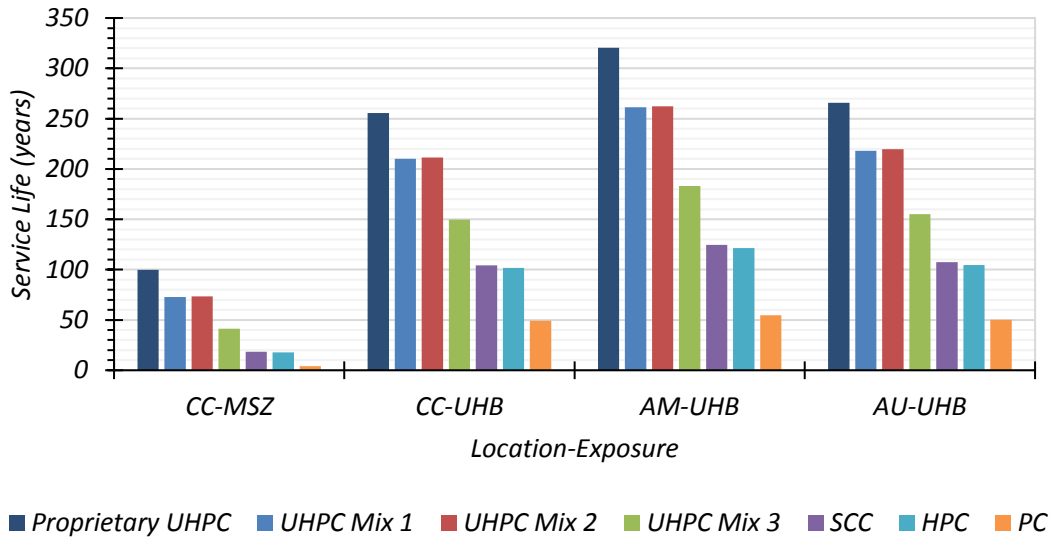
Figure 5.13. Service Life Predictions for UHPC, HPC, SCC, and a Conventional PC Mix for a 30x30 in. (762x762 mm) Beam (Tx54)

5.7. Conclusions

Life-365 provides service life calculations based on the mechanisms of typical concrete mixtures and for structural components. The limitations of Life-365 for UHPC were noted because the actual mechanism of UHPC is very different from a conventional system. Adjustments were made in the UHPC predictions and comparisons to limit the influence of these parameters. By using the diffusion coefficient based on the formation factor and using the smallest diffusion decay index allowed, this study attempted to bypass some of these limitations, which include the mix proportion inputs and *w/cm* influence. However, these limitations remain, and the results should not be taken as definite values for service life. When the service life for the non-proprietary UHPC mixes is compared using the error function solution to Fick's second law and Life-365, the predictions using only Fick's second law are significantly lower. However, that equation could produce unrealistically low results for more conventional systems which was shown in the literature (Spragg et al. 2019). When using the same parametric comparisons, like the diffusion coefficient, it has been shown that even the non-proprietary UHPC mix with the lowest predictions, which is the most unconventional UHPC mixture design because of the low SCM content, still exceeds those of SCC, HPC, and conventional PC mixes across all methods of study. These relative comparisons have their own limitations in accuracy because they are based on the absolute values but can provide additional understanding on the influence of various parameters in Life-365.

6. SUMMARY, CONCLUSIONS, AND FUTURE RESEARCH

RECOMMENDATIONS

6.1. Summary

The objectives of this research were to determine the durability, in terms of permeability, and service life of non-proprietary UHPC made with local Texas materials for use in pretensioned bridge girders. The materials include a Type I/II cement, silica fume, Class F fly ash, HRWR, river sand smaller than a No. 16 sieve, and 0.5 in. (13 mm) long with 0.008 in. (0.2 mm) diameter steel fibers. Steel fibers were included in the abrasion resistance testing at 1.5 percent by volume.

6.1.1. Durability Testing

Through RCPT, resistivity, and the formation factor, indirect verification of permeability is made for each non-proprietary UHPC mixture. Bulk and surface resistivity are nondestructive tests and allowed for multiple measurements on the same specimen over the course of testing. Measurements were recorded at 7, 14, 28, and 56 days. At 56 days, select specimens were used for RCPT, and those remaining were tested for resistivity again at 90 days. The bulk resistivity measurements at 28 days are used to calculate a formation factor that can describe the pore connectivity and porosity of the system.

Mix 1 and 2 have similar mix design characteristics due to the higher SCM contribution, and they also have a significantly higher SCM contribution than Mix 3. Mix 1 has 12.5 percent silica fume and 4.2 percent fly ash, while Mix 2 has a slightly lower

silica fume proportion at 10.7 percent, but a much higher fly ash proportion at 17.9 percent. The higher SCM proportion is typical of both proprietary and non-proprietary UHPC mixes. Mix 3 has 3.6 percent silica fume and 6.8 percent fly ash and is the most unconventional of the UHPC mixes studied due to its low SCM contribution. This mix was created with the explicit goal of achieving high early strength without heat-treatment or an accelerator agent for prestressing.

Supplemental testing for abrasion resistance was performed for all three mixes using two different dressing wheels. Three surface preparations were also tested and include cast, ground, and molded surfaces.

6.1.2. Service Life Study

After the laboratory evaluation on durability, the three non-proprietary UHPC mixes underwent a further study to calculate the service life. The service life was defined as including only the initiation period, or the time it takes to reach the chloride threshold. A parametric study using Life-365 was performed to determine the effect of silica fume, fly ash, structural component, exposure, w/cm, and location on service life, and determine the limitations of the default values calculated by the program. Once the limitations for UHPC applicability were better understood, steps were taken to minimize or bypass default parameters in Life-365. Calculations for service life using the error function to Fick's second law helped facilitate the implementation of the formation factor into the service life prediction, while also serving as an additional comparison to the Life-365 service life predictions. The formation factor can be used to calculate the diffusion coefficient. Subsequent manipulation of both the diffusion coefficient and the diffusion decay index

allowed better implementation of UHPC and provided the opportunity for a comparative assessment. However, certain limitations in accuracy remain.

Using the customized entries in Life-365, the three non-proprietary UHPC mixes were modeled for three structural components. An 8.5 in. (216 mm) thick deck with a 2.5 in. (64 mm) reinforcement cover dimension was modeled to simulate a bridge deck while two beams, one 25x25 in. (635x635 mm) and another 30x30 in. (762x762 mm), were modeled to simulate bridge girders with a cross-sectional area and cover distance comparable to a Tx34 and Tx54 bridge girder. Three locations across Texas were studied along with two exposure conditions.

Three additional mixes, including SCC, HPC, and conventional PC mix designs were also modeled and used the same custom diffusion coefficient entry to calculate service life. The service life predictions of the supplementary mixes were compared to the non-proprietary UHPC mix designs to provide additional understanding on the influence of the parameters in Life-365 and the benefits of UHPC.

6.2. Conclusions

Based on the results of this study, the following conclusions were made.

6.2.1. Rapid Chloride Penetration Test

1) Mix 1 and 2 measured charge passed values below 100 Coulombs. This correlates to a negligible chloride ion penetration classification.

6.2.2. Resistivity

1) Surface resistivity testing correlates to RCPT classifications and by 14 days all mixtures without steel fibers measure in the low or very low chloride ion penetration range. By 28 days, Mix 3 also classifies in the very low classification.

2) Bulk resistivity values for Mix 3 are between 50 and 75 percent of the values of Mix 2. As the specimen ages, the difference in resistivity values between these two mixes increases. Mix 1 follows a trend similar to Mix 2, which indicates that Mix 1 and 2 have a lower permeability than Mix 3.

3) The differences in Mix 1 and 2 and Mix 3 resistivity data could be attributed to the large difference in SCM contribution. Silica fume typically provides additional benefits like filling micropores, accelerating cement hydration, or undergoing pozzolanic reaction at early ages, and when combined with fly ash, could explain the difference in measurements.

4) Steel fibers significantly impacted the resistivity readings. The mixture with steel fibers measured 75 percent lower than the same mixture without steel fibers.

6.2.3. Pore Solution Resistivity

1) Pore solution resistivity was estimated for the three non-proprietary UHPC mixes using the NIST model, and all values are below 0.05 Ω-m.

2) Due to the higher cementitious content and low *w/cm* in UHPC, the pore solution concentration of UHPC could be higher, which means conductivity will be higher,

and the resulting pore solution resistivity should be lower. However, using the 0.1 Ω-m pore solution resistivity assumption still provided adequate results.

6.2.4. Formation Factor

1) When using the estimated pore solution resistivity of 0.1 Ω-m, all formation factors correlate to a chloride ion penetration of very low at 28 days.

6.2.5. Abrasion Resistance

1) The different sized dressing wheels produced opposite results for the surface types tested. Under the 1.5 in. (38 mm) dressing wheels, the molded surface specimens experienced less total mass loss than the cast surface specimens for two of the mixes, while the 2-3/8 in. (60 mm) dressing wheel caused the cast surface specimens to experience a higher percentage of total mass loss than the molded surface specimens for all three mixes.

2) The ground surface exhibited the lowest total mass loss for all mixes and dressing wheels tested.

3) Mix 3 performed better under the larger dressing wheel for the cast, ground, and molded surface when compared to Mix 1 and Mix 2. However, under the smaller dressing wheel Mix 1 and 2 experienced slightly less total mass loss.

6.2.6. Service Life Predictions

1) Life-365 can calculate the service life for structural components but does not account for the entire structure or the differences in durability from one component to another.

2) The parametric study on Life-365 indicated that this software has a sensitivity to silica fume contribution, which can result in inflated service life predictions.

3) Life-365 is intended for conventional concrete, and the mechanism of silica fume in the software may not be representative of the mechanism of silica fume in UHPC. UHPC has the added benefit of particle packing density and low water content which, on its own, creates positive changes in the system that are not present in the conventional system.

4) Limitations for Life-365 were found for UHPC applications. These limitations include,

    a. SCM proportions limited to Class F fly ash, silica fume, and slag,

    b. Silica fume mechanism is based on a conventional concrete system,

    c. *w/cm* cannot be less than 0.25,

    d. Superplasticizer input is not available to offset the high powder content,

    e. Mixture proportions are entered in percent instead of weight,

    f. Aggregate input is not available, and

    g. Diffusion coefficient and *w/cm* relationship are based on concrete mixtures containing aggregates of normal density.

5) Based on these limitations, Life-365 is unable to give a definite service life prediction for UHPC mixtures.

6) Because Life-365 service life predictions are influenced by SCM proportion, particularly silica fume, is it possible that Life-365 overpredicts the service life of Mix 1 and Mix 2 while underpredicting the service life of Mix 3.

7) Life-365 predicts a higher service life for Mix 1 and Mix 2 compared to Mix 3 across all locations and exposures studied.

8) A custom diffusion coefficient and diffusion decay index were entered that were more reflective of the UHPC diffusion coefficient found in literature and the results from the durability testing. When a similar procedure is used for the SCC, HPC, and conventional PC mixtures and the resulting service life predictions are compared to the non-proprietary UHPC predictions, Life-365 calculates a lower service life prediction for the supplementary mixes than for the UHPC mixes.

9) When the service life predictions for non-proprietary UHPC are compared using the error function solution to Fick's second law and the custom diffusion coefficients in Life-365, the predictions from Fick's second law are between 50 and 86 percent lower than the Life-365 predictions for the two structural components studied.

10) When the service life predictions for proprietary and non-proprietary UHPC are compared using the custom diffusion coefficient input, Life-365 predicts a service life for the non-proprietary Mix 1 and 2 that is approximately 27 percent lower than the proprietary UHPC mix under the MSZ exposure for all structural components and 18 percent lower in the UHB exposure for the girder components. The non-proprietary Mix 3, compared to the proprietary UHPC, has a service life prediction in Life-365 approximately 59 percent lower in the MSZ for all structural components studied and 42 percent lower in the UHB exposure for the girder components.

11) While the service life predictions in Life-365 are not absolute, for the bridge girder simulations Life-365 predicts a service life for SCC and HPC that is approximately 56 lower than UHPC Mix 3 in the marine spray zone exposure condition and 32 percent lower in the urban highway bridge exposure condition across the three locations of study. Life-365 predicts a service life for the conventional PC mix that is 90 percent lower than UHPC Mix 3 in the marine spray zone and 68 percent lower in the urban highway bridge exposure condition across the three locations. Similar relative values were found for the bridge deck simulation and are also not absolute due to the limitations in Life-365 for UHPC.

12) UHPC has a lower diffusion coefficient than SCC, HPC, and conventional PC mixtures which, despite a higher diffusion decay index being used for the supplementary mixes, still causes Life-365 to predict longer service life for UHPC.

13) The service life predictions for an 8.5 in. (216 mm) deck with a 2.5 in. (64 mm) cover exceeded the predictions of the two beams, one 25x25 in. (635x635 mm) and another 30x30 in. (762x762 mm), that have comparable areas and cover distances to a Tx34 and Tx54 bridge girder across all locations and exposure combinations studied.

14) The service life simulations in the Amarillo region produced higher service life predictions than the simulations in the Corpus Christi or Austin region under the same exposure type.

15) The largest differences in service life predictions, calculated by Life-365, between UHPC and the supplementary mixes occurred under the Corpus Christi marine spray zone exposure conditions.

16) Combined with the laboratory durability testing and service life study through Life-365, initial studies indicate that the three non-proprietary UHPC mixtures exhibit lower permeability and higher abrasion resistance while also providing a high service life prediction when using a diffusion coefficient based on the formation factor.

17) These non-proprietary mixes could be beneficial for prestressed girders or other bridge applications.

6.3. Future Research Recommendations

1) Measurements for resistivity provided useful insight into the development of the non-proprietary UHPC mixes. By removing the influence of steel fibers, the differences in the SCM contribution to the mix designs may be more evident and could prove to be a beneficial tool in future UHPC mixture designs. If resistivity can be used to aid in understanding not only the mix design phase but also the role SCMs play in the UHPC system, the importance of resistivity measurements could increase.

2) A more accurate method for characterizing the PSR in UHPC is necessary. Paired with the user-friendly and cost-efficient resistivity tests, if a more reliable method for PSR characterization is found, the formation factor could gain importance as a numerical characterization for UHPC.

3) Service life predictions for UHPC using Life-365 should not be taken as definite values and additional caution should be taken on the interpretation of the results. Additional research is required to improve Life-365 or other software to better capture the unique mixture designs and mechanisms of UHPC.

REFERENCES

AASHTO PP84 (2018). "Standard Practice for Developing Performance Engineered Concrete Pavement Mixtures." American Association of State Highway and Transportation Officials, Washington, D.C.

AASHTO T358 (2017). "Standard Method of Test for Surface Resistivity Indication of Concrete's Ability to Resist Chloride Ion Penetration." American Association of State Highway and Transportation Officials, Washington, D.C.

Acker, P., and Behloul, M. "Ductal® Technology: A Large Spectrum of Properties, a Wide Range of Applications." *Proc., Proceedings of the International Symposium on Ultra High Performance Concrete*, 11-23.

Ahlborn, T. M., Peuse, E. J., and Misson, D. L. (2008). "Ultra-High-Performance-Concrete for Michigan Bridges Material Performance - Phase I." Michigan Department of Transportation, Lansing, MI.

Alkaysi, M., and El-Tawil, S. (2016). "Effects of variations in the mix constituents of ultra high performance concrete (UHPC) on cost and performance." *Materials and Structures*, 49(10), 4185-4200.

Alkaysi, M., El-Tawil, S., Liu, Z., and Hansen, W. (2016). "Effects of Silica Powder and Cement Type on Durability of Ultra High Performance Concrete (UHPC)." *Cement and Concrete Composites*, 66, 47-56.

ASTM C39 (2018). "Standard Test Method for Compressive Strength of Cylindrical Concrete Specimens." ASTM International, West Conshohocken, PA.

ASTM C192 (2016). "Standard Practice for Making and Curing Concrete Test Specimens in the Laboratory." ASTM International, West Conshohocken, PA.

ASTM C944 (2012). "Standard Test Method for Abrasion Resistance of Concrete or Mortar Surfaces by the Rotating-Cutter Method." ASTM International, West Conshohocken, PA.

ASTM C1202 (2017). "Standard Test Method for Electrical Indication of Concrete's Ability to Resist Chloride Ion Penetration." ASTM International, West Conshohocken, PA.

ASTM C1437 (2015). "Standard Test Method for Flow of Hydraulic Cement Mortar." ASTM International, West Conshohocken, PA.

ASTM C1760 (2012). "Standard Test Method for Bulk Electrical Conductivity of Hardened Concrete." ASTM International, West Conshohocken, PA.

ASTM C1856 (2017). "Standard Practice for Fabricating and Testing Specimens of Ultra-High-Performance Concrete." ASTM International, West Conshohocken, PA.

ASTM C1876 (2019). "Standard Test Method for Bulk Electrical Resistivity or Bulk Conductivity of Concrete." ASTM International, West Conshohocken, PA.

Batoz, J. F., and Behloul, M. (2011). "UHPFRC Development: Experience with Ductal® over the Past Two Decades." *Designing Building with UHPFRC*, 43-62.

Bentz, D. P., Guthrie, W. S., Jones, S. Z., and Martys, N. S. (2014). "Predicting Service Life of Steel-Reinforced Concrete Exposed to Chlorides." *Concrete International*, 36(9), 55-64.

Bernardi, S., Jacomo, D., and Boudry, F. "Overlay Ductal®: a durable solution for bridges retrofitting." *Proc., International Interactive Symposium on Ultra-High Performance Concrete*, Iowa State University Digital Press.

Berry, M., Snidarich, R., and Wood, C. (2017). "Development of Non-Proprietary Ultra-High Performance Concrete." Montana Department of Transportation, Helena, MT.

Bierwagen, D., Moore, B., Keierleber, B., Sritharan, S., Wipf, T., and Abu-Hawash, A. "Design of Buchanan county, Iowa, bridge, using ultra-high performance concrete and pi-girder cross section." *Proc., 3rd International fib Congress and Exhibition, Incorporating the PCI Annual Convention and Bridge Conference: Think Globally, Build Locally, Proceedings*.

Brühwiler, E., and Denarié, E. (2013). "Rehabilitation and Strengthening of Concrete Structures Using Ultra-High Performance Fibre Reinforced Concrete." *Structural Engineering International*, 23(4), 450-457.

Dean, N., Stevens, C., and Hastings, J. "Accelerated Bridge Construction Methods for Bridge 1-438 Replacement." *Proc., International Interactive Symposium on Ultra-High Performance Concrete*, Iowa State University Digital Press.

Denarié, E. (2005). "Full scale application of UHPFRC for the rehabilitation of bridges–from the lab to the field." SAMARIS Management Group.

Ehlen, M. A. 2018. Life-365 Service Life Prediction Model and Computer Program for Predicting the Service Life and Life-Cycle Cost of Reinforced Concrete Exposed to Chlorides, version 2.2.3.

El-Tawil, S., Tai, Y.-S., Meng, B., Hansen, W., and Liu, Z. (2018). "Commercial Production of Non-Proprietary Ultra High Performance Concrete." Michigan Department of Transportation, Lansing, MI.

Farris, J. F., and Bettis, G. (2019). "Everyday ABC in Texas." *International Accelerated Bridge Construction.* Miami, FL.

FHWA (2019). "North American Deployments of UHPC in Highway Bridge Construction." <https://usdot.maps.arcgis.com/apps/webappviewer/index.html?id=41929767ce164eba934d70883d775582>. (April, 2020).

Giesler, A. J., McGinnis, M. J., and Weldon, B. D. (2018). "Flexural behavior and analysis of prestressed ultra-high-performance concrete beams made from locally available materials." *PCI Journal*, 63(6).

Graybeal, B. A. (2006). "Material Property Characterization of Ultra-High Performance Concrete." Federal Highway Administration, McLean, VA.

Graybeal, B. A. (2009). "UHPC in the U.S. Highway Infrastructure." *International Workshop on UHPFRC.* Marseille, France.

Graybeal, B. A. (2011). "Ultra-High Performance Concrete." Federal Highway Administration, McLean, VA.

Graybeal, B. A. (2013). "Development of Non-Proprietary Ultra-High Performance Concrete for Use in the Highway Bridge Sector: TechBrief." Federal Highway Administration.

Graybeal, B. A. (2019). "Design and Construction of Field-Cast UHPC Connections." Federal Highway Administration, McLean, VA.

Haber, Z. B., De la Varga, I., Graybeal, B. A., Nakashoji, B., and El-Helou, R. (2018). "Properties and Behavior of UHPC-Class Materials." Federal Highway Administration, McLean, VA.

Haber, Z. B., Munoz, J. F., and Graybeal, B. A. (2017). "Field Testing of an Ultra-High Performance Concrete Overlay." Federal Highway Administration, McLean, VA.

Hartwell, D. R. (2011). "Laboratory testing of Ultra High Performance Concrete deck joints for use in accelerated bridge construction." Master of Science, Iowa State University, Ames, IA.

Jensen, B. (2015). "Historic Road Infrastructure of Texas, 1866-1965." *National Register of Historic Places*, Texas Department of Transportation, Environmental Affairs, Austin, TX.

Khayat, K. H., and Valipour, M. (2018). "Design and Performance of Cost-Effective Ultra High Performance Concrete for Bridge Deck Overlays." Missouri Department of Transportation, Jefferson City, MO.

Kim, H. (2016). "Design and field construction of Hawkeye Bridge using ultra high performance concrete for accelerated bridge construction." Master of Science, University of Iowa, Iowa City, Iowa.

Kim, Y. J. (2018). "Development of Cost-Effective Ultra-High Performance Concrete (UHPC) for Colorado's Sustainable Infrastructure." Colorado Department of Transportation, Denver, CO.

Layssi, H., Ghods, P., Alizadeh, A. R., and Salehi, M. (2015). "Electrical Resistivity of Concrete: Concepts, applications, and measurement techniques." *Concrete International*, 37(5), 41-46.

Mendonca, F., El-Khier, M. A., Morcous, G., and Hu, J. (2020). "Feasibility Study of Development of Ultra-High Performance Concrete (UHPC) for Highway Bridge Applications in Nebraska." Nebraska Department of Transportation, Lincoln, NE.

Mindess, S., Young, J. F., and Darwin, D. (2003). *Concrete*, Prentice Hall, Upper Saddle River, NJ.

Mukhopadhyay, A., and Saraswatula, P. (8/2020). "TxDOT Project 0-6958: Developing Performance Specifications for High-Performance Concrete." Texas Department of Transportation, Austin, TX.

Nassif, H., Rabie, S., Na, C., and Salvador, M. (2015). "Evaluation of Surface Resistivity Indication of Ability of Concrete to Resist Chloride Ion Penetration." New Jersey Department of Transportation, Trenton, NJ.

NIST (2017). "Estimation of Pore Solution Conductivity." <https://www.nist.gov/el/materials-and-structural-systems-division-73100/inorganic-materials-group-73103/estimation-pore>. (May, 2020).

Park, J.-S., Kim, Y. J., Cho, J.-R., and Jeon, S.-J. (2015). "Early-age strength of ultra-high performance concrete in various curing conditions." *Materials*, 8(8), 5537-5553.

Pyo, S., Abate, S. Y., and Kim, H.-K. (2018). "Abrasion resistance of ultra high performance concrete incorporating coarser aggregate." *Construction and Building Materials*, 165, 11-16.

Qiao, P., Zhou, Z., and Allena, S. (2016). "Developing Connections for Longitudinal Joints between Deck Bulb Tees-Development of UHPC Mixes with Local Materials." Washington State Department of Transportation, Olympia, WA.

Riding, K., Schindler, A. K., Pesek, P., Drimalas, T., and Folliard, K. J. (2017). "ConcreteWorks v3 training/user manual (P1): ConcreteWorks software (P2)." The University of Texas at Austin Center for Transportation Research, Austin, TX.

Rupnow, T. D., and Icenogle, P. (2011). "Evaluation of Surface Resistivity Measurements as an Alternative to the Rapid Chloride Permeability Test for Quality Assurance and Acceptance." Louisiana Transportation Research Center, Baton Rouge, LA.

Russell, H. G., and Graybeal, B. A. (2013). "Ultra-High Performance Concrete: A State-of-the-Art Report for the Bridge Community." Federal Highway Administration, McLean, VA.

Snyder, K. A. (2001). "The relationship between the formation factor and the diffusion coefficient of porous materials saturated with concentrated electrolytes: theoretical and experimental considerations." *Concrete Science and Engineering*, 3, 216-224.

Spragg, R., Bu, Y., Snyder, K., Bentz, D., and Weiss, J. (2013). "Electrical Testing of Cement-Based Materials: Role of Testing Techniques, Sample Conditioning, and Accelerated Curing." Joint Transportation Research Program Purdue University, Indianapolis, IN.

Spragg, R., De la Varga, I., Montanari, L., and Graybeal, B. (2019). "Using Formation Factor to Define the Durability of Ultra-High Performance Concrete." *Second International Interactive Symposium on UHPC*, Federal Highway Administration, Albany, NY.

Spragg, R., Villani, C., Snyder, K., Bentz, D., Bullard, J. W., and Weiss, J. (2013). "Factors that Influence Electrical Resistivity Measurements in Cementitious Systems." *Transportation Research Record: Journal of the Transportation Research Board*, 2342(1), 90-98.

Sritharan, S. (2015). "Design of UHPC Structural Members: Lessons Learned and ASTM Test Requirements." *Advances in Civil Engineering Materials*, 4(2), 113-131.

Subedi, D., Moustafa, M. A., and Saiidi, M. S. (2019). "Non-Proprietary UHPC for Anchorage of Large Diameter Column Bars in Grouted Ducts." California Department of Transportation, Sacramento, CA.

Tanesi, J., Ardani, A., and Montanari, L. (2019). "Formation Factor Demystified and its Relationship to Durability." Federal Highway Administration, McLean, VA.

Thomas, M., Green, B., O'Neal, E., Perry, V., Hayman, S., and Hossack, A. "Marine Performance of UHPC at Treat Island." *Proc., Proceedings of the 3rd International Symposium on UHPC and Nanotechnology for High Performance Construction Materials*, 365-370.

Trejo, D., Hueste, M. B. D., Kim, Y. H., and Atahan, H. (2008). "Characterization of Self-Consolidating Concrete for Design of Precast, Prestressed Bridge Girders." Texas Transportation Institute, Texas Department of Transportation.

TxDOT (2020). "Bridge Design Manual - LRFD." Texas Department of Transportation, Austin, TX.

TxDOT Project 0-6958 (8/2020). "Developing Performance Specifications for High-Performance Concrete." PI: Anol Mukhopadhyay, and Z. G. Team: Kai-Wei Liu, Stefan Hurlebaus, Dan Zollinger, and Andrew Wimsatt, eds.

Ulm, F. (2004). "Bending and shear design of Iowa DOT sample bridge: Update Design Review of Mars Hill Bridge." *Massachusetts Institute of Technology for the Iowa Department of Transportation*.

WALO USA (2018). "Floyd River Bridge, Iowa." <https://walo.com/case-studies/floyd-river-bridge-sheldon-ia/>. (April, 2020).

Weiss, W. J., Spragg, R. P., Isgor, O. B., Ley, M. T., and Van Dam, T. (2018). "Toward Performance Specifications for Concrete: Linking Resistivity, RCPT and Diffusion Predictions Using the Formation Factor for Use in Specifications." *High Tech Concrete: Where Technology and Engineering Meet*, Springer, Cham, 2057-2065.

Weldon, B. D., Jauregui, D. V., Newtson, C. M., Taylor, C. W., Montoya, K. F., and Allena, S. (2010). "Feasibility Analysis of Ultra High Performance Concrete for Prestressed Concrete Bridge Applications." New Mexico Department of Transportation, Albuquerque, NM.

Wibowo, H., and Sritharan, S. (2018). "Use of Ultra-High-Performance Concrete for Bridge Deck Overlays." Iowa Highway Research Board Iowa Department of Transportation, Ames, IA.

Wille, K., Naaman, A. E., and Parra-Montesinos, G. J. (2011). "Ultra-High Performance Concrete with Compressive Strength Exceeding 150 MPa (22 ksi): A Simpler Way." *ACI Materials Journal*, 108(1).

Yuan-Hui, L., and Gregory, S. (1974). "Diffusion of Ions in Sea Water and in Deep-Sea Sediments." *Geochimica et Cosmochimica Acta*, 38(5), 703-714.

APPENDIX A

LABORATORY TEST RESULTS FOR DURABILITY

Table A.1. Abrasion Resistance Results for 2-3/8 in. Dressing Wheels

Mix	Surface Preparation	Diameter (in.) 1	Diameter (in.) 2	Height (in.) 1	Height (in.) 2	Height (in.) 3	Height (in.) 4	Avg Diameter (in.)	Avg Height (in.)	Initial Mass (g)	Mass 1 (g)	Mass 2 (g)	Mass 3 (g)	Mass 4 (g)	Mass 5 (g)
1	Cast	4.06	4.01	2.55	2.52	2.54	2.51	4.03	2.53	1247.9	1243.5	1242.2	1239.0	1237.1	1235.1
		4.06	4.00	2.52	2.52	2.53	2.53	4.03	2.53	1258.7	1254.7	1250.5	1246.9	1243.3	1240.0
		4.05	4.01	2.49	2.47	2.55	2.53	4.03	2.51	1277.1	1272.2	1269.5	1266.5	1263.6	1260.9
	Ground	4.02	4.00	2.56	2.59	2.56	2.55	4.01	2.56	1260.5	1259.6	1258.8	1258.4	1257.7	1257.5
		3.99	4.02	2.64	2.65	2.65	2.64	4.00	2.64	1310.4	1309.4	1308.9	1308.5	1308.0	1307.3
		4.01	4.01	2.53	2.52	2.52	2.51	4.01	2.52	1246.5	1245.4	1244.7	1244.1	1243.4	1242.7
	Molded	3.96	3.97	2.51	2.51	2.52	2.51	3.97	2.51	1228.4	1226.7	1226.0	1224.9	1223.3	1222.0
		3.97	3.96	2.43	2.42	2.41	2.43	3.96	2.42	1204.0	1201.3	1199.9	1198.3	1196.9	1195.4
		3.96	3.96	2.49	2.49	2.49	2.49	3.96	2.49	1231.5	1229.1	1227.0	1225.5	1224.1	1222.8
2	Cast	4.01	4.01	2.53	2.56	2.56	2.57	4.01	2.56	1237.9	1236.0	1232.2	1229.5	1227.5	1226.0
		4.04	4.02	2.51	2.51	2.53	2.53	4.03	2.52	1247.9	1245.3	1243.2	1241.5	1240.1	1238.4
		4.04	4.04	2.55	2.54	2.54	2.55	4.04	2.54	1252.4	1248.5	1246.0	1244.2	1242.1	1240.6
	Ground	3.98	4.02	2.60	2.60	2.57	2.58	4.00	2.59	1267.8	1267.0	1266.7	1266.7	1265.4	1264.9
		4.02	4.02	2.57	2.55	2.55	2.53	4.02	2.55	1249.8	1248.4	1247.5	1247.5	1245.9	1245.2
		4.01	4.01	2.63	2.63	2.60	2.61	4.01	2.62	1291.6	1290.4	1289.1	1288.4	1287.4	1286.7
	Molded	3.96	3.96	2.46	2.46	2.45	2.47	3.96	2.46	1200.7	1198.7	1198.0	1196.9	1196.0	1195.2
		3.97	3.97	2.55	2.53	2.54	2.53	3.97	2.54	1230.4	1228.3	1226.9	1225.6	1224.6	1224.0
		3.97	3.95	2.45	2.45	2.45	2.47	3.96	2.45	1193.5	1188.5	1186.7	1185.6	1184.7	1183.6
3	Cast	3.99	4.01	2.51	2.57	2.55	2.52	4.00	2.53	1283.4	1278.9	1277.9	1276.6	1275.3	1273.7
		4.01	4.01	2.69	2.70	2.65	2.62	4.01	2.66	1335.0	1331.5	1330.7	1329.4	1328.0	1326.8
		4.00	4.04	2.65	2.62	2.61	2.66	4.02	2.64	1342.1	1338.2	1337.4	1335.5	1333.4	1331.3
	Ground	3.99	4.05	2.56	2.54	2.54	2.54	4.02	2.55	1299.0	1297.8	1297.5	1297.2	1297.0	1296.7
		4.00	3.99	2.44	2.41	2.42	2.41	4.00	2.42	1230.2	1228.9	1228.7	1228.3	1227.7	1227.3
		4.02	4.00	2.50	2.50	2.52	2.53	4.01	2.51	1284.0	1283.1	1282.8	1282.6	1282.1	1281.8
	Molded	3.96	3.97	2.50	2.48	2.49	2.49	3.97	2.49	1264.0	1262.8	1262.3	1261.0	1260.0	1258.9
		3.97	3.97	2.45	2.44	2.45	2.45	3.97	2.45	1235.3	1234.0	1233.2	1232.0	1230.7	1229.7
		3.95	3.96	2.45	2.46	2.47	2.45	3.95	2.45	1240.0	1239.0	1237.7	1236.3	1235.0	1233.7

Table A.2. Abrasion Resistance Results for 1.5 in. Dressing Wheels

Mix	Surface Preparation	Diameter (in.)		Height (in.)				Avg Diameter (in.)	Avg Height (in.)	Initial Mass (g)	Mass 1 (g)	Mass 2 (g)	Mass 3 (g)	Mass 4 (g)	Mass 5 (g)
		1	2	1	2	3	4								
1	Cast	4.01	4.01	2.65	2.65	2.68	2.69	4.01	2.67	1310.8	1309.5	1308.5	1307.6	1306.9	1306.1
	Ground	4.00	4.04	2.69	2.69	2.68	2.68	4.02	2.69	1335.6	1335.5	1335.2	1335.1	1334.9	1334.6
	Molded	3.99	3.97	2.31	2.30	2.29	2.30	3.98	2.30	1140.5	1139.2	1137.9	1136.8	1135.3	1134.1
2	Cast	4.08	4.01	2.62	2.62	2.63	2.70	4.04	2.64	1334.7	1333.5	1331.8	1331.0	1330.0	1329.1
	Ground	4.25	3.98	2.41	2.40	2.41	2.40	4.11	2.41	1181.9	1181.4	1181.1	1180.8	1180.5	1180.2
	Molded	3.97	3.96	2.48	2.47	2.47	2.50	3.96	2.48	1215.9	1214.7	1213.8	1212.9	1211.9	1211.0
3	Cast	4.01	4.05	2.70	2.71	2.68	2.70	4.03	2.69	1385.1	1383.0	1381.6	1380.1	1379.1	1378.2
	Ground	4.01	4.01	2.53	2.52	2.52	2.54	4.01	2.53	1293.5	1293.1	1292.8	1292.6	1292.5	1292.2
	Molded	3.96	3.97	2.37	2.39	2.36	2.37	3.96	2.37	1194.8	1193.2	1192.2	1191.1	1189.7	1188.3

Table A.3. Surface Resistivity Values at 7 Days

Mix	Batch	Surface Resistivity (kΩ-cm)								Specimen			Batch			Mix		
		0°	90°	180°	270°	0°	90°	180°	270°	Avg (kΩ-cm)	Std Dev	COV (%)	Avg (kΩ-cm)	Std Dev	COV (%)	Avg (kΩ-cm)	Std Dev	COV (%)
1	a	11.0	11.0	14.0	13.0	14.0	17.0	11.0	9.0	12.5	2.3	18.8	12.6	2.1	16.8	-	-	-
		15.0	11.0	14.0	13.0	9.0	14.0	17.0	13.0	13.3	2.3	17.2				-	-	-
		10.0	12.0	13.0	14.0	10.0	12.0	14.0	12.0	12.1	1.5	12.0				-	-	-
	b	31.0	28.0	23.0	24.0	24.0	28.0	23.0	26.0	25.9	2.7	10.5	24.5	2.1	8.7	23.7	1.9	7.8
		24.0	22.0	25.0	23.0	22.0	24.0	25.0	23.0	23.5	1.1	4.8						
		24.0	23.0	27.0	25.0	23.0	23.0	23.0	25.0	24.1	1.4	5.7						
	c	23.0	26.0	22.0	23.0	23.0	25.0	25.0	26.0	24.1	1.5	6.0	23.3	1.6	7.0			
		20.0	22.6	24.0	22.0	22.0	24.0	24.0	23.0	22.7	1.3	5.7						
		23.0	22.0	22.0	21.0	23.0	22.0	21.0	22.0	22.0	0.7	3.2						
		22.0	21.0	23.0	24.0	22.0	23.0	24.0	25.0	23.0	1.2	5.3						
		23.0	26.0	27.0	24.0	22.0	26.0	26.0	23.0	24.6	1.7	7.0						
2	a	28.0	29.0	29.0	30.0	29.0	30.0	30.0	30.2	29.4	0.7	2.5	30.0	0.9	3.1	26.3	3.3	12.5
		30.0	32.0	29.0	31.0	30.0	31.0	29.0	30.0	30.3	1.0	3.2						
		31.3	30.3	31.0	30.0	29.0	31.0	30.0	31.0	30.5	0.7	2.4						
	b	26.0	28.0	27.0	28.0	25.0	29.0	28.0	27.0	27.3	1.2	4.4	24.1	1.9	8.0			
		23.0	21.0	24.0	25.0	23.0	22.0	24.0	24.0	23.3	1.2	5.2						
		23.0	22.0	23.0	25.0	25.0	21.0	22.0	23.0	23.0	1.3	5.8						
		24.0	23.0	23.0	22.0	24.0	23.0	24.0	24.0	23.4	0.7	3.0						
		23.0	25.0	24.0	25.0	24.0	22.0	23.0	24.0	23.8	1.0	4.1						
3	a	16.0	17.0	16.7	16.9	16.4	16.5	16.7	16.9	16.6	0.3	1.9	16.8	0.4	2.3	16.6	0.6	3.7
		17.7	16.3	16.7	17.2	17.4	16.8	16.5	17.1	17.0	0.4	2.6						
		16.7	16.8	16.5	16.3	16.4	16.2	16.4	16.5	16.5	0.2	1.1						
		17.1	16.9	17.3	16.1	16.7	17.0	17.0	17.3	16.9	0.4	2.1						
		17.0	17.0	17.2	16.8	17.4	16.5	16.4	16.8	16.9	0.3	1.9						
	b	17.0	16.5	17.2	17.5	15.2	17.2	15.3	16.6	16.6	0.8	4.9	16.5	0.8	4.8			
		16.4	16.7	15.8	16.0	16.0	16.8	17.0	16.6	16.4	0.4	2.5						
		16.3	16.4	15.3	15.5	15.5	15.9	15.0	15.4	15.7	0.5	2.9						
		16.0	17.6	17.3	17.6	17.6	17.4	17.0	17.3	17.2	0.5	2.9						

Table A.4. Surface Resistivity Values at 14 Days

Mix	Batch	Surface Resistivity (kΩ-cm)								Specimen			Batch			Mix		
		0°	90°	180°	270°	0°	90°	180°	270°	Avg (kΩ-cm)	Std Dev	COV (%)	Avg (kΩ-cm)	Std Dev	COV (%)	Avg (kΩ-cm)	Std Dev	COV (%)
1	a	15.0	20.0	18.0	17.0	16.0	21.0	16.0	15.0	17.3	2.1	12.2	16.6	3.7	22.2	-	-	-
		13.0	23.0	14.8	23.0	15.0	22.0	14.0	23.0	18.5	4.3	23.4				-	-	-
		16.0	17.0	12.0	12.0	12.0	18.0	16.0	10.0	14.1	2.8	19.5				-	-	-
	b	47.0	49.6	49.0	47.4	46.0	46.0	47.0	48.0	47.5	1.2	2.6	46.7	2.2	4.7	44.7	2.9	6.4
		49.0	49.2	47.6	50.0	48.0	47.3	47.5	48.0	48.3	0.9	1.9						
		43.0	46.0	46.1	42.0	45.0	45.0	44.0	42.0	44.1	1.6	3.5						
	c	40.0	40.0	46.0	39.0	42.0	42.0	45.0	41.0	41.9	2.3	5.5	43.6	2.7	6.2			
		47.0	48.0	45.0	47.0	48.0	45.0	44.0	47.0	46.4	1.4	3.0						
		44.0	43.0	44.0	43.0	46.0	45.0	45.0	42.0	44.0	1.2	2.8						
		42.0	48.0	43.0	45.0	43.0	50.0	43.0	43.0	44.6	2.7	6.0						
		41.0	39.0	42.0	41.0	43.0	40.0	43.0	40.0	41.1	1.4	3.3						
2	a	43.9	53.1	51.6	52.5	49.0	51.0	51.3	51.6	50.5	2.7	5.4	50.3	1.9	3.8	45.6	3.9	8.6
		50.8	47.0	48.8	49.7	51.0	48.9	51.6	49.5	49.7	1.4	2.8						
		51.1	49.7	50.7	50.2	52.5	50.2	50.0	51.4	50.7	0.9	1.7						
	b	45.0	40.0	43.0	41.0	46.0	42.0	45.0	43.0	43.1	2.0	4.6	42.8	1.3	3.1			
		40.0	43.0	42.0	43.0	42.0	42.0	43.0	44.0	42.4	1.1	2.6						
		41.0	44.0	44.0	42.0	42.0	45.0	44.0	43.0	43.1	1.3	2.9						
		41.0	43.0	41.0	43.0	42.0	43.0	42.0	43.0	42.3	0.8	2.0						
		42.0	43.0	43.0	44.0	43.0	43.0	44.0	44.0	43.3	0.7	1.5						
3	a	28.0	28.8	28.7	28.2	28.8	29.5	29.4	28.3	28.7	0.5	1.8	27.9	1.0	3.7	28.8	1.4	5.0
		27.3	26.7	27.8	28.8	28.1	27.9	28.5	29.8	28.1	0.9	3.1						
		27.2	27.0	27.4	29.0	27.3	28.4	27.4	29.0	27.8	0.8	2.8						
		27.7	27.2	27.3	27.6	28.2	27.3	28.7	29.8	28.0	0.8	3.0						
		26.8	25.1	27.6	28.5	28.0	26.0	26.3	26.2	26.8	1.1	4.0						
	b	30.0	30.0	31.0	27.1	31.0	30.9	30.0	30.3	30.0	1.2	4.0	30.0	0.8	2.8			
		29.1	29.6	31.0	29.5	29.0	31.0	29.6	29.0	29.7	0.8	2.6						
		30.0	29.0	29.9	30.5	31.0	30.0	30.2	30.5	30.1	0.5	1.8						
		28.8	30.5	30.0	30.6	30.3	31.0	30.7	29.5	30.2	0.7	2.2						

Table A.5. Surface Resistivity Values at 28 Days

Mix	Batch	Surface Resistivity (kΩ-cm)								Specimen			Batch			Mix		
		0°	90°	180°	270°	0°	90°	180°	270°	Avg (kΩ-cm)	Std Dev	COV (%)	Avg (kΩ-cm)	Std Dev	COV (%)	Avg (kΩ-cm)	Std Dev	COV (%)
1	a	28.0	22.0	23.0	27.0	29.0	31.0	36.0	27.0	27.9	4.1	14.8	29.1	4.5	15.6	-	-	-
		29.0	36.0	31.0	30.0	29.0	39.0	32.0	32.0	32.3	3.3	10.3				-	-	-
		28.0	32.0	21.0	23.0	28.0	33.0	22.0	30.0	27.1	4.3	15.9				-	-	-
	b	121	115	118	118	122	115	120	117	118	2.4	2.1	118	3.1	2.6	106	9.0	8.4
		122	119	119	123	118	117	116	123	120	2.5	2.1						
		117	116	115	113	116	112	117	112	115	2.0	1.7						
	c	99.0	95.0	97.0	98.0	101	96.0	101	101	98.5	2.2	2.3	99.8	2.3	2.3			
		99.0	103	102	100	100	101	103	101	101	1.4	1.3						
		103	97.0	99.0	105	95.0	96.0	99.0	102	99.5	3.3	3.3						
		101	100	100	99.0	100	102	102	97.0	100	1.5	1.5						
		99.0	101	97.0	101	98.0	99.0	99.0	102	99.5	1.6	1.6						
2	a	120	119	117	113	117	118	117	112	117	2.6	2.2	117	3.2	2.7	106	9.6	9.1
		114	117	114	114	116	116	116	113	115	1.3	1.2						
		121	118	125	118	120	116	123	121	120	2.7	2.3						
	b	95.0	99.0	100	96.0	100	97.0	99.0	98.0	98.0	1.7	1.8	98.5	2.9	2.9			
		96.0	99.0	94.0	96.0	95.0	97.0	96.0	94.0	95.9	1.5	1.6						
		104	104	101	100	101	105	102	103	103	1.7	1.6						
		99.0	97.0	97.0	93.0	96.0	97.0	96.0	97.0	96.5	1.6	1.6						
		98.0	99.0	101	100	97.0	101	98.0	102	99.5	1.7	1.7						
3	a	59.0	50.3	57.0	58.1	57.3	52.9	62.0	60.0	57.1	3.6	6.2	54.7	3.2	5.9	56.5	3.4	6.1
		51.6	56.7	52.4	55.0	58.0	58.1	51.6	58.0	55.2	2.7	5.0						
		54.2	54.2	59.0	57.0	53.3	58.0	57.9	52.0	55.7	2.4	4.3						
		55.0	50.0	54.0	51.3	52.0	49.0	50.1	54.9	52.0	2.2	4.2						
		54.1	52.9	56.6	52.3	49.0	55.1	55.5	52.0	53.4	2.3	4.2						
	b	56.0	55.0	57.9	55.0	59.0	56.4	58.5	56.3	56.8	1.4	2.5	58.9	2.0	3.3			
		60.0	58.1	60.0	57.0	60.0	61.0	59.6	60.4	59.5	1.2	2.1						
		58.0	57.0	60.9	62.0	60.0	61.0	63.1	60.1	60.3	1.9	3.1						
		58.0	60.0	58.2	58.0	57.6	61.4	60.0	58.4	59.0	1.3	2.1						

Table A.6. Surface Resistivity Values at 56 Days

Mix	Batch	Surface Resistivity (kΩ-cm)								Specimen			Batch			Mix		
		0°	90°	180°	270°	0°	90°	180°	270°	Avg (kΩ-cm)	Std Dev	COV (%)	Avg (kΩ-cm)	Std Dev	COV (%)	Avg (kΩ-cm)	Std Dev	COV (%)
1	a	67.6	66.7	52.3	49.8	63.0	66.3	43.4	50.2	57.4	8.9	15.5	57.8	9.4	16.3	-	-	-
		58.9	78.3	63.0	67.9	53.8	72.5	61.4	66.0	65.2	7.3	11.1				-	-	-
		44.0	50.2	58.7	53.1	43.3	49.4	57.9	49.4	50.8	5.3	10.4				-	-	-
	b	226	226	222	224	222	227	217	227	224	3.2	1.4	226	4.4	1.9	211	12.5	5.9
		223	225	226	222	224	222	223	224	224	1.3	0.6						
		229	230	232	230	232	231	235	234	232	1.9	0.8						
	c	208	203	209	200	214	203	204	195	205	5.5	2.7	202	4.7	2.3			
		207	200	206	200	207	206	205	204	204	2.7	1.3						
		206	193	204	202	204	197	214	195	202	6.4	3.1						
		202	204	200	204	201	202	196	202	201	2.4	1.2						
		199	200	204	196	199	202	199	196	199	2.5	1.3						
2	a	232	233	237	235	234	235	236	237	235	1.7	0.7	237	2.4	1.0	214	18.3	8.6
		237	239	234	236	235	239	238	238	237	1.7	0.7						
		240	238	239	238	242	237	240	236	239	1.8	0.7						
	b	193	190	202	201	208	205	203	200	200	5.6	2.8	200	4.5	2.2			
		203	200	204	200	199	190	203	197	200	4.2	2.1						
		206	205	203	202	204	197	200	203	203	2.7	1.3						
		192	195	196	201	203	198	195	198	197	3.3	1.7						
		203	202	200	204	201	191	196	204	200	4.2	2.1						
3	a	90.0	84.5	106	108	102	97.5	106	108	100	8.3	8.3	100	5.3	5.3	-	-	-
		102	98.0	104	109	99.0	104	104	107	103	3.5	3.3				-	-	-
		94.0	97.0	102	94.7	95.3	102	99.2	97.2	97.7	2.9	3.0				-	-	-
		103	95.0	96.0	100	99.0	102	104	109	101	4.2	4.2				-	-	-
		97.0	105	100	108	100	94.9	97.5	98.0	100	4.1	4.1				-	-	-
	b	-	-	-	-	-	-	-	-	-	-	-	-	-	-	-	-	-
		-	-	-	-	-	-	-	-	-	-	-	-	-	-	-	-	-
		-	-	-	-	-	-	-	-	-	-	-	-	-	-	-	-	-
		-	-	-	-	-	-	-	-	-	-	-	-	-	-	-	-	-

Table A.7. Surface Resistivity Values at 90 Days

Mix	Batch	Surface Resistivity (kΩ-cm)								Specimen			Batch			Mix		
		0° (kΩ-cm)	90° (kΩ-cm)	180° (kΩ-cm)	270° (kΩ-cm)	0° (kΩ-cm)	90° (kΩ-cm)	180° (kΩ-cm)	270° (kΩ-cm)	Avg (kΩ-cm)	Std Dev	COV (%)	Avg (kΩ-cm)	Std Dev	COV (%)	Avg (kΩ-cm)	Std Dev	COV (%)
1	a	58.0	72.0	83.0	60.0	65.0	69.0	73.0	56.0	67.0	8.5	12.7	69.9	11.1	15.9	-	-	-
		62.0	64.0	79.0	80.0	95.0	70.0	82.0	73.0	75.6	10.0	13.3				-	-	-
		51.0	79.0	68.0	54.0	73.0	70.0	87.0	54.0	67.0	12.2	18.2				-	-	-
	b	283	288	273	284	278	271	275	286	280	6.0	2.1	277	7.2	2.6	-	-	-
		275	260	281	284	267	271	286	271	274	8.3	3.0				-	-	-
		271	274	281	267	277	277	271	287	276	5.9	2.2				-	-	-
	c	-	-	-	-	-	-	-	-	-	-	-	-	-	-	-	-	-
		-	-	-	-	-	-	-	-	-	-	-	-	-	-	-	-	-
		-	-	-	-	-	-	-	-	-	-	-	-	-	-	-	-	-
		-	-	-	-	-	-	-	-	-	-	-	-	-	-	-	-	-
		-	-	-	-	-	-	-	-	-	-	-	-	-	-	-	-	-
2	a	324	324	320	325	316	321	317	322	321	3.1	1.0	321	7.0	2.2	-	-	-
		313	322	320	309	312	317	315	321	316	4.4	1.4				-	-	-
		324	340	324	312	336	319	330	320	326	8.7	2.7				-	-	-
	b	-	-	-	-	-	-	-	-	-	-	-	-	-	-	-	-	-
		-	-	-	-	-	-	-	-	-	-	-	-	-	-	-	-	-
		-	-	-	-	-	-	-	-	-	-	-	-	-	-	-	-	-
		-	-	-	-	-	-	-	-	-	-	-	-	-	-	-	-	-
		-	-	-	-	-	-	-	-	-	-	-	-	-	-	-	-	-
3	a	-	-	-	-	-	-	-	-	-	-	-	-	-	-	-	-	-
		-	-	-	-	-	-	-	-	-	-	-	-	-	-	-	-	-
		-	-	-	-	-	-	-	-	-	-	-	-	-	-	-	-	-
		-	-	-	-	-	-	-	-	-	-	-	-	-	-	-	-	-
	b	-	-	-	-	-	-	-	-	-	-	-	-	-	-	-	-	-
		-	-	-	-	-	-	-	-	-	-	-	-	-	-	-	-	-
		-	-	-	-	-	-	-	-	-	-	-	-	-	-	-	-	-
		-	-	-	-	-	-	-	-	-	-	-	-	-	-	-	-	-

Table A.8. Bulk Resistivity Values at 7 Days

Mix	Batch	Bulk Resistivity (kΩ-cm)	Batch			Mix		
			Avg (kΩ-cm)	Std Dev	COV (%)	Avg (kΩ-cm)	Std Dev	COV (%)
1	a	6.7	6.3	0.3	5.2	-	-	-
		6.4				-	-	-
		5.9				-	-	-
	b	23.8	24.0	0.1	0.5	23.4	0.4	1.8
		24.1						
		24.0						
	c	23.0	23.1	0.2	1.1			
		23.3						
		22.8						
		23.5						
		23.0						
2	a	24.8	24.9	0.2	0.7	23.6	1.0	4.4
		24.7						
		25.1						
	b	22.7	22.8	0.1	0.6			
		22.6						
		22.9						
		22.8						
		23.0						
3	a	17.6	17.5	0.2	1.2	17.7	0.3	1.5
		17.6						
		17.1						
		17.6						
		17.7						
	b	17.9	17.9	0.1	0.7			
		17.8						
		17.8						
		18.1						

Table A.9. Bulk Resistivity Values at 14 Days

Mix	Batch	Bulk Resistivity (kΩ-cm)	Batch			Mix		
			Avg (kΩ-cm)	Std Dev	COV (%)	Avg (kΩ-cm)	Std Dev	COV (%)
1	a	13.7	13.0	0.7	5.5	-	-	-
		13.2				-	-	-
		12.0				-	-	-
	b	48.5	48.7	0.2	0.3	46.6	1.7	3.7
		48.9						
		48.7						
	c	45.2	45.3	0.3	0.6			
		45.3						
		45.4						
		45.7						
		44.9						
2	a	51.4	51.3	0.3	0.6	47.2	3.3	6.9
		50.9						
		51.6						
	b	44.6	44.8	0.3	0.7			
		44.3						
		45.2						
		44.9						
		45.0						
3	a	30.2	30.2	0.3	0.9	30.6	0.6	1.9
		30.1						
		29.7						
		30.3						
		30.5						
	b	30.9	31.2	0.3	1.0			
		30.9						
		31.2						
		31.7						

Table A.10. Bulk Resistivity Values at 28 Days

Mix	Batch	Bulk Resistivity (kΩ-cm)	Batch Avg (kΩ-cm)	Batch Std Dev	Batch COV (%)	Mix Avg (kΩ-cm)	Mix Std Dev	Mix COV (%)
1	a	30.7	28.9	1.6	5.6	-	-	-
		29.3				-	-	-
		26.8				-	-	-
	b	109	110	0.9	0.9	106	3.0	2.9
		109						
		111						
	c	103	104	0.8	0.8			
		104						
		103						
		105						
		103						
2	a	118	117	0.8	0.7	107	8.1	7.6
		116						
		117						
	b	100	101	1.2	1.2			
		100						
		103						
		100						
		101						
3	a	58.3	58.0	0.5	0.9	58.7	1.0	1.7
		57.6						
		57.3						
		58.2						
		58.8						
	b	58.8	59.6	0.7	1.2			
		58.9						
		60.0						
		60.5						

Table A.11. Bulk Resistivity Values at 56 Days

Mix	Batch	Bulk Resistivity (kΩ-cm)	Batch Avg (kΩ-cm)	Batch Std Dev	Batch COV (%)	Mix Avg (kΩ-cm)	Mix Std Dev	Mix COV (%)
1	a	59.1	55.5	3.2	5.8	-	-	-
		56.2				-	-	-
		51.3				-	-	-
	b	219	221	1.7	0.8	207	11.0	5.3
		220						
		223						
	c	195	199	2.3	1.2			
		200						
		198						
		202						
		198						
2	a	233	233	1.2	0.5	208	19.9	9.6
		231						
		234						
	b	193	193	3.3	1.7			
		194						
		198						
		188						
		191						
3	a	105	105	1.0	0.9	-	-	-
		105				-	-	-
		104				-	-	-
		105				-	-	-
		107				-	-	-
	b	-	-	-	-	-	-	-
		-	-	-	-	-	-	-
		-	-	-	-	-	-	-
		-	-	-	-	-	-	-

Table A.12. Bulk Resistivity Values at 90 Days

Mix	Batch	Bulk Resistivity (kΩ-cm)	Batch		
			Avg (kΩ-cm)	Std Dev	COV (%)
1	a	75.7	71.0	4.2	6.0
		71.8			
		65.4			
	b	281	281	2.9	1.0
		285			
		278			
	c	-	-	-	-
		-	-	-	-
		-	-	-	-
		-	-	-	-
		-	-	-	-
2	a	312	311	0.9	0.3
		310			
		312			
	b	-	-	-	-
		-	-	-	-
		-	-	-	-
		-	-	-	-
		-	-	-	-
3	a	-	-	-	-
		-	-	-	-
		-	-	-	-
		-	-	-	-
		-	-	-	-
	b	-	-	-	-
		-	-	-	-
		-	-	-	-
		-	-	-	-